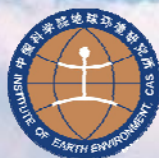


11st National Aerosol Conference and
10th Cross-strait Workshop for Aerosol Science and Technology

十一届全国气溶胶会议暨
第十届海峡两岸气溶胶技术研讨会

摘要集

中国气溶胶专业委员会
中国科学院地球环境研究所
中国科学院大气物理研究所
武汉大学
华中农业大学
国际空气与废弃物管理学会
北京粉体技术协会
丹东市百特仪器有限公司
广州禾信分析仪器有限公司



中国·武汉
2013.5.16~19

目 录

| | |
|--|----|
| 中国近海海域气溶胶反演及验证 | 1 |
| （边健，曹亚楠，徐梦春，徐青山） | |
| Evaluating the degree of oxygenation of organic aerosols during foggy and hazy days in Hong Kong using high-resolution time-of-flight aerosol mass spectrometry （HR-ToF-AMS） | 2 |
| （Li Yongjie, Berto Paul Yok Long Lee, Chak K. Chan） | |
| Recent research advances of PM _{2.5} monitoring and sampling techniques | 3 |
| （蔡春進） | |
| 台灣科學園區周界大氣氣膠特性研究 | 4 |
| （蔡仁雄，陳瑞仁，蔡朋枝，謝連德，林人杰） | |
| 兰州地区气溶胶消光特性研究 | 5 |
| （曹贤洁，张镭，田鹏飞） | |
| 周边气象条件对南京城区污染颗粒物及气体污染物浓度的影响研究 | 6 |
| （常炉予，赵天良，何金海，汤莉莉，于红霞） | |
| 土地覆被资料改变及对空气污染模拟影响的初步分析 | 7 |
| （常鸣，陈伟华，王雪梅） | |
| CARSNET 气溶胶关键光学特性参数反演研究 | 8 |
| （车慧正，夏祥鳌，张小曳，王亚强，张晓春，孙俊英） | |
| 基于 CMB 模型的南京市分级颗粒物来源解析研究 | 9 |
| （陈璞珑，王体健，胡忻） | |
| 珠三角地区细颗粒物质量浓度和化学组分变化趋势 | 10 |
| （陈伟华，王雪梅） | |
| 基于卫星遥感和地面观测资料分析苏皖两省一次空气污染过程 | 12 |
| （陈焯鑫，朱彬，侯雪伟，尹聪） | |
| 台灣大氣中 PM _{2.5} 區域性來源之模擬分析 | 13 |
| （陳杜甫，張良輝） | |
| 西安市大气中二次有机气溶胶的季节组成及变化 | 15 |
| （成春雷，王格慧） | |
| 武汉市大气灰霾期 PM _{1.0} 水溶性组分污染特征研究 | 16 |
| （成海容，王祖武，张帆，吕效谱，刘佳，王新明） | |
| 东亚季风减弱背景下我国空气质量变化的模拟研究 | 17 |
| （程叙耕，赵天良，徐祥德，Liu Feng, 韩永翔，车慧正，何金海） | |
| PM _{2.5} and PM _{10-2.5} chemical composition and source apportionment near a Hong Kong roadway | 18 |
| （Y. Cheng, S. C. Lee, Z. L. Gu, K. F. Ho, Y. W. Zhang, Y. Huang, J. C. Chow, J. G. Watson, J. J. Cao, R. J. Zhang） | |
| 大气环境对博物馆内文物的影响 | 19 |
| （程燕，郭伟，樊巍巍，张云伟，张仁健） | |
| 大气及气溶胶中有机氮研究进展 | 20 |
| （程玉婷，王格慧） | |
| 江苏省城市灰霾变化趋势 | 21 |

| | |
|--|----|
| (戴灵慧, 田心如, 韩永翔, 赵天良) | |
| Characteristics of atmospheric visibility and its affecting factors in five typical cities across the Taiwan Strait..... | 22 |
| (邓君俊, 杜可) | |
| 广州市大气汞的湿沉降特征及影响因素分析 | 23 |
| (邓思欣, 王雪梅, 董汉英, 鲍若峪) | |
| 一次严重灰霾过程的气溶胶光学特性垂直分布 | 24 |
| (邓涛, 吴兑, 邓雪娇, 谭浩波, 李菲, 陈欢欢) | |
| 广州地区 PM ₁ 气溶胶、湿度效应与能见度的函数关系 | 25 |
| (邓雪娇, 张芷言, 李菲, 王宝民, 吴兑, 郁建珍, 卞奇婧, 谭浩波, 邓涛) | |
| 一种国内外首创的重量法 PM _{2.5} 自动监测系统 | 26 |
| (董青云, 马明杰, 杨卫东, 李晓旭) | |
| The “Dual-Spot” Aethalometer: real-time source apportionment of fossil fuel vs. biomass combustion aerosols..... | 27 |
| (G. MOČNIK, L. DRINOVEC, P. ZOTTER, A.S.H. PRÉVÔT, C. RUCKSTUHL, J. SCIARE , J.-E. PETIT, R. SARDA ESTEVE, A.D.A. HANSEN) | |
| 人为活动对室内空气质量的影响分析 | 29 |
| (郭伟, 程燕, 晁攸闯, 樊巍巍) | |
| 中国春季人为和沙尘气溶胶对大气辐射的影响 | 30 |
| (韩志伟, 李嘉伟, 夏祥鳌, 张仁健) | |
| Characteristics, distribution and source apportionment of polycyclic aromatic hydrocarbons in fine particulate in Nanjing, China | 31 |
| (He Jiabao, Fan Shuxian, Zu Fan, Meng Qingzi, Zhang Jian, Sun Yu) | |
| 應用 WRF/Chem 模式研析熱帶氣旋對南台灣大氣臭氧濃度流佈與累積現象 | 32 |
| (洪崇軒, 羅國誠, 袁中新) | |
| Continuous observations of water-soluble ions in PM _{2.5} over different seasons in Beijing: Variability, ions formation, and aerosol acidity | 33 |
| (Hu Guoyuan, Zhang Yangmei, Sun Junying, Lin Weili, Yang Yun) | |
| 西安市 PM _{2.5} 中主要成分的质量浓度和数量浓度对比分析 | 34 |
| (胡塔峰, 曹军骥) | |
| Effect of NH ₃ on the Formation of Indoor Secondary Pollutants from Ozone/Monoterpenes Reactions | 35 |
| (Huang Yu, Lee Shun Cheng, Ho Kin Fai, Wang Jiaping, Niu Xinyi) | |
| 利用多通道扫描式激光雷达监测大气污染物的 3D 分布 | 36 |
| (黄忠伟, 倪简白, 周天) | |
| 評估堆肥場生物危害特性 | 37 |
| (黃筱茜, 楊心豪, 王嗣涵, 洪柏宸, 羅金翔) | |
| 抗菌沸石去除室內空氣中生物性氣膠之研究 | 38 |
| (黃于珊, 謝祝欽, 翁郁絜) | |
| 应用颗粒物化学组分监测仪 (ACSM) 实时快速在线测定致霾细粒子化学组分和有机组分 | 39 |
| (江琪, 孙业乐, 王自发, 银燕, 王飞) | |
| Observation and Analysis of Optical Properties of Atmospheric Aerosols in Beijing Urban Area..... | 40 |

| | |
|--|----|
| (Jing Junshan, Zhang Renjian, Che Huizheng, Wu Yunfei, Xia Xiangao, Yan Peng, Zhao Deming) 多環芳烴在台灣南部熱帶地區空氣氣態-顆粒態之濃度及分布 | 41 |
| (柯風溪, 鄭金娥, 李宗霖) | |
| Similarities and diversities of PM _{2.5} , PM ₁₀ and TSP profiles for fugitive dust in a coastal oilfield city, China | 42 |
| (Kong Shaofei, Ji Yaqin, Lu Bing, Zhao Xueyan, Bai Zhipeng) | |
| 固定源排放 PM ₁₀ 和 PM _{2.5} 无机组分特征研究 | 43 |
| (孔少飞, 姬亚芹, 李志勇, 白志鹏) | |
| 台灣中南部地區大氣垂直剖面臭氧濃度及光化指標特性之調查 | 45 |
| (賴進興, 吳義林, 林清和, 葉淑杏, 葉旗福) | |
| Aqueous-phase photochemical oxidation and direct photolysis of vanillin as a model compound of methoxy-phenols from biomass burning | 46 |
| (Li Yong Jie, Heidi H.Y. CHEUNG, Huang Dan Dan, Fan Wei Hong, Liya E. YU, Chak K. CHAN) | |
| Aerosol radiative effects on the meteorology and concentrations of pollutants in Mega-Cities | 48 |
| (Li Guohui, Bei Naifang, Luisa T. Molina) | |
| Influences of Fireworks Display on Gaseous Ambient Air Pollutants and Titration Effects during the Taiwanese Lantern Festival | 49 |
| (Yuan ChungShin, Lee ChangGai) | |
| 冬季兰州城市大气 PM _{2.5} 中碳气溶胶的污染特征与来源 | 50 |
| (李刚, 石广玉, 李宏宇, 邓祖琴) | |
| 2011 年夏季新疆天山大气 PM _{2.5} 中碳气溶胶特征与来源分析 | 51 |
| (李刚, 周军, 石广玉, 李忠勤, 王文彬, 李宏宇, 邓祖琴) | |
| Preliminary study of the influence of OH radical source on the formation process of secondary organic aerosol in smog chamber experimen | 52 |
| (Li Hong, Kei SATO, Akinori TAKAMI, Wang Xuezhong) | |
| 操作電壓對靜電集塵器收集微粒效率之影響 | 53 |
| (李嘉塗, 莊崇賢) | |
| 二維噴管內氣流流動數值模擬研究 | 54 |
| (李嘉塗, 邱怡樺) | |
| 2010 年春季东亚地区气溶胶的模拟研究 | 55 |
| (李嘉伟, 韩志伟, 张仁健) | |
| 基于 CMAQ 模式的珠三角地区碳气溶胶排放研究 | 56 |
| (李楠, 傅宗玖, 曹军骥) | |
| 人类黑碳气溶胶与东亚夏季气候年代际变化 | 57 |
| (李双林, Rashed Mahmood, 万江华) | |
| Reduction of both NO _x and PM emission by using water containing diesel fuels | 58 |
| (Chang YuCheng, Lee WenJhy) | |
| 气溶胶标准化发展概况及对策 | 60 |
| (李兆军, 李劲松) | |
| 閩江口大氣懸浮微粒濃度季節變化趨勢及污染源貢獻量分析 | 61 |
| (廖建欽, 李宗璋, 張正馳, 陳光暉, 袁中新, 張章堂, 江士豪) | |
| 大氣中 VOC 垂直層化分佈觀測及其對臭氧空氣品質之影響探討 | 62 |

| | |
|---|----|
| (廖思婷, 高英暉, 林啟燦, 洪崇軒, 袁中新) | |
| Study of long-range transport air pollutants to Taiwan during Southeast Asia biomass burning events | 63 |
| (Chuan Yao Lin, Chun Zhao, Liu Xiaohong, Lin NengHuei, Chi KaiHsien) | |
| 高雄市都會區大氣細懸浮微粒濃度時空變異特徵 | 64 |
| (林銳敏, 李瑞龍) | |
| Development of an optimal method for ¹⁴ C-based source apportionment of PM _{2.5} carbonaceous aerosols at a background site in East China | 65 |
| (Liu Di, Li Jun, Zhang Yanlin, Xu Yue, Liu Xiang, Ding Ping, Shen Chengde, Chen Yingjun , Tian Chongguo, Zhang Gan) | |
| 重慶城市灰霾特征与数值模拟研究 | 67 |
| (刘红年, 吕梦瑶) | |
| 全球沙尘气溶胶源汇分布及其变化特征的模拟分析 | 68 |
| (刘建慧, 赵天良, 韩永翔, S.L.Gong, 熊洁) | |
| 武汉光谷地区春季大气颗粒物的粒径分布特征 | 70 |
| (刘珏, 胡辉, 刘立) | |
| The PAH concentrations and compositions in aerosol over Marginal and Open sea in the North Pacific Ocean | 71 |
| (Liu Junwen, Xu Yue, Li Jun , Zhang Gan) | |
| 东莞市不同区域气溶胶细粒子 PM ₁ 及其中重金属元素的污染特征 | 72 |
| (刘立, 胡辉, 李嫻, 黄奂彦, 蔡勋江, 张国斐) | |
| 南京城市群区大气污染对地表气象要素及能量收支的影响研究 | 73 |
| (刘丽霞, 凌肖露, 郭维栋) | |
| Is formation of NH ₄ NO ₃ a critical factor for the growth of > 10 nm new particles to cloud condensation nuclei size in marine boundary layer? | 74 |
| (Liu Xiaohuan, Zhu Yujiao, Gao Huiwang, Zhang Tianran, Xiaohong Yao) | |
| 长江三角洲地区 1980-2009 年灰霾分布特征及影响因子研究 | 75 |
| (刘晓慧, 朱彬, 王红磊, 张恩红) | |
| 臺中市政府清潔隊柴油車輛裝置濾煙器試範運行成果 | 76 |
| (劉邦裕) | |
| 二行程機車青白煙檢測與改善成效探討 | 77 |
| (劉邦裕, 江嘉, 鐘文舜, 姜禹丞, 盧昭暉) | |
| 臺中市清潔隊柴油車輛加裝濾煙器試範運行成效探討 | 78 |
| (劉邦裕, 余忠賢, 游雲欽, 陳以松, 盧昭暉) | |
| 自動貝他計和手動採樣器之 PM _{2.5} 量測結果差異探討 | 79 |
| (劉俊男, 亞瓦希 阿米, 洪毅弘, 蔡春進, 巫月春, 陳重方) | |
| 福建省大气污染物排放清单的初步估算研究 | 80 |
| (鲁斯唯, 吴水平, 陈晓秋) | |
| 近 50 年中国气溶胶光学厚度反演及长期变化特征的分析 | 81 |
| (罗建国, 吴润) | |
| 利用影像處理技術評估大氣能見度與 PM _{2.5} 之關係 | 82 |
| (羅金翔, 楊心豪, 黃筱茜, 王嗣涵) | |
| 混合气溶胶吸湿性研究 | 83 |

| | |
|--|-----|
| (马庆鑫, 刘畅, 马金珠, 贺泓) | |
| 雾化液滴对湿法采集纳米 TiO ₂ 气溶胶的影响研究 | 84 |
| (茆平, 冯曙艳, 杨毅, 刘梦楚, 周阳, 陈守文, 王正萍) | |
| Water-soluble secondary organic aerosol in Qinghai Lake: implication for sources, formation, and degradation during long-range transport | 85 |
| (Meng Jingjing, Wang Gehui, Li Jianjun, Cheng Chunlei, Cao Junji) | |
| Particle size distribution and characteristics of Polycyclic Aromatic Hydrocarbons during an autumn haze episode in Nanjing, China | 86 |
| (Meng Qingzi, Fan Shuxian, Zu Fan, He Jiabao, Zhang Jian, Sun Yu) | |
| Ambient Ammonia and Ammonium Observed at a Remote Mountain Site in Western China | 87 |
| (Meng Zhaoyang, Jia Xiaofang, Ma Jianzhong, Wang JianQiong, Yu Xiaolan, Jiang YiAn) | |
| 西安水溶性类腐殖质气溶胶 (HULIS) 的污染特征及其来源 | 88 |
| (倪海燕, 韩永明, 曹军骥) | |
| 乌鲁木齐市大气 PM _{2.5} 和 PM _{2.5-10} 中有机碳、元素碳的粒径分布及季节性分布 | 89 |
| (热比古力·达木拉, 迪丽努尔·塔力甫, 王新明, 丁翔, 阿不力孜·伊米提) | |
| 武汉市雾霾期间 PM _{2.5} 浓度和气象因子对能见度影响分析 | 91 |
| (沈龙娇, 王建民, 胡珂) | |
| Seasonal and day-night variations of chemical species in PM ₁₀ over Xi'an, China: Implications of water-soluble organic carbon (WSOC) sources | 92 |
| (Shen Zhenxing, Cao Junji, Zhang Qian, Li Jianjun, Liu Suixin) | |
| Aerosol Variations in Boundary Atmospheres: Review and Prospect | 93 |
| (Shi Guangyu, Chen Bin) | |
| 青岛市区春、夏季生物气溶胶浓度及影响因子分析 | 94 |
| (宋志文, 吴等等, 钱生财, 徐爱玲, 夏岩) | |
| Column-integrated aerosol optical properties over Xi'an, China | 95 |
| (Su Xiaoli, Cao Junji, Li Zhengqiang, Lin Meijing, Wang Gehui) | |
| The molecular composition and mass-size distribution of biogenic secondary organic aerosol from Xi'an .. | 96 |
| (Sun Tao, Wang Gehui, Li Jianjun) | |
| An Observational Study of the Hygroscopic Properties of Aerosols over the Pearl River Delta Region | 97 |
| (Tan Haobo, Yin Yan, Gu Xuesong, Li Fei, P.W. Chan, Xu Hanbing, Deng Xuejiao) | |
| 东南极大陆沿岸黑碳气溶胶的本底特征研究 | 98 |
| (汤洁, 卞林根, 逯昌贵) | |
| 北京一次持续雾霾天气过程的气象特征分析 | 99 |
| (唐宜西, 张小玲, 熊亚军) | |
| CARSNET 太阳光度计室内积分球标定方法研究 | 101 |
| (陶然, 车慧正, 鲁赛) | |
| Development of an integrating sphere calibration method for China Aerosol Remote Sensing NETwork Cimel sunphotometer | 102 |
| (Tao Ran, Che Huizheng, Chen Quanliang, Wang Yaqiang, Sun Junying, Zhang Xiaochun, Lu Sai, Guo Jianping, Wang Hong, Zhang Xiaoye) | |
| 大型燃烧腔的设计、特征与实验测试——生物质露天燃烧的室内模拟 | 103 |
| (田杰, 韩永明, 倪海燕, L.-W.A. Chen, 曹军骥) | |

| | |
|---|-----|
| Aerosol vertical distribution and seasonal variation over SACOL derived from CALIPSO lidar observations | 104 |
| (Tian Pengfei, Zhang Lei, Cao Xianjie) | |
| 北京城区夏季大气气溶胶亲水性特征研究 | 105 |
| (田平, 张仁健, 颜鹏, 王广甫, 武云飞) | |
| Impact of meteorological parameters and gaseous pollutants (SO_2 and NO_2) on $\text{PM}_{2.5}$ and PM_{10} mass concentrations during 2010 in Xi'an, China..... | 106 |
| (Wang Ping, Cao Junji, Han Yongming, Huang Yu, Lee Shuncheng) | |
| 青海湖地区单颗粒黑碳气溶胶的特性 | 107 |
| (王启元, 曹军骥, 胡塔峰) | |
| Investigation of NR- PM_1 Species and Effect on Visibility in Xi'an, China | 108 |
| (Wang Yichen, Cao Junji) | |
| 台灣北部三個空氣品質測站之大氣微粒來源及特性研究 | 109 |
| (危涵, 劉俊男, 蔡春進, 巫月春, 陳重方) | |
| 同时测定大气中气态和颗粒态多环芳烃及其含氧/氮衍生物的新方法 | 110 |
| (魏崇, Benjamin A. Musa Bandowe, Hannah Meusel, 何建辉, 韩永明, 曹军骥, Thorsten Hoffmann, Wolfgang Wilcke) | |
| 气溶胶中硫酸根离子的 FTIR 定量分析 | 111 |
| (魏秀丽, 高闽光, 刘建国, 刘娜, 徐亮, 童晶晶, 金岭) | |
| 青岛市不同功能区冬季空气微生物群落代谢与多样性特征 | 112 |
| (吴等等, 宋志文, 徐爱玲, 郑远, 夏岩) | |
| Characteristics of aerosol transport and distribution in East Asia | 114 |
| (吴润, 郭俊, 赵得明) | |
| 台灣柴油車 NO_x 排放管制成效探討 | 115 |
| (吳容輝, 林文淵, 顏瑞瑩, 許仲景, 莊志偉, 盧昭暉, 林建良) | |
| 北京夏季大气气溶胶吸收特性—多仪器比对观测 | 116 |
| (武云飞, 张仁健, 颜鹏, 田平, 张养梅, 陈聪) | |
| 2000-2010 年中国地区人为排放源年际变化趋势研究 | 117 |
| (谢祖欣, 韩志伟) | |
| 青藏高原沙漠化对东亚沙尘气溶胶贡献的敏感性模拟试验分析 | 118 |
| (熊洁, 赵天良, 刘煜, 韩永翔, Feng Liu) | |
| 米散射微脉冲激光雷达应用的探讨 | 119 |
| (徐赤东, 纪玉峰, 徐青山) | |
| Inter-annual variability of wintertime $\text{PM}_{2.5}$ chemical composition in Xi'an, China: Implications of Emission Changes | 120 |
| (H.M. Xu, J.J. Cao, K.F. Ho) | |
| 上海市大气散射系数的季节变化特征 | 121 |
| (徐薇, 修光利, 陶俊, 王丽娜, 朱梦雅, 冯玲, 张大年) | |
| Estimation of aerosol refractive index and optical properties during summer and winter time at a regional background station in Yangtze River Delta Region of China..... | 122 |
| (Yan Peng, Zhou Xiuji) | |

| | |
|---|-----|
| 纳米流体注入过程中咸水层二氧化碳迁移数值分析 | 123 |
| (杨多兴, 张毅) | |
| 黏粉原料配比及粒徑對於拜香燃煙特徵之影響 | 124 |
| (楊奇儒, 林建佑, 葉秀緯, 李孫榮, 張翊峰) | |
| Preparation of Titania-Silica Aerogels and Their Application to VOC Degradation..... | 125 |
| (姚尚汶, 郭修伯) | |
| 不同尺度非控制型重油燃燒對多環芳香烴污染物排放的影响 | 126 |
| (葉旗福, 賴進興, 林清和, 鄭立新, 陳明仁, 蔡匡忠, 陳宣匡) | |
| 工业纳米颗粒气溶胶测量及数值模型构建 | 127 |
| (于明州, Martin Seinenbusch, Gerhard Kasper) | |
| 分光光度法测定大气气溶胶细粒子中的阴离子表面活性物质 | 128 |
| (于彦婷, 李红, 张庆竹, 段鹏丽, 曹冠, 李雷) | |
| 在线单颗粒气溶胶质谱仪在香烟口感及烟气气溶胶老化过程检测中的应用 | 129 |
| (粘慧青, 庄雯, 李梅, 周振) | |
| VOCs 廢氣治理與溶劑回收之最佳可行技術與案例探討 | 130 |
| (粘愷峻, 簡弘民, 張豐堂) | |
| 铅锌冶炼区大气颗粒物中典型重金属及来源分析 | 131 |
| (张凯, 柴发合, 李倦生, 郑子龙, 王静, 杨 晴) | |
| 砒矾岛国家大气背景站 PM _{2.5} 化学组成及来源分析 | 132 |
| (张帆, 王晓平, 陈颖军, 田崇国, 王艳) | |
| 武汉秋季灰霾和非灰霾天气 PM _{2.5} 中水溶性离子的特征研究 | 133 |
| (张帆, 成海容, 王祖武, 吕效谱) | |
| 海峽兩岸大氣中懸浮微粒模擬結果之性能評估 | 134 |
| (張良輝, 陳杜甫, 蔡長祐) | |
| Chemical composition and source characterization of Fugitive Dust over Xi'an in theSouth Margin of the Loess Plateau, China | 135 |
| (Zhang Qian, Mu Jiao, Shen Zhenxing) | |
| Spatial and Seasonal Variations of Mass and Chemical Composition for PM ₁₀ in Xi'an, China | 136 |
| (T. Zhang, J.J. Cao, S.X. Liu, S.X. Yang) | |
| 1964—2010 年四川能见度及消光系数特征及变化趋势 | 137 |
| (张小娟, 韩永翔, 陈娟, 郑小波) | |
| 华北平原区域雾霾天气分析与数值试验 | 138 |
| (张小玲, 唐宜西, 赵秀娟, 熊亚军) | |
| Observation of submicron aerosols at Mount Tai in east China from 2010 to 2012:Impact of different air masses on chemical components and size distribution..... | 139 |
| (Y.M. Zhang, X.Y. Zhang, J.Y. Sun, G.Y. Hu, X.J. Shen, T.T. Wang, D.Z. Wang, Y. Zhao) | |
| 北京市大气中醛酮化合物和 BTEX 来源和浓度变化特征..... | 140 |
| 行驶车辆对城市街谷内空气流动与污染物扩散的影响-基于拉格朗日模型的数值模拟 | 141 |
| (张云伟, 顾兆林, 段翠娥, 苏磊杰) | |
| 以臺南市大氣粒狀物所含重金屬比例判斷重金屬污染源變異性 | 142 |
| (張皇珍, 邱瑞基, 林徽雅, 涂良君) | |

| | |
|---|-----|
| 臺南市細懸浮微粒變化趨勢及區域污染特性分析 | 143 |
| (張皇珍, 邱瑞基, 呂鴻毅, 蔡宜倫, 黃琬鈴) | |
| 福州與馬祖地區酸雨化學成份及雨水酸化之探討 | 144 |
| (張章堂, 林凱隆, 袁中新, 施志恆, 陳玉利, 江士豪, 陳光暉) | |
| Analysis and characteristics of visibility in Shenyang from 2010—2012 | 145 |
| (Zhao Hujia, Che Huizheng, Zhang Xiaoye, Ma Yanjun, Wang Yangfeng) | |
| 新国标下峡口地形城市冬季大气污染的时空分布变化规律研究 | 146 |
| (赵克明, 李霞, 卢新玉, 冯志敏, 王磊, 马超) | |
| Effects of meteorological conditions on high BC concentration at Xi'an from 2003 to 2007 | 147 |
| (Zhao Shuyu) | |
| 大气边界层中 VOCs 层化分布与逆温现象之相关性探讨 | 148 |
| (郑佳俊, 林启灿, 袁中新, 洪崇轩, 廖思婷) | |
| 株洲市工业区大气颗粒物污染特征研究 | 149 |
| (郑子龙, 张凯, 柴发合, 杨晴, 李倦生, 刘运年) | |
| 探寻 IMPROVE 和 NIOSH 法元素碳 (EC) 测定结果的数学联系 | 150 |
| (支国瑞, 陈颖军, 李洋) | |
| 利用 CALIPSO 星载激光雷达资料研究我国 PM ₁₀ 浓度分布特征 | 152 |
| (周天, 黄忠伟) | |
| Investigations of the Chemical Characteristics from an Intensive Sainampling of Ambient Particles in Shanghai, China | 153 |
| (Zhu Chong shu, Cao Jun ji) | |
| 大气细颗粒物对人体健康的影响 | 154 |
| (朱彤) | |
| 武汉市道路一侧 PM _{2.5} 和 PM ₁₀ 浓度监测 | 155 |
| (朱颖, 李可, 刘彬, 向荣彪) | |
| Comparing new particle formation events between in highly and less polluted atmosphere: Implication of a critical role of anthropogenic pollutants in growing new particles to CCN size | 156 |
| (Y.J. Zhu, H.W. Gao, Z.Q. Duan, G.J. Evans, X. H. Yao) | |
| Characterization of Springtime Atmospheric Organic and Elemental Carbon of PM _{2.5} in a Typical Semi-Arid Area of Northeastern China | 157 |
| (Renjian Zhang, Jun Tao, K.F. Ho, Zhenxing Shen) | |
| 直接称量法环境空气颗粒物自动监测系统 | 158 |
| Real-time Measurements of Secondary Organic Aerosol from the Photooxidation of Naphthalene using Single Particle Mass Spectrometry | 159 |
| (Ang Chen, Robert M. Healy, Shouming Zhou, John C., WengYer) | |
| 半干旱区气溶胶物理特性的观测研究 | 160 |
| (张武, 冯岚, 李娜, 颜娇珑, 王雅萍, 柳丹, 黄晨然) | |
| 长三角臭氧和细颗粒污染及其对区域污染控制和污染-气候相互作用的启示: SORPES 观测站最新进展 | 161 |
| (丁爱军, 符淙斌, 杨修群, 孙鉴泞, 聂玮, 谢郁宁, 齐西蒙, E. Herrmann, T. Petäjä, V.-M. Kerminen, M. Kulmala) | |
| 亚洲沙尘的演化和非均相光化学过程研究 | 162 |

| | |
|--|-----|
| (聂玮, 王韬, 丁爱军, 薛丽坤, 王文兴) | |
| 西安 2008 年冬季地表臭氧变化模拟及其主要影响因素 | 163 |
| Black carbon variation during a high pollution haze episode in Beijing, China..... | 164 |
| (Qingyang Liu, Yanju Liu, Yi Gao, Meigen Zhang, Renjian Zhang, Hui Ding , Xuekui Qi) | |
| 大型环境舱协助改进外排式空气净化设备性能的评价测..... | 165 |
| (杨华, 王欣欣, 刘清珺, 刘艳菊, 邵薇) | |

中国近海海域气溶胶反演及验证

(边健^{1,2,3} 曹亚楠^{1,2} 徐梦春^{1,2} 徐青山¹)

(1 中国科学院安徽光学精密机械研究所中国科学院大气成分与光学重点实验室, 安徽 合肥 230031; 2 中国科学院大学, 北京, 100039; 3 合肥学院, 数学与物理系, 安徽, 合肥, 230601)

摘 要:基于中分辨率成像光谱仪(TERRA/MODIS)的一级数据和相应的辅助数据, 利用 Junge 谱近似实际大气气溶胶模型, 从 MODIS 两近红外通道卫星数据同时反演中国近海海洋上空气溶胶光学厚度和 Junge 谱指数, 并将反演结果与 MODIS 产品和 AERONET 数据作对比分析, 验证了此方法的可行性与可靠性, 得到了合理的气溶胶 Junge 谱指数与气溶胶光学厚度的空间分布。

关键词: 气溶胶光学厚度, Junge 谱, MODIS, AERONET

Evaluating the degree of oxygenation of organic aerosols during foggy and hazy days in Hong Kong using high-resolution time-of-flight aerosol mass spectrometry (HR-ToF-AMS)

(Yongjie Li¹, Berto Paul Yok Long Lee¹, Chak K. Chan^{1, 2})

¹ Division of Environment,

² Department of Chemical and Biomolecular Engineering,

Hong Kong University of Science and Technology, Clear Water Bay, Hong Kong, keckchan@ust.hk

Abstract: The role of aqueous-phase chemistry in the formation of secondary organic aerosols (SOA) is still poorly constrained. Here we present observation results of the degree of oxygenation of organic aerosols (OA) based on high-resolution time-of-flight aerosol mass spectrometer (HR-ToF-AMS) measurements made at a coastal site in Hong Kong from late April to the end of May, 2011 for 37 days. Two foggy periods and one hazy period were chosen for detailed analysis to compare the changes in degree of oxygenation of OA due to different processes. The Extended Aerosol Inorganic Model (E-AIM) predicted fine particle liquid water content (LWC_{fp}) was up to $85 \mu\text{g}/\text{m}^3$ during the foggy days. Particle concentration as measured by the HR-ToF-AMS was up to $60 \mu\text{g}/\text{m}^3$ during the hazy days. The degree of oxygenation of OA, as indicated by several parameters including fraction of m/z 44 in organic mass spectra (f_{44}), oxygen to carbon elemental ratio (O:C), and carbon oxidation state was evaluated against odd oxygen (O_x) concentration, LWC_{fp} , ionic strength (IS), and in-situ pH (pH_{is}). Results suggested that for the hazy period, the high concentration of OA (on average $11 \mu\text{g}/\text{m}^3$) and the high degree of oxygenation were mainly due to gas-phase oxidation. During the foggy periods with low photochemical activities, the degree of oxygenation of OA was almost as high as that in the hazy days and significantly higher than that during non-fog/non-haze days. However, the evolution of OA behaved quite differently in these two foggy periods. The first foggy period in late April and early May had larger LWC_{fp} and lower O_x concentration and the OA had more semi-volatile oxygenated organic aerosols (SVOOA) as resolved by positive matrix factorization (PMF). The second foggy period in mid-May had higher O_x concentration and lower LWC_{fp} , and produced more low-volatility oxygenated organic aerosols (LVOOA). Examination into the particle-phase constituents suggests that partitioning may be the dominating process that incorporates oxygenated species into the particle phase for the first foggy period, while oxidation may be the dominating process for the second foggy period. Both physical and chemical processes are important in multi-phase mechanisms for oxygenated organic aerosol formation.

ACKNOWLEDGMENTS

This work was supported by the University Grants Committee (Special Equipment Grant, SEG-HKUST07) and the Environment and Conservation Funds (ECF) of Hong Kong SAR (project number: ECWW09EG04).

Recent research advances of PM_{2.5} monitoring and sampling techniques

(蔡春進 (Tsai, Chuen-Jinn))

新竹交通大學環境工程研究所, 新竹, 台灣, 30010

Abstract: Accurate sampling and analysis of PM_{2.5} is essential to determine the compliance with promulgated ambient PM_{2.5} standards and identify the sources of PM_{2.5} pollutants. USA PM_{2.5} FRM (federal reference method) manual samplers or FEM (federal equivalent method) monitors are commonly used but there are still rooms to improve the accuracy. In several air monitoring stations in Taiwan, it was found PM_{2.5} concentrations are over-estimated by the VEREWA-F701 BAM (beta attenuation monitor) by as much as 58.4 %, and 28.4-29.8 % by the earlier version of the Met-One BAM-1020s (without FEM designation). In this talk, reasons why PM_{2.5} concentrations are overestimated by automatic beta attenuation monitors, including positive artifacts due to acid gas adsorption by the glass fiber filter tapes used in the monitors, aerosol water content and volatilization loss of inorganic semi-volatile species will be presented (Liu et al., 2013a). Then the size-selective inlets of current manual PM samplers, including impactors and cyclones, will be reviewed and problems associated with particle bounce, evaporation loss, ambient relative humidity and substrate coating conditions will be discussed. It was found that the BGI VSCC (very sharp cut cyclone) has a better solid particle loading performance than that of the WINS impactor and oil-coated Teflon substrates are capable of resolving solid particle loading problems in impactors (Tsai et al., 2012). The results of using the newly developed MFPPS (multi-filter PM₁₀-PM_{2.5} sampler) in NCTU (Liu et al., 2011) to determine artifacts during filter sampling and conditioning of PM_{2.5} manual samplers will be presented. The evaluation of PM_{2.5} monitoring accuracy of the Model 1405-DF TEOM-FDMS, which is capable of correcting for positive and negative PM_{2.5} artifacts, will also be presented. For obtaining accurate size-classified aerosol samples, a newly developed 10-stage NCTU micro-orifice cascade impactor (NMCI, 56 nm to 10 μm) which contains new nozzle plates with smooth nozzle shape made by the LIGA (Lithography, Electroplating, and Molding) process, will be introduced (Liu et al., 2013b). The laboratory and field comparison test results showed the NMCI outperforms the widely used micro-orifice uniform deposit impactor (MOUDI, MSP Model 110).

Keywords: PM_{2.5}, sampling artifacts, impactor, cyclone, PM sampling, monitoring

references

- Liu, C.-N., Awasthi, A., Hung, Y.-H., Gugamsetty, B., Tsai, C.-J., Wu, Y.-C., Chen, C.-F., Differences in 24-h average PM_{2.5} concentrations between the beta attenuation monitor (BAM) and the dichotomous sampler (Dichot), *Atmos. Environ.*, doi: 10.1016/j.atmosenv.2013.04.062, 2013a.
- Liu, C.-N., Chen, S.-C. and Tsai, C.-J., A Novel Multi-Channel PM₁₀-PM_{2.5} sampler (MCPPS), *Aerosol Sci. Technol.*, 45: 1480-1487, 2011.
- Tsai, C.-J., Liu, C.-N., Hung, S.-M., Chen, S.-C., Uang, S.-N., Cheng, Y.-S., Zhou, Y., A Novel Active Personal Nanoparticle Sampler (PENS) for the Exposure Assessment of Nanoparticles in Workplaces, *Environ. Sci. Technol.*, 46: 4546-4552, 2012.
- Liu, C.-N., Awasthi, A., Tsai, C.-J., Collection Efficiency and Interstage Loss of Nanoparticles in Micro-orifice-based Cascade Impactors, *Atmos. Environ.*, 69: 325-333, 2013b.

台灣科學園區周界大氣氣膠特性研究

(蔡仁雄¹, 陳瑞仁^{1,*}, 蔡朋枝², 謝連德¹, 林人杰¹)

1 屏東科技大學環境工程與科學系, 屏東, 91201;

2 中國醫藥大學職業安全與衛生學系, 台中, 40402

摘要: 為瞭解台灣科學園區周界大氣氣膠特性, 本研究於 2012 年春季及夏季於中科后里園區周界之后里聚落(Houli-settlement)、中科后里辦公室(Houli's office of Central Taiwan Science Park)、鯉魚潭淨水廠(Liyutan Water Treatment Plant)及九甲聚落(Jiujia-settlement)等四採樣點以分道採樣器(Dichot)進行大氣懸浮粗、細懸浮微粒採樣, 採得之微粒樣品以離子層析儀分析微粒上水溶性離子成分。初步結果顯示: 春、夏兩季採樣期間四採樣點大氣 $PM_{2.5}$ 及 $PM_{2.5-10}$ 濃度以鯉魚潭淨水廠之測值較高, 九甲聚落及后里聚落之值次之, 而以中科后里辦公室之測值最小; 園區周界大氣懸浮微粒(PM_{10})有近 50~60%是由細微粒($PM_{2.5}$)所提供; 且后里園區大氣 $PM_{2.5}$ 及 $PM_{2.5-10}$ 約一半質量是由水溶性離子組成, 且粗細微粒上之水溶性離子均以 SO_4^{2-} 、 NO_3^- 及 NH_4^+ 等衍生性氣膠為主(佔 80% 以上); 在細微粒($PM_{2.5}$)上以 SO_4^{2-} 之含量最多, 而在粗微粒($PM_{2.5-10}$)上以 NO_3^- 之含量最高。

关键字: 科學園區, $PM_{2.5}$, $PM_{2.5-10}$, 水溶性離子, 衍生性氣膠

兰州地区气溶胶消光特性研究

(曹贤洁 张镭 田鹏飞)

兰州大学半干旱气候变化教育部重点实验室

兰州大学大气科学学院

摘 要：利用 2005 年 9 月-2008 年 7 月微脉冲激光雷达 CE370-2 观测资料，分析了无降水和无沙尘条件下的兰州市气溶胶消光系数和光学厚度的统计特征，如月平均和日平均气溶胶光学厚度的变化特征、日平均气溶胶光学厚度的频数分布特征，以及气溶胶垂直分布的季节变化特征。结果表明：兰州大学半干旱气候与环境观测站（SACOL）综合站和城市站点分别有 87.8%和 78.2%的气溶胶光学厚度小于 0.4，且两者的频数分布特征基本一致；秋冬季的气溶胶光学厚度较春夏偏大，郊区（综合站）的气溶胶光学厚度比市区（城市站）的偏小。从垂直分布而言，气溶胶主要集中在 4km 以下，气溶胶消光系数随高度的增加而减小。1.5km 以下秋冬的气溶胶消光系数较春夏的偏大，1.5km-4km 高度层内则刚好相反。

关键词：消光系数，光学厚度，垂直分布，激光雷达

周边气象条件对南京城区污染颗粒物及气体污染物浓度的影响研究

(常炉予¹ 赵天良² 何金海¹, 汤莉莉³, 于红霞⁴)

1 南京信息工程大学气象灾害省部共建教育部重点实验室, 南京, 210044

2 南京信息工程大学大气物理学院, 南京, 210044

3 江苏省环境监测中心, 南京, 210029

4 江苏省环境保护厅, 南京, 210036

摘 要: 本文将 NCEP/NCAR 6 小时再分析资料作为驱动场, 利用 WRF 模式处理得到时空尺度更为精细的风场资料, 发现青奥会时段 (2010 年 8 月) 南京地区主导风向为海洋吹响大陆的东南风以及来自内陆的西南风。结合南京草场门观测点的污染物浓度资料, 通过相关分析以及合成分析, 得到了该时段南京地区主要污染物 (SO_2 , NO_2 , PM_{10}) 来源的关键输送通道: (1) 来自于南京西南部 (江西、湖南、湖北等地区) 的中远距离输送是对南京地区 SO_2 浓度影响的关键通道; (2) 来自于南京东南方向 (浙江、上海一带) 的近距离输送是对南京地区 NO_2 浓度影响的关键通道; (3) 来自于南京西南部 (湖南一带) 的中远距离输送是对南京地区 PM_{10} 浓度影响的关键通道。

关键词: 南京市, 污染物, 气象条件, 输送通道

土地覆被资料改变及对空气污染模拟影响的初步分析

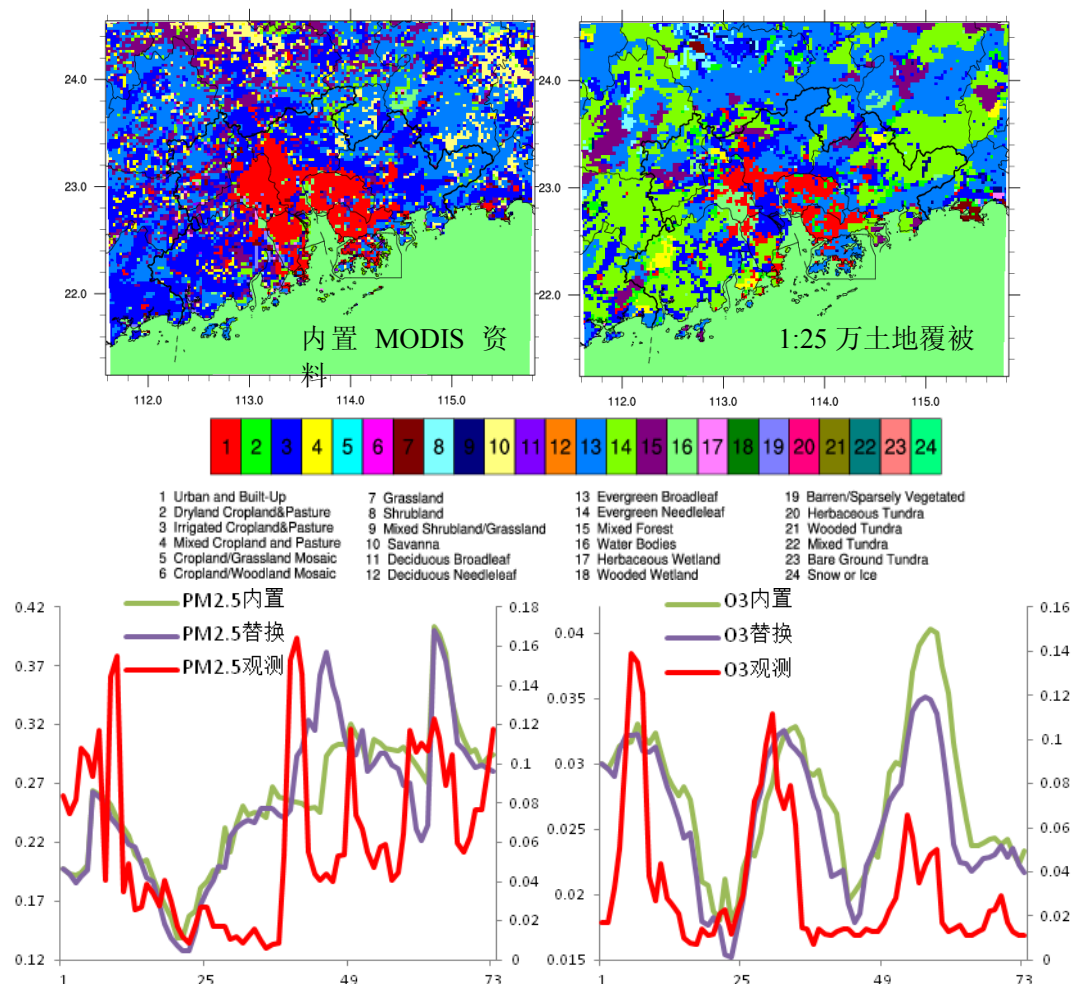
(常鸣 陈伟华 王雪梅*)

中山大学环境科学与工程学院 广州 510275

*Email: eeswxm@sysu.edu.cn

摘要: 土地利用/覆盖类型决定了地表反照率、空气动力粗糙度等参数的取值, 从而影响模式中地表-大气系统的能量、物质和动量交换过程的模拟。采用较为准确和与模拟时间接近的下垫面资料, 是提高区域气象和污染物模拟准确性的有力支持。伴随着城市化的过程, 土地覆被/利用类型发生了很大的转变。然而在 WRF/Chem 模式中, 土地覆被资料的更新往往跟不上土地用途改变的速率, 且珠三角地区与实际覆被有较大不同, 使得模拟的结果在部分区域有所偏差。

本研究基于我国 1:25 万土地覆被资料, 与内置的静态地理资料(Static Geographical Datasets)进行融合, 并与 2008 年 11 月 1 日-4 日广州中山大学站观测的结果对比, 分析了资料更新对数值模拟结果的影响。结果表明: 更为准确的土地利用数据可以明显提高 WRF 模式在城市周边复杂区域对风速的模拟能力, 而由于污染源清单的不确定性, 污染物模拟结果与观测值偏差较大。但从趋势上看, 更新了的土地覆被资料对于广州中山大学站 $PM_{2.5}$ 、 O_3 模拟的趋势相比模式内置的资料与观测结果更为接近。



关键词: WRF/Chem, 土地覆被改变, 数值模拟

CARSNET 气溶胶关键光学特性参数反演研究

(车慧正^{1*}, 夏祥鳌², 张小曳², 王亚强¹, 张晓春³, 孙俊英¹)

¹ 工作单位, 地址, 邮编

1. 中国气象科学研究院, 中关村南大街 46 号, 北京 100081, 中国
2. 中国科学院大气物理研究所, 北京 100029, 中国
3. 中国气象局气象探测中心, 北京 100081, 中国

*Email: chehz@cams.cma.gov.cn

摘 要: 以中国气溶胶地基遥感监测网 (China Aerosol Remote Sensing Network-CARSNET) 北京-CAMS观测数据为个例, 运用Dobvic算法反演分析了气溶胶光学特性, 包括光学厚度、Angstrom波长指数、单次散射反照率、粒子体积谱分布、相函数、粗细模态粒子有效半径等。分析结果表明, 不同仪器之间气溶胶光学特性呈现出很好的一致性, 气溶胶光学厚度较SSA等参数相关性更高; 同时比较CARSNET反演结果与AERONET同步观测结果的差异, 结果表明, 二者之间仍然存在很好一致性, 说明CARSNET反演结果具有较好的精度和可信性, 为今后中国地区气溶胶卫星遥感结果验证、模式模拟、气溶胶气候效应研究都具有重要意义。

关键词: CARSNET; 气溶胶; 光学特性;

Aerosol optical properties over different regions of China measured by CARSNET

Huizheng CHE^{1*}, Xiangao XIA², Xiaoye ZHANG¹, Yaqiang Wang(initial surname)¹, Xiaochun ZHANG³, Junying SUN¹

¹ Chinese Academy of Meteorological Sciences, Beijing 100081, China

² Institute of Atmospheric Physics, Chinese Academy of Sciences, Beijing, China, 100029

³ Meteorological Observation Centre, CMA, Beijing 100081, China

Abstract : Aerosol optical properties such as aerosol optical depth (AOD), Angstrom Exponent, single scattering albedo, volume size distribution, phase function, radius of fine and coarse particles at Beijing have been retrieved by using Cimel sunphotometer measurements of China Aerosol Remote Sensing Network-CARSNET. The results show different aerosol optical properties over different regions of China. Validation of CARSNET's retrieval results has been done comparing with the simultaneous measurements of AERONET ones. There is good consistency between two networks' result, which indicates CARSNET data quality can be assured to be used by satellite validation, modeling input, and aerosol climatology studies.

Keywords: CARSNET, aerosol, optical property

基于 CMB 模型的南京市分级颗粒物来源解析研究

(陈璞珑¹ 王体健^{*1} 胡忻²)

1 南京大学大气科学学院, 南京 210093

2 南京大学现代分析中心, 南京 210093

摘 要: 大气颗粒物现已成为南京首要空气污染物, 利用 CMB 模型研究南京大气颗粒物的来源有重要意义。本文对南京市 2010 年 4 月至 2011 年 5 月鼓楼浦口两个站点分级颗粒物样品和各排放源样品进行浓度和化学成分的特征分析比较, 结合 CMB 模型解析南京市城、郊颗粒物来源, 得到分级颗粒物各类排放源贡献。分析结果表明鼓楼、浦口 PM₁₀ 浓度年均值分别为 $135.8 \pm 66.4 \mu\text{g}/\text{m}^3$ 、 $139.9 \pm 77.3 \mu\text{g}/\text{m}^3$, 最主要的化学成分是 SO_4^{2-} 、 NO_3^- 、Ca、 NH_4^+ 、Cl⁻、Fe、Al、K 等。PM_{2.5} 两个站点浓度年均值分别为 $55.1 \pm 36.3 \mu\text{g}/\text{m}^3$ 、 $71.7 \pm 48.0 \mu\text{g}/\text{m}^3$, 最主要的化学成分是 SO_4^{2-} 、 NO_3^- 、 NH_4^+ 、Cl⁻、K、Fe、Ca、Zn、Na、Al 等。各类排放源分别为煤烟尘、建筑尘、冶炼尘、土壤尘、汽车尾气、二次气溶胶以及海盐。颗粒物来源解析结果表明, 粗粒径颗粒物谱段两个站点贡献最大排放源为建筑尘 (58.9%、47.3%) 和冶炼尘 (14.1%、19.7%); 细粒径颗粒物谱段中两个站点贡献最大排放源为二次无机盐气溶胶 (58.8%、44.2%) 和煤烟尘 (15.9%、39.5%)。

关键词: 颗粒物分级; PM₁₀; PM_{2.5}; CMB 模型; 排放源源谱; 来源解析

珠三角地区细颗粒物质量浓度和化学组分变化趋势

(陈伟华¹, 王雪梅^{1*})

¹ 中山大学环境科学与工程学院, 广东, 广州, 510275

*Email: eeswxm@mail.sysu.edu.cn

摘要: 珠江三角洲 (PRD) 近年来面临着越来越严重的大气污染问题, 其中大气颗粒物污染问题尤为突出。为了解珠三角地区细颗粒物的长期变化趋势, 本文收集 2000-2010 年文献中珠三角地区细颗粒物的相关数据, 总结细颗粒物的质量浓度和化学组分长期变化特征, 及其与污染源排放的关系。结果发现, 2000-2010 年珠三角地区细颗粒物质量浓度先上升后下降, 2004-2005 年浓度最高, 达到 $85\mu\text{g}/\text{m}^3$, 整体呈下降趋势, 从 2000 年的 $49\mu\text{g}/\text{m}^3$ 下降到 2010 年的 $37\mu\text{g}/\text{m}^3$, 11 年的平均质量浓度为 $59.1\mu\text{g}/\text{m}^3$ 。细颗粒物中的含碳物质 OC 和 EC 变化趋势与 $\text{PM}_{2.5}$ 相同, 先上升后下降, 整体呈下降趋势, 2004 年含碳物质质量浓度达到最高值, 分别为 19.4 和 $12.4\mu\text{g}/\text{m}^3$ 。主要是因 2004 年广州市灰霾天数达到 131 天, 为近十年来灰霾天数最多年份, 佛山市 2004 年能见度较其他年份也有所下降, 2004 年珠三角地区空气污染严重, 污染物浓度较高 (黄健, 等, 2008; 陈欢欢, 等, 2010; 陈慧娴, 2011)。分析 $\text{PM}_{2.5}$ 与化学组分的相关性发现, $\text{PM}_{2.5}$ 与 OC、EC 相关性最高, 达到 0.575 和 0.553。细颗粒物中的水溶性离子 SO_4^{2-} 、 NO_3^- 和 NH_4^+ 均呈上升趋势, 分别从 2000 年的 10.2、1.5 和 $2.9\mu\text{g}/\text{m}^3$ 上升到 2010 年的 12.2、6.4、 $5.3\mu\text{g}/\text{m}^3$, 平均质量浓度分别为 12.2、3.4、 $4.3\mu\text{g}/\text{m}^3$ 。由于城市化的发展, 珠三角地区工业烟尘、粉尘的直接排放量虽大幅度减少, 但是 SO_2 和 NO_x 等二次粒子的前体物排放量仍然很大, 且 O_3 浓度不断增加, 大气氧化性增强, 有利于无机二次颗粒物的生成 (Wang et al., 2003; Zhang et al., 2004; Zheng et al., 2010), 珠三角地区细颗粒物的无机二次污染日趋严重。珠三角地区细颗粒物中 SO_4^{2-} 、 NO_3^- 、 NH_4^+ 、OC 和 EC 所占百分比分别为 24%、6%、8%、21% 和 11%, 共占细颗粒物百分达到 70%, 其中 SO_4^{2-} 和 OC 贡献所占百分比最高。珠三角地区 OC/EC 比值主要介于 2-5 之间, 表明珠三角地区二次有机碳的生成比较显著。通过对 PRD 不同功能区的细粒子颗粒物进行分析发现, 道路和工业区细颗粒物质量浓度最高, 可达到 $90\mu\text{g}/\text{m}^3$, 城市和近郊约为 $60\mu\text{g}/\text{m}^3$, 背景点浓度最低为 $38\mu\text{g}/\text{m}^3$ 。水溶性离子 SO_4^{2-} 、 NO_3^- 和含碳物质均为工业区最高, 城市和近郊次之。而 NH_4^+ 为近郊浓度最高, 工业区和道路反而较低, 主要与近郊区的农业活动有关。通过分析水溶性离子与污染源的相关性发现, SO_4^{2-} 与电力消费量达到显著相关 ($\alpha=0.05, R=0.626$), 火力发电燃煤产生的 SO_2 通过化学反应产生 SO_4^{2-} 对于细颗粒物中的 SO_4^{2-} 有重要贡献。 NO_3^- 与机动车保有量 ($\alpha=0.05, R=0.663$)、电力消费 ($\alpha=0.05, R=0.625$) 达到显著相关, 机动车尾气和火电厂排放的 NO_x 通过光化学反应生成的 NO_3^- 是大气中 NO_3^- 的重要来源 (Zheng et al., 2009); NH_4^+ 与农业化肥施用量 ($R=0.699$) 达到显著相关, 说明农业活动排放的 NH_3 对于 NH_4^+ 有重要影响 (Zheng et al., 2012)。总体来说, 珠三角地区细颗粒物二次污染问题突出, 细粒子污染与珠三角地区不断增强的大气氧化性有关外, 与工业、机动车尾气排放有很大关系, 因此改善珠三角地区的细颗粒物污染问题, 控制其前体物的排放是关键因素之一。

关键字: 珠三角, 细颗粒物, 质量浓度, 化学组分, 长期变化

参考文献

- 陈欢欢, 吴兑, 谭浩波, 等. 珠江三角洲 2001-2008 年灰霾天气过程特征分析. 热带气象学报, 2010, 26, (2): 147-155.
黄健, 吴兑, 黄敏辉, 等. 1954-2004 年珠江三角洲大气能见度变化趋势. 应用气象学报, 2008, 19(1).

陈慧娴.近 10 年佛山市大气能见度变化特征及气象因子.广东气象,2011,33(1): 32-34.

Wang T., Ding A.J., Blake D.R., et al. Chemical characterization of the boundary layer outflow of air pollution to Hong Kong during February- April 2001. *Journal of Geophysical Research*, 2003, 108(D20): 8787-8801, doi:10.1029/2002JD003272.

Zhang Y.H., Zhu X.L., Slanina S., et al., Aerosol pollution in some Chinese cities (IUPAC Technical Report) . *Pure and Applied Chemistry*, 2004, 76(6): 1227-1239.

Zheng J.Y., Zhang L.J., Che W.W., et al. A highly resolved temporal and spatial air pollutant emission inventory for the Pearl River Delta region, China and its uncertainty assessment. *Atmospheric Environment*, 2009, 43: 5112-5122.

Zheng J.Y., Yin S.S., Kan D.W., et al. Development and uncertainty analysis of a high-resolution NH₃ emissions inventory and its implications with precipitation over the Pearl River Delta region, China. *Atmospheric Chemistry and Physics*, 2012, 12: 7041-7058.

Zheng J.Y., Zhong L.J., Wang Tao., et al., Ground-level ozone in the Pearl River Delta region: Analysis of data from a recently established regional air quality monitoring network. *Atmospheric Environment*, 2010, 44: 814-823.

基于卫星遥感和地面观测资料分析苏皖两省一次空气污染过程

(陈烨鑫¹, 朱彬¹, 侯雪伟¹, 尹聪¹)

1. 南京信息工程大学大气物理学院, 南京, 210044

摘 要:2012 年 6 月 8-11 日, 江苏安徽两省发生了一次持续性的空气污染过程。本文利用 MODIS 卫星观测的气溶胶产品和地面气象观测资料, 并结合火点监测资料和 HYSPLIT 后向轨迹模式, 分析了苏皖两省该时间段的气溶胶光学厚度(Aerosol Optical Depth, AOD)、细粒子比例(Fine Mode Fraction, FMF)、空气污染指数(Air Pollution Index, API)的特征, 探究了这次空气污染的可能原因。研究表明, 这次过程中苏皖两省 8 个代表城市的能见度绝大部分时间低于 10km, 相对湿度低于 90%, API 均达到污染等级, AOD 也出现显著增长。利用 FMF 资料, 计算出污染期间, 定义的区域细粒子比例(Regional Fine Mode Fraction, RFMF)高达 0.79, 并且污染期间, 高 FMF 出现的概率高达 74.8%, 表明了此次污染事件中污染物以人类活动产生的细粒子为主。此次污染过程中, 苏皖两省天气形势稳定, 不利于污染物扩散。6 月 8-11 日, 在苏皖两省(北部地区为主), 出现大量的火点, 表明有秸秆焚烧现象的存在, 为污染物提供了充足的源。从 HYSPLIT 模式的模拟结果来看, 在污染期间, 苏皖两省 8 个代表城市主要受到偏西方向的气流以及局地气流的影响, 偏西方向的气流有利于外部秸秆焚烧的污染物经过输送影响苏皖两省, 同时本地区自身排放的污染物在局地气流的影响下, 不利于扩散出去, 从而造成污染物积累, 形成污染。

关键词: MODIS, 空气污染, AOD, FMF

Study on a continuous air pollution event in Jiangsu and Anhui provinces on the basis of satellite remote sensing and field observation data

Chen Ye-xin¹, Zhu bin¹, Hou Xue-wei¹, YIN Cong¹ ((School of Atmospheric Physics, Nanjing University of Information Science and Technology, Nanjing 210044)

Abstract: From 8 to 11 June 2012, a serious air pollution event occurred in Jiangsu and Anhui provinces. On the basis of MODIS satellite aerosol production, meteorological data, and fire spot data, using HYSPLIT backward trajectory simulation, the variation features of Aerosol Optical Depth(AOD), Fine Mode Fraction(FMF) and Air Pollution Index(API) was investigated, to inferring the possible causes of the air pollution event. The study indicated that, in Jiangsu and Anhui provinces, during this process, most of time, the visibility was less than 10km, the relative humidity was below 90%, and there was a significant increasing in API and AOD. During the event, the defined Regional Fine Mode Fraction(RFMF) was calculated to get to the value of 0.79, and the ratio of high value of FMF was 74.8%, which meant the major pollutants in air was the aerosol fine particles which was produced by human activities. The atmosphere was stable in Jiangsu and Anhui provinces, providing an inconvenient condition to the diffusion of pollutants. Between Jun.8 to Jun.11, in Jiangsu and Anhui provinces(especially in north area), lots of fire burning spots were detected by MODIS sensor, which suggested that biomass burning had been happened repeatedly and provided an abundant source of pollutants. Backward trajectory analysis indicated that the air mass mainly originated from west, which passed through the region with the air pollutants from biomass burning. In addition, local circulation was not conducive for the diffusion of air pollutants, all of factors led to the air pollution event.

Key words: MODIS, Air pollution, AOD, FMF

台灣大氣中 PM_{2.5} 區域性來源之模擬分析

(陳杜甫、張良輝*)

雲林科技大學環境與安全衛生工程系，台灣

摘 要：近十年來東亞地區經濟及工業快速發展，使得由人、交通及工業所排放的空氣污染物隨之日益增加(Ohara et al., 2007)，使得空氣污染問題也日益嚴重，污染物不僅會對排放源當地空氣品質造成影響，亦會經由長程傳輸亦會使得其他鄰近國家的空氣品質受到影響，對常處於污染物出流處的鄰近國家而言，境外傳輸的影響為當地空氣污染物污染之來源的一個很重要的來源之一(Shimadera et al., 2009; Koo et al., 2008; Wang, 2005)。台灣位於東亞地區，隔著台灣海峽緊鄰中國大陸，因此對台灣大氣中之 PM_{2.5} 而言，除台灣本島排放之影響外，由境外傳輸至台灣的污染物，亦是另一個重要的影響來源。台灣於 2012 年公告了相當嚴格的 PM_{2.5} 空氣品質標準，要達成此空氣品質標準需要針對 PM_{2.5} 影響來源實施適當的管制措施，因此需釐清台灣大氣中 PM_{2.5} 濃度區域性來源之相對重要性。本研究以 MM5/CMAQ 為工具，進行全年三層巢狀網格套疊模擬(如圖 1)，探討 2007 年東亞污染物排放對台灣大氣 PM_{2.5} 之貢獻來源。要釐清台灣大氣中 PM_{2.5} 區域性來源之貢獻比例，需進行四種不同排放案例模擬，包括(A)基準排放案例：考慮區域內台灣與所有東亞其他國家之排放；(B)東亞零排放案例：僅考慮台灣排放，東亞其他國家零排放；(C)台灣零排放案例：僅考慮東亞其它國家排放，台灣零排放；(D)全部零排放案例：區域內台灣與東亞其他國家皆零排放。

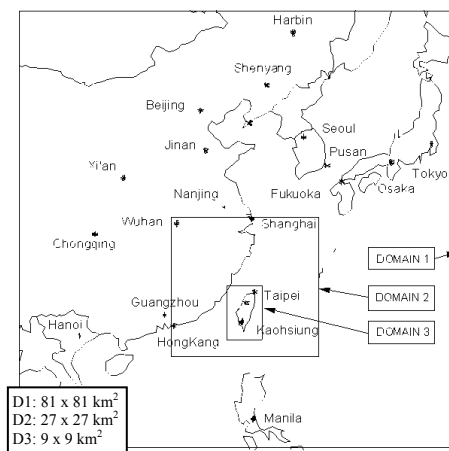


圖 1 三層巢狀網格模式模擬範圍示意圖

研究結果顯示，全年台灣大氣中 PM_{2.5} 區域性來源，台灣本身佔有最高之貢獻比例約為 60%，東亞長程傳輸貢獻約 37% (直接貢獻為 27%，間接貢獻為 9%)，東亞背景貢獻乃為全球排放對東亞區域之整體影響，此影響僅約 3%，如表 1 所示。在表中之季節變化上，夏季台灣 PM_{2.5} 受東亞排放長程傳輸的影響較輕微(僅 14%)，主要受台灣本身排放生成之影響(81%)。在其餘三季節，境外傳送對於台灣 PM_{2.5} 污染均扮演重要角色，東亞長程傳輸貢獻均達 40%，但仍有高達 57%-58%來自台灣本身之貢獻。

東亞長程傳輸之間接貢獻代表境外污染物傳送至台灣與台灣本地污染物之交互作用對台灣 PM_{2.5} 濃度之貢獻，換言之，此間接貢獻乃屬台灣可控制之影響；而直接貢獻則是境外污染物直接傳送至台灣之貢獻，此直接貢獻乃屬台灣不可控制之影響。在衍生 PM_{2.5} 成分(表 2)中，間接貢獻對硝酸鹽與

銨鹽具有較大影響(各別為 36%、24%)，而直接貢獻則是對硫酸鹽有較大影響(57%)。換言之，台灣硫酸鹽不易透過台灣本地污染物排放控制降低長程傳輸之影響，而硝酸鹽與銨鹽之長程傳輸影響，則相當程度可透過台灣本地污染物排放控制降低對台灣 PM_{2.5} 的影響。

表 1 2007 年各季台灣大氣中 PM_{2.5} 區域性來源之貢獻比例(%)

| | 台灣本身 | 東亞長程傳輸 | | 東亞背景 |
|----|------|--------|------|------|
| | | 直接 | 間接 | |
| 春 | 56.9 | 30.1 | 10.2 | 2.8 |
| 夏 | 81.0 | 8.8 | 5.8 | 4.3 |
| 秋 | 57.7 | 29.0 | 9.9 | 3.4 |
| 冬 | 57.5 | 30.5 | 9.8 | 2.3 |
| 全年 | 60.3 | 27.3 | 9.4 | 3.0 |

表 2 2007 年台灣大氣中各類衍生 PM_{2.5} 區域性來源之貢獻比例(%)

| | 台灣本身 | 東亞長程傳輸 | | 東亞背景 |
|-------------------------------|------|--------|------|------|
| | | 直接 | 間接 | |
| SO ₄ ²⁻ | 31.9 | 56.8 | 6.0 | 5.2 |
| NO ₃ ⁻ | 57.5 | 6.9 | 35.6 | 0.0 |
| NH ₄ ⁺ | 43.2 | 32.4 | 24.2 | 0.2 |
| SOA | 73.8 | 10.2 | 16.0 | 0.0 |
| 衍生 PM _{2.5} 合計 | 44.6 | 34.5 | 18.6 | 2.3 |

西安市大气中二次有机气溶胶的季节组成及变化

(成春雷, 王格慧*)

中国科学院地球环境研究所, 黄土与第四纪地质国家重点实验室, 陕西西安 710075

摘 要:二次有机气溶胶是一类重要的大气致霾粒子,为探讨西安市大气二次有机气溶胶的来源和形成机制,本研究以二元羧酸类二次有机气溶胶为对象,分析其组成和来源.本研究采集了西安市 2009 年冬夏季的 PM_{10} 样品,并利用 GC/MS 对样品中二元羧酸进行了化学表征,同时分析了 WSOC, WSIC, OC 及 EC.研究表明二元羧酸中草酸(C_2)浓度最高(冬季: $1162 \pm 570 ng m^{-3}$;夏季: $767 \pm 574 ng m^{-3}$),其次,冬季是对苯二甲酸(tPh)($250 \pm 118 ng m^{-3}$),夏季是邻苯二甲酸(Ph)($103 \pm 50 ng m^{-3}$).这和其他亚洲城市以丁二酸(C_4)浓度居第二位的分布规律不同.在冬季高浓度的 tPh 是因为塑料制品和垃圾焚烧产生,而 Ph 则是因为前体物多环芳烃(PAHs)通过燃煤和机动车尾气大量排放后氧化降解形成.夏季壬二酸(C_9)的含量比冬季高 4 倍,因为植物排放的长链烃类及脂肪酸(C_{18})化合物远多于冬季.WSOC, WSIC, OC 及 EC 的浓度呈现出明显的冬高夏低规律,冬季取暖造成来自燃煤排放源的污染物起主导作用,西安市地理位置不利于污染物扩散,灰霾天气频繁出现.WSOC/OC 比值夏季($78 \pm 16\%$)远高于冬季($56 \pm 15\%$),表明夏季气溶胶水溶性成分比重大,氧化更严重,二次有机气溶胶(SOA)转化的比例更大.二元羧酸(diacids)和酮酸(ketoacids)的相关性夏季好于冬季表明夏季氧化程度更深.本研究分别挑选了冬夏季灰霾天气采集的样品,研究了有机气溶胶和含碳化合物组成及比例的区别.冬夏季灰霾期相比,除 C_2, C_3, C_4, C_9 夏季高,其他组分冬季灰霾期更高.但是灰霾期内 C_2 /diacids, C_3/C_4 , WSOC/OC 都是夏季显著高于冬季.二元羧酸在 WSOC 中的比值(仅计算含碳成分)同样表现出夏季灰霾期高于冬季灰霾期的规律.夏季光化学氧化和液相氧化反应速度更快,一次污染物被氧化后,转化为水溶性的二次污染物;冬季因为温度低,光照时间短,大量一次污染物累积在大气中诱发灰霾形成.通过对二元羧酸类有机气溶胶组成的分析表明冬夏季灰霾的成因不同。

关键词: PM_{10} ; 二元羧酸; 灰霾; 二次有机气溶胶; 光化学氧化

武汉市大气灰霾期 $\text{PM}_{1.0}$ 水溶性组分污染特征研究

(成海容¹, 王祖武^{*1}, 张帆¹, 吕效谱, 刘佳¹, 王新明²)

(1 武汉大学资源与环境科学学院环境工程系, 湖北武汉 430079; 2. 中国科学院广州地球化学研究所有机重点实验室, 广州 510640)

摘 要: 2013 年 1 月, 利用大流量 $\text{PM}_{2.5}$ 采样器采集武汉市大气灰霾天和正常天气细颗粒物 ($\text{PM}_{1.0}$) 样品并对其水溶性离子进行测定。武汉市大气中 $\text{PM}_{1.0}$ 质量浓度平均值为 $117.8 \pm 51.5 \mu\text{g}/\text{m}^3$, 灰霾天气 $\text{PM}_{1.0}$ 以及其重要水溶性离子的质量浓度远高于正常天气。灰霾期间移动源 (机动车) 对 $\text{PM}_{1.0}$ 中水溶性离子组分的贡献比较大, 而正常天气固定源 (工厂) 对 $\text{PM}_{1.0}$ 中水溶性离子的贡献较大。

关键词: 武汉市, 大气, $\text{PM}_{1.0}$, 水溶性离子

东亚季风减弱背景下我国空气质量变化的模拟研究

(程叙耕¹, 赵天良^{1,*}, 徐祥德², Feng Liu³, 韩永翔¹, 车慧正⁴, 何金海¹)

¹ 南京信息工程大学 大气物理学院, 江苏 南京 210044

² 中国气象科学研究院灾害天气国家重点实验室 北京 10081

³ Center for Atmospheric Science, Division of Illinois State Water Survey, Prairie Research Institute, University of Illinois at Urban-Champaign, Champaign, Illinois, USA

⁴ 中国气象科学研究院, 中国气象局大气成分观测与服务中心, 中国气象局大气化学重点开放实验室, 北京 100081

摘 要: 本文采用的全球空气质量模型系统 (GEM-AQ/EC), 设计了一个 10 年 (1995-2004 年) 全球气溶胶气候模拟的敏感性试验, 设定 10 年间模拟中全球人为气溶胶 (硫酸盐, 黑碳和有机碳) 排放源无年际变化, 即取除了气溶胶排放源因素变化对中国区域大气环境的影响, 利用这一途径分离出气象条件对气溶胶浓度影响贡献, 模拟分析出在东亚季风减弱背景下中国区域大气环境的变化。研究结果显示: 夏季季风减弱使黄河以南到华南广大地区地面气溶胶浓度全部呈现上升的趋势, 环渤海湾地区气溶胶浓度下降趋势。环渤海湾地区的气溶胶浓度与风场间的相关关系弱, 而黄河以南地区二者有强反相关关系, 所以季风环流的变化是影响夏季黄河以南区域气溶胶浓度的主要因素, 此外, 与季风风雨带相联系的湿沉降过程亦会影响东部地区气溶胶浓度的分布。冬季, 全国除青藏高原东部、贵州东部和广西以外, 冬季地面气溶胶浓度在 1995-2004 年十年间均呈上升趋势, 同时冬季风有减弱趋势, 气溶胶浓度与风场有反相关关系, 所以大气环流仅是影响冬季中国东部气溶胶浓度因素之一。在研究冬季强弱季风年浓度与干沉降合成差图对比分析发现二者分布类型呈反向一致, 干沉降清除是影响冬季中国中东部地区气溶胶浓度的又一因素。

关键词: 季风减弱, 气溶胶浓度, 空气质量

PM_{2.5} and PM_{10-2.5} chemical composition and source apportionment near a Hong Kong roadway

(Y. Cheng^{a,b,c,*}, S. C. Lee^c, Z. L. Gu^a, K. F. Ho^d, Y. W. Zhang^a, Y. Huang^c, J. C. Chow^{a,b,e}, J. G. Watson^{a,b,e}, J. J. Cao^b, and R. J. Zhang^f)

^a Department of Environmental Science and Technology, School of Human Settlements and Civil Engineering, Xi'an Jiaotong University, No.28 Xianning West Road, Xi'an, Shaanxi, 710049, China

^b State Key Laboratory of Loess Quaternary Geology, Institute of Earth and Environment, CAS, Xi'an, Shaanxi, 710075, China

^c Department of Civil and Structural Engineering, Research Center for Environmental Technology and Management, The Hong Kong Polytechnic University, Hung Hom, Kowloon, Hong Kong

^d School of Public Health and Primary Care, The Chinese University of Hong Kong

^e Division of Atmospheric Sciences, Desert Research Institute, Reno, Nevada, USA

^f Key Laboratory of Regional Climate-Environment Research for Temperate East Asia, Institute of Atmospheric Physics, Chinese Academy of Sciences, Beijing, 100029, China

*Corresponding author. Tel.: 029-83395078

E-mail address: chengyan@mail.xjtu.edu.cn

Abstract: Twenty-four-hour PM_{2.5} and PM₁₀ samples were collected simultaneously at a highly-trafficked roadside station in Hong Kong every sixth day from October 2004 to September 2005. Mass concentrations of PM_{2.5}, PM_{10-2.5} (or PM_{coarse}, defined as PM₁₀ – PM_{2.5}), organic carbon (OC), elemental carbon (EC), water-soluble ions, and up to 25 elements were determined. Investigation on the chemical compositions and potential sources of aerosols shows distinct differences between PM_{2.5} and PM_{10-2.5}. Annual average mass concentration was 55.4±25.5 µg m⁻³ and 25.9±15.5 µg m⁻³ for PM_{2.5} and PM_{10-2.5}, respectively. EC, OM (OM=OC×1.4), and ammonium sulfate (NH₄)₂SO₄ comprised over ~82% of PM_{2.5}, accounting for ~29%, ~27%, and ~25% of the PM_{2.5} mass, respectively. Low OC/EC ratios (less than 1) in PM_{2.5} suggested influence from fresh diesel-engine exhaust. Seven factors were resolved for PM_{2.5} data by Positive Matrix Factorization (PMF) Model, including vehicle emissions (~29%), secondary aerosol (~27%), waste incinerator/biomass burning (~23%), residual oil combustion (~10%), marine aerosol (~6%), industrial exhaust (~4%), and resuspended road dust (~1%). PM_{10-2.5} showed significant difference in chemical composition as compared to PM_{2.5}, with geological material and trace elements being the most abundant components (~28%), followed by unidentified material (~26%), OM(~12%), sea salt (~10%), and ammonium nitrate (NH₄NO₃, ~10%). EC and (NH₄)₂SO₄, the major components (>54%) in PM_{2.5}, each accounted for only ~7% of PM_{10-2.5}. Average OC/EC ratio in PM_{10-2.5} was 7.8±14.2, suggesting the impact from combustion sources other than vehicular exhaust. The sources for PM_{10-2.5} comprised of ~20% vehicle-related resuspended dust (e.g., tire dust/brake linear/petrol evaporation), ~17% local resuspension road dust, ~17% marine aerosol, ~12% secondary aerosol/field burning, ~11% vehicle emissions, and ~23% unidentified material.

Key word: PM_{2.5}, PM_{10-2.5}, roadside monitoring

大气环境对博物馆内文物的影响

(程燕^{1,*}, 郭伟¹, 樊巍巍¹, 张云伟¹, 张仁健²)

1 西安交通大学人居环境与建筑科学学院地球环境科学系, 西安, 710049;

2 中国科学院大气物理研究所, 北京, 10029

*通讯作者: 程燕, 邮箱: chengyan@mail.xjtu.edu.cn

摘 要: 越来越多的国内外研究结果表明, 大气环境问题成为造成文物古迹损害的重要因素^[1]。其中影响最大的是降尘、酸雨、酸性气体和菌类微生物等。根据近年来关于大气环境对博物馆内文物影响的研究文献, 本文主要侧重收集了气溶胶、酸性气体、大气微生物以及温湿度对文物的影响研究文献, 并论述了其对文物的损害机理以及分析研究的方法, 并从大气污染、生物侵害等方面着手, 对博物馆环境的主要影响因素进行分析并提出相应改善对策。现将有关问题作扼要综述。

关键词: 酸性气体, 大气微生物, 温湿度, 馆藏文物

大气及气溶胶中有机氮研究进展

(程玉婷¹ 王格慧¹)

1 中国科学院地球环境研究所, 西安, 710075

摘 要: 有机氮是大气中含氮物质的重要组成部分。近年来世界各地的监测数据都表明有机氮在大气颗粒物、雨水和雾滴中普遍存在。这些有机氮化合物会影响生态系统的营养收支、大气化学过程以及空气质量, 从而对人体健康、能见度和全球气候变化都产生重要影响。通过对国内外文献的总结, 综述了还原态有机氮化合物的来源、分析方法、浓度分布以及环境和健康效应, 最后, 指出了未来对大气中有机氮研究应该加强的方面。

关键字: 气溶胶, 有机氮, 氨基酸, 尿素, 有机胺

江苏省城市灰霾变化趋势

(戴灵慧¹, 田心如², 韩永翔¹, 赵天良¹)

1 南京信息工程大学, 南京, 210000

2 江苏省气象局, 南京, 21000

摘 要: 本文使用江苏省 33 个观测站 1960 至 2010 年观测资料, 分析江苏地区霾的时空分布、气候特征, 并初步探讨霾天气的成因, 结果发现, 江苏有两个霾污染严重区: 苏北的徐州、东海一带, 尤其是 1990 年前; 江苏的西南地区, 尤其是南京; 江苏约 82% 的城市霾日有增加的趋势, 南京霾天增长最为迅速, 增长系数为 4.185, 苏南及徐州等地的增长系数也较大, 苏中霾天增长系数较小, 有的城市还呈负增长。江苏各城市霾天月变化明显, 7、8、9 三月霾天最少, 主要受气象条件影响, 11 月到次年 1 月霾天最多, 6 月和 10 月, 霾天略有增加, 主要受生物质燃烧的影响。

关键词: 江苏, 霾, 秸秆焚烧

Characteristics of atmospheric visibility and its affecting factors in five typical cities across the Taiwan Strait

(Junjun Deng (邓君俊), Ke Du (杜可))

Institute of Urban Environment, Chinese Academy of Sciences, Xiamen 361021, China

(中国科学院城市环境研究所, 厦门, 361021)

Abstract: The rapid industrial development and urbanization has lead to increasing particulate matter pollution over the region across the Taiwan Strait, which has significant impacts on atmospheric visibility degradation. Long-term visibility trends in five typical cities across the Taiwan Strait (i.e., Xiamen and Fuzhou in the Western Taiwan Strait (WTS) region and Taipei, Taichung and Tainan in Taiwan) and its correlation with air quality and meteorological conditions were investigated by using visibility and meteorological data during 1973-2011 and critical air pollutant data during 2009-2011. Average visibilities in the WTS region were better than those in Taiwan for the period 1973-2011, with an average of 16.8, 16.6, 8.5, 10.3 and 9.0 km in Fuzhou, Xiamen, Taipei, Taichung and Tainan, respectively. Decline trends with decreasing rates of -0.5 — -0.1 km/yr existed in all the cities except Taipei, which had an improvement in visibility after 1992. All seasons had decreasing trends during the last 39-year period except in Taipei. The WTS region had the worse change trend comparing with Taiwan. No statistically significant weekend effect in visibility is found over the region. Visibilities were better in summer and autumn, while worse in winter and spring. Correlation analysis revealed the significant negative correlations existed between visibility and NO₂ and particles PM₁₀ and PM_{2.5}; PM_{2.5} played an important role in visibility degradation. High temperature and low pressure is beneficial for better visibility. Principal component analysis further confirmed the impacts of high concentrations of air pollutants and stable synoptic systems with high pressure and low temperature on poor visibility in the region. In addition, case studies highlighted characteristics and potential causes of typical regional low visibility episodes over the region.

Keywords: Atmospheric visibility, Air pollutant, Meteorological parameter, Principal component analysis, Taiwan Strait

广州市大气汞的湿沉降特征及影响因素分析

(邓思欣¹, 王雪梅^{1*}, 董汉英¹, 鲍若峪¹)

¹ 中山大学环境科学与工程学院, 广东, 广州, 510275

*Email: eeswxm@mail.sysu.edu.cn

摘 要: 汞是一种持续性生物累积毒性的化学物质, 能够随着大气沉降进入生态系统, 并且会通过食物链逐级富集, 最终对人类的健康构成严重威胁。大气沉降是陆地和水生生态系统中汞的主要来源, 而大气汞沉降又是以湿沉降为主。本研究采用原子荧光法(方法检出限为 $0.02\mu\text{g}\cdot\text{L}^{-1}$)对广州市(城市下垫面)进行为期三年(2010年1月至2012年12月)的湿沉降化学组分分析。监测项目包括 Hg、Cd、Cu、Zn、Pb、Cr、Ni、K、Na、Mg、Ca 等降水化学组成成分。结果表明, 广州汞湿沉降浓度三年雨量加权平均值为 $0.086\mu\text{g}\cdot\text{L}^{-1}$, 其中 2010~2012 年雨量加权平均浓度分别为 $0.074\mu\text{g}\cdot\text{L}^{-1}$ 、 $0.050\mu\text{g}\cdot\text{L}^{-1}$ 、 $0.131\mu\text{g}\cdot\text{L}^{-1}$ 。湿沉降通量三年平均值为 $119.4\mu\text{g}\cdot\text{m}^{-2}\cdot\text{yr}^{-1}$, 其中 2010~2012 年分别为 $108.2\mu\text{g}\cdot\text{m}^{-2}\cdot\text{yr}^{-1}$ 、 $64.4\mu\text{g}\cdot\text{m}^{-2}\cdot\text{yr}^{-1}$ 、 $185.6\mu\text{g}\cdot\text{m}^{-2}\cdot\text{yr}^{-1}$, 汞湿沉降量是全球汞湿沉降年均沉降通量的($12\sim 25\mu\text{g}\cdot\text{m}^{-2}$)的 4.8~10.0 倍, 处于我国已有监测数据的较高水平(沉降量: $6.1\sim 447.68\mu\text{g}\cdot\text{m}^{-2}$), 降雨量与汞湿沉降量有显著的正相关关系。研究期间汞湿沉降浓度和通量的年际变化较大, 湿沉降汞浓度和沉降量的季节变化一致, 均为: 夏季>春季>秋季>冬季, 大气臭氧浓度的变化和汞沉降的变化特征有明显相似的趋势。通过因子分析发现广州汞湿沉降主要受土壤扬尘、建筑水泥扬尘以及燃煤排放的影响。

关键字: 汞湿沉降, 降雨量, 臭氧浓度, 主成分因子分析

一次严重灰霾过程的气溶胶光学特性垂直分布

(邓涛^{1*}, 吴兑¹, 邓雪娇¹, 谭浩波¹, 李菲¹, 陈欢欢^{1,2})

(1. 中国气象局广州热带海洋气象研究所, 广东 广州 510080; 2. 汕头气象局, 广东 汕头 515000)

摘要: 本文利用激光雷达在广州地区一次严重灰霾过程进行探测, 并反演气溶胶消光系数及退偏比, 分析边界层结构演变对气溶胶消光系数廓线分布的影响。结果表明, 气溶胶主要在 1.5km 以下。发生灰霾天气时, 霾层达到在 1km, 午后可达 1.5km, 发生严重灰霾天气时, 霾层只有 500m。气溶胶消光系数随高度分布在清洁过程呈线性递减, 标高为 1490m, 灰霾过程呈指数递减, 标高为 789.5m。从气溶胶消光系数廓线变化可以很好地反演边界层结构的演变。气溶胶消光系数在残留层顶出现极大值。气溶胶退偏比有明显的日变化, 白天的退偏比比夜间的高, 午后出现峰值。该次过程水云和气溶胶的退偏比小于 0.2, 高云退偏比大于 0.3。本地气溶胶廓线只有在清洁过程时与 elterman 廓线接近。

关键词: 激光雷达, 气溶胶消光系数, 灰霾, 退偏比

The vertical distribution of aerosol optical properties in a serious haze process.

DENG Tao^{1,*}, WU Dui¹, DENG Xue-jiao¹, TAN Hao-bo¹, LI Fei¹, CHEN Huanhuan^{1,2}

(1. Institute of Tropical and Marine Meteorology, Guangzhou, China Meteorological Administration, Guangzhou 510080, China; 2. Shantou Meteorological Bureau, Shantou 515000, China)

Abstract: In this paper, lidar was used to detect a serious haze process in the Guangzhou area. The aerosol extinction coefficient and depolarization ratio were inverses, to analyze the impact of the boundary layer structure evolution to the distribution of aerosol extinction coefficient profile. The results showed that aerosol gathered below 1.5km. In haze day, the haze layer up to 1km, and 1.5km in the afternoon, but only 500m in the severe haze day. The aerosol extinction coefficient decreased linearly with height distribution, and 1490m of the elevation in the cleaning process, but exponentially decreasing and 789.5m of the elevation in the haze process. The evolution of boundary layer could be well inverses from the change of aerosol extinction coefficient profile. There was a maximum value of aerosol extinction coefficient at the top of the residual layer. The aerosol depolarization ratio had obvious diurnal variation, and higher value in daytime than in night, and peak value in the afternoon. In this process, the depolarization ratio of water cloud and aerosol was less than 0.2, the depolarization ratio of high cloud was greater than 0.3. The local aerosol profile was close to the elterman profile only in the cleaning process.

Key words: lidar; aerosol extinction coefficient; haze; depolarization ratio

广州地区 PM₁ 气溶胶、湿度效应与能见度的函数关系

(邓雪娇^{1,2}, 张芷言^{1,2}, 李菲¹, 王宝民², 吴兑¹, 郁建珍³, 卞奇婧³, 谭浩波¹, 邓涛¹)

1 中国气象局广州热带海洋气象研究所, 广州, 510080;

2 中山大学大气科学系, 广州, 510275;

3 香港科技大学, 香港

摘 要: 利用粒子谱、膜采样成分谱分析与能见度等观测资料, 分析广州地区的气溶胶粒子谱、湿度增长函数的变化特征, 并重新构建广州地区的能见度参数化计算函数关系式。连续 7 年 (2005—2012) 观测资料统计表明广州地区的 PM₁ 气溶胶数浓度占总粒子数的 99.8%, 广州地区能见度恶化主要由 PM₁ 气溶胶所引起。分析发现能见度与 PM₁ 在 70%≤RH<80% 区间相关性最高; 通常情况下 RH 为 60~70%, PM₁ 约为 50 μg/m³, 能见度即可低至 10 km; 当 RH 为 80%, PM₁ 仅为 20 μg/m³, 能见度即可低至 10 km; 当 RH>90%, PM₁ 仅为 3 μg/m³, 能见度也可低至 10 km, 说明气溶胶湿度增长对能见度恶化的影响十分明显。广州地区观测资料拟合得到的气溶胶吸湿增长因子与相对湿度之间的关系为: $f(RH) = 0.265(1 - RH/100)^{-1.458} + 0.8$, $f(RH)$ 与 IMPROVE 的湿度增长曲线在相对湿度为 50-80% 之间具有可比性。能见度仪器在高能见度情景下往往高估了能见度测量数值, 在实际应用中, 如把能见度仪观测的高视程资料当作有效样本资料参与重构能见度参数化方案, 将可能显著降低拟合的硫酸盐、硝酸盐、有机质的单位质量比消光系数。广州地区的能见度计算方案初步确定为 $B_{ext} = 2.04 \left([(NH_4)_2SO_4] + [NH_4NO_3] + [NH_4HSO_4] \right) \times f(RH) + 1.82 [SOC \times 1.8 + POC \times 1.4] + 8.28 EC + [soil] + 0.6[CM] + 10$ 其合理性有待进一步评估。

关键字: PM₁, 粒子谱, 湿度效应, 能见度, 广州

一种国内外首创的重量法 $\text{PM}_{2.5}$ 自动监测系统

(董青云、马明杰、杨卫东、李晓旭)

摘 要：本文提出了一种新的环境空气颗粒物 $\text{PM}_{2.5}$ 自动监测方法——重量法自动监测方法。着重介绍了实现这种方法的仪器结构组成、工作原理、数据发布方式以及为提高称量精度而设立的标准化的称量环境。通过仪器的原理和工作过程描述论证了这种方法具有更高的准确性；通过初步监测数据证明这种系统具有良好的稳定性和一致性。作者认为，这种监测 $\text{PM}_{2.5}$ 含量的自动监测方法就是基础验证法的自动化和智能化，或者说是自动化和智能化的基础验证法。它消除了现行的间接监测方法的量值转换误差，是一种更科学、准确的环境空气颗粒物自动监测的方法，具有广阔应用和推广前景。

关键词：直接称量法,可入肺颗粒物, $\text{PM}_{2.5}$

The “Dual-Spot” Aethalometer: real-time source apportionment of fossil fuel vs. biomass combustion aerosols

(G. MOČNIK¹, L. DRINOVEC¹, P. ZOTTER², A.S.H. PRÉVÔT², C. RUCKSTUHL³, J. SCIARE⁴, J.-E. PETIT⁴, R. SARDA ESTEVE⁴, A.D.A. HANSEN^{1,5})

¹ Aerosol d.o.o., SI-1000 Ljubljana, Slovenia; ² Paul Scherrer Institut, CH-5232 Villigen, Switzerland

³ inNET Monitoring AG, CH- 6460 Altdorf, Switzerland

⁴ LSCE CNRS-CEA-IPSL, F-91191 Gif-sur-Yvette, France

⁵ Magee Scientific Corp., Berkeley, CA 94704, USA

Abstract: Filter-based measurements of aerosol optical absorption are widely used to determine Black Carbon (BC) concentrations in real time. Measurements at multiple wavelengths (Sandradewi 2008) can identify the contributions from different combustion sources, separating ‘Black Carbon’ (BC) from ‘Brown Carbon’ (BrC). These methods sometimes show non-linearity due to ‘loading effects’ of increasing aerosol deposit on the filter (Gundel, 1984; Weingartner, 2003; Arnott, 2005; Virkkula, 2007). These effects are highly variable and cannot be treated by static algorithms, either in post-processing of the data or fixed in the instrument firmware. A dynamical and auto-adaptive approach is required, in order to capture the details and variability of the aerosol optical properties and allow for accurate real-time source apportionment.

We have developed a new Aethalometer®, Model AE33, in which two parallel sampling channels collect the aerosol simultaneously at different loading rates. Combining the data from the two parallel analyses eliminates the ‘loading effect’ and yields an accurate measurement of BC together with a dynamical value of the non-linearity parameter which is indicative of aerosol properties. These analyses are performed for multiple optical wavelengths spanning the range from 370 nm to 950 nm and with a time resolution as rapid as 1 second. The results show greatly improved analytical performance for measurement of BC. The instrument is network-ready and is designed for both research and routine monitoring operations.

We present results from the use of this new instrument in urban and rural measurement campaigns in Switzerland, France, Austria, and Slovenia. The data show high sensitivity and time resolution, with a complete absence of loading artifacts. We have developed a real-time application based on a published method (Sandradewi, 2008) for source apportionment to separate contributions of biomass and fossil fuel combustion to ambient aerosols.

The diurnal concentrations of black carbon in Klagenfurt, Austria, show a two peak diurnal pattern: a morning peak associated with traffic and an evening peak which starts as traffic dominated, but then emissions from wood combustion start to dominate (Figure 1). The concentrations of all aerosolized carbonaceous matter (CM) apportioned to fossil fuel combustion (CM_{ff}) inside the city show a distinct enhancement when compared to the background station in the same basin. Wood-smoke, that is the carbonaceous matter apportioned to wood burning (CM_{wb}) shows much smaller variation over the course of the day.

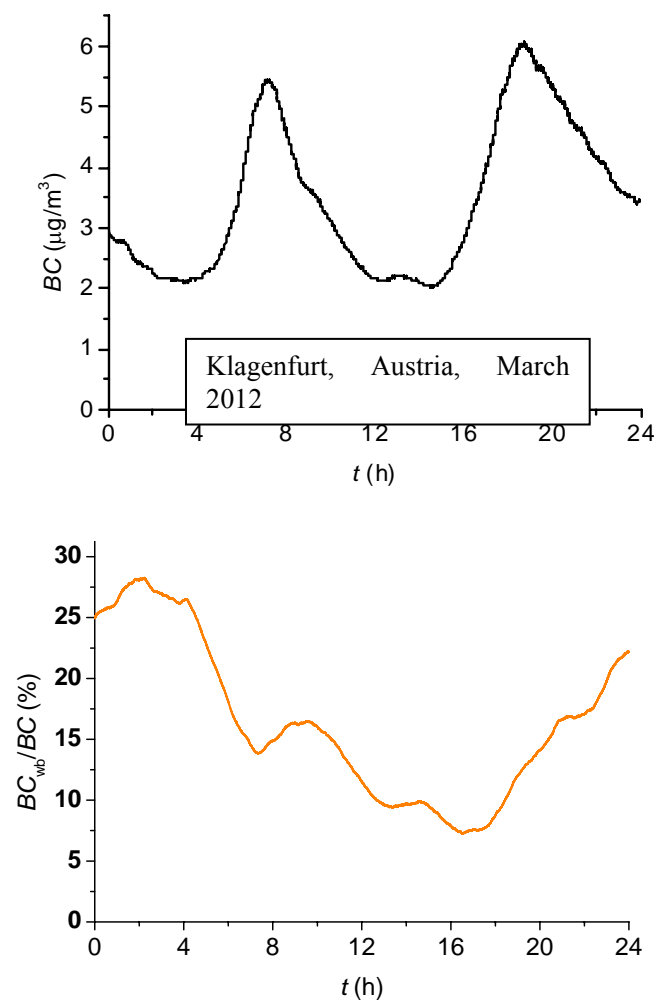


Figure 1. Diurnal variation of BC (top) and the fraction apportioned to wood combustion (bottom).

Keywords: black carbon; source apportionment; optical properties; aerosol absorption.

人为活动对室内空气质量的影响分析

(郭伟, 程燕*, 晁攸闯, 樊巍巍)

西安交通大学 人居环境与建筑工程学院 地球环境科学系, 西安, 710049;

*通讯作者: 程燕, 邮箱: chengyan@mail.xjtu.edu.cn

摘 要: 为了探讨人为活动对导致室内环境空气质量恶化的影响程度, 分析研究不同人为活动对室内颗粒物的贡献, 为人们科学从事室内活动, 提高室内空气质量提供依据。作者于 2012 年 4 月选择西安交通大学兴庆校区五个代表性人为活动点为监测点, 同步实时监测室内颗粒物数浓度和 PM_{2.5} 质量浓度的变化, 并记录人为活动和相关通风信息。采样结果显示不同人为活动产生的颗粒物数浓度和 PM_{2.5} 质量浓度有所差异。其中食堂所测平均数浓度和平均质量浓度分别为 242266 particles·cm⁻³、124.2ug·m⁻³, 远远高于其他室内活动对颗粒物浓度的影响, 其值分别是打印店、图书馆、健身房、宿舍正常观测值平均值的 3.1、1.7 倍, 3.8、4.5 倍, 3.6、1.6 倍, 3.9、1.6 倍。在各项人为活动中, 拖地时产生的颗粒物数浓度和质量浓度最低。人们在进行室内活动时, 特别是烹饪等污染物排放量较高的活动, 应尽量缩短工作时间, 同时加强通风, 降低在高危污染环境中的暴露风险。

关键词: 人为活动, 颗粒物数浓度, PM_{2.5}

The analysis of human activities impact on indoor air quality

Abstract: To investigate air quality deterioration in the indoor environment which human activities cause and analyze the difference they contribute, which may supply the basic data for people engaged in indoor activities scientific and improving indoor air quality. Five representative places in Xi 'an Jiaotong university were selected for monitoring point during April 2012. Number concentration and PM_{2.5} mass concentration changing were monitored at same time and human activities and related ventilation information were recorded. The sampling results show that different human activities caused the different particle number concentration and PM_{2.5} mass concentration. The dining hall particle number average concentration and PM_{2.5} mass average concentration were 242266 particles·cm⁻³ and 124.2 ug·m⁻³, respectively. It's far higher than other indoor activities, expect mop the floor. People should shorten working hours and enhance ventilation to reduce risk during they exposure in high-risk environmental pollution, especially the higher emissions of pollutants activity, such as cooking.

Keywords: human activities; number concentration; PM_{2.5}

中国春季人为和沙尘气溶胶对大气辐射的影响

(韩志伟, 李嘉伟, 夏祥鳌, 张仁健)

中国科学院大气物理研究所, 东亚区域气候-环境重点实验室, 北京 100029

摘 要: 利用区域大气化学/气溶胶-气候耦合模式 RIEMS-Chem 详细研究了 2010 年我国春季气溶胶对大气辐射的影响以及沙尘和人为气溶胶产生的短波、长波和净辐射强迫。2010 年 3 月 19-22 日发生了一次特大沙尘暴, 使我国东部广大地区颗粒物浓度严重超标。

研究发现在这次特大沙尘暴期间, 我国戈壁沙漠地区气溶胶地面短波、长波辐射强迫最大达到 -90 W/m^2 和 $+40 \text{ W/m}^2$ 。月均地面沙尘净辐射强迫在起沙区为 $-9 \sim -24 \text{ W/m}^2$, 在广大的黄河和长江流域为 $-6 \sim -21 \text{ W/m}^2$, 而大陆上大部分地区大气顶的辐射强迫在 $0 \sim +6 \text{ W/m}^2$ 。根据中国东部平均和月平均, 沙尘、人为气溶胶和总气溶胶在地表的净辐射强迫分别为 -8.4 W/m^2 , -10.2 W/m^2 , -18.0 W/m^2 , 在大气顶的辐射强迫分别为 $+1.2 \text{ W/m}^2$, -4.3 W/m^2 , -3.1 W/m^2 , 表明春季沙尘对大气的增暖作用和总体气溶胶的制冷作用。其中京津冀、长三角、珠三角地区总体气溶胶直接辐射强迫分别为 $-21 \sim -27 \text{ Wm}^{-2}$, $-18 \sim -24 \text{ Wm}^{-2}$, $-12 \sim -15 \text{ Wm}^{-2}$, 京津冀地区辐射强迫最强, 这是因为我国北方沙尘气溶胶浓度更高, 对大气辐射的影响也更大。

研究发现沙尘对总体气溶胶地面辐射强迫的贡献可达 42%, 反映了我国春季沙尘气溶胶对辐射的影响具有与人为气溶胶相当的贡献。研究还发现沙尘的半直接效应可以通过减少云量影响大气辐射, 进而间接影响气溶胶辐射强迫。

Characteristics, distribution and source apportionment of polycyclic aromatic hydrocarbons in fine particulate in Nanjing, China

(Jiabao He¹, Shuxian Fan^{1,2}, Fan Zu¹, Qingzi Meng¹, Jian Zhang¹, Yu Sun¹)

1. Department of Atmospheric Physics, Nanjing University of Information Science and Technology, Nanjing 210044, China

2. Key Laboratory for Meteorological Disaster, Ministry of Education, Nanjing University of Information Science and Technology, Nanjing 210044, China

Abstract: A study of 16 EPA priority polycyclic aromatic hydrocarbons (PAHs) associated with particulate matter (PM_{2.1}) in the ambient air in Nanjing was carried out from November 2009 to July 2010. Total PAH concentrations during the sampling period were in the range of 25.91-102.25 ng/m³ (average value: 58.09 ng/m³), with relatively higher values in nighttime rather than daytime. Differing from other studies, PM_{2.1}-bound PAHs were found to be more abundant at suburban site, which was due to the sharp increase in vehicle numbers for recent years in suburban along with the development of urbanization and the unique industrial circumstance around the suburban site. What's more, similarities between the profiles for two sites were identified by using coefficient of divergence, predicting PAHs from the two districts have common sources. Correlation analysis proved the PM_{2.1}-bound PAHs mainly derived from combustion activities and the species of BbF, Chr, Fla, InP, BeP, BghiP, all of which were vehicle markers, dominated the PAH profiles. The average concentrations in four seasons were in the order of winter > spring > autumn > summer, owing to both pollution sources local or external and meteorological factors. Apportioned by Diagnostic ratios and Principal component analyses (PCA), yearly potential sources of PM_{2.1}-bound PAHs in Nanjing were traffic exhaust and coal consumption including coal combustion, coal gas production and coke oven. During autumn, local emission provided a higher level of contribution with the source of wood/biomass burning supplied. However, air masses in spring and winter were relatively aged and influenced more by long range transport. Particulates in summer were diluted by Asian monsoon with much degradation happened.

Key words: Concentration; Polycyclic aromatic hydrocarbons; Correlation; sources

應用 WRF/Chem 模式研析熱帶氣旋對南台灣大氣臭氧濃度流佈與累積現象

(洪崇軒^{1,*}, 羅國誠¹, 袁中新²)

1 高雄第一科技大學環境與安全衛生工程系, 高雄。

2 中山大學環境工程研究所, 高雄。

摘要: 夏季期間本來為南台灣地區的大氣空氣品質, 較佳的季節, 然而當熱帶氣旋(颱風)侵台前, 南台灣空氣污染物濃度有短時間(1-2 日)偏高現象。因此, 基於希望能夠瞭解熱帶氣旋對此區域空氣品質之影響, 本研究旨在嘗試應用新一代的氣象/空品數值模式—WRF/Chem, 模擬研析熱帶氣旋對南台灣大氣臭氧濃度變化的影響, 並解析導致臭氧濃度累積的主要因素。本研究模擬南瑪都颱風侵台前後期間(2011 年 8 月 24-30 日), 南臺灣大氣臭氧濃度變化情形。研究中分析海上颱風警報發布前後 72 小時期間, 臭氧濃度變化的趨勢。模擬結果顯示: 於海上颱風警報發布日之前一日午後, 南台灣林園、大寮等區域臭氧有濃度較高的現象(90 ppb 以上)。由於臭氧為光化反應之二次污染物產物, 太陽輻射強弱與大氣擴散條件, 為影響該濃度高低分佈的主要因素。導致颱風侵台期間, 具有較高臭氧濃度的主要原因, 係因為南台灣地區之盛行風向為北風及西向風, 當颱風環流系統逐漸接近, 其地面風場與高層風場(500 hpa)形成相對高壓氣象場, 導致高雄區域形成局部低壓環流。當熱帶氣旋(颱風)受到導引而逐漸接近台灣南部區域前, 高層大氣燥熱下沉, 白晝雲量稀少, 太陽輻射較強, 導致大氣臭氧濃度的累積。本研究透過 WRF/Chem 光化反應模式, 模擬光化污染物臭氧濃度變化趨勢, 顯示氣象因素為影響此區域大氣空氣品質的重要關鍵因素。

關鍵字: WRF/Chem, 熱帶氣旋, 臭氧, 模式模擬

Continuous observations of water-soluble ions in PM_{2.5} over different seasons in Beijing: Variability, ions formation, and aerosol acidity

(Guoyuan Hu¹, Yangmei Zhang^{2,*}, Junying Sun², Weili Lin³, Yun Yang²)

1. Wuhan University, Wuhan, China
2. Key Laboratory for Atmospheric Chemistry, Chinese Academy of Meteorological Sciences, Beijing, China;
3. Meteorological observation Center, Beijing, China

Abstract : Hourly real-time measurements of water-soluble ions including sulfate, nitrate, ammonium, sodium, calcium et al., in PM_{2.5} were employed at an urban station from June to December in 2009. The average concentrations of total water soluble ions were 44 $\mu\text{g m}^{-3}$, accounting for 38% of PM_{2.5} mass concentration. Monthly characterizations of these water-soluble ions in aerosol and gas phase were summarized. The highest concentration also with highest sulfate is in July, lowest in September and October. SO₂ and NO_x concentration increase while decrease for O₃ in November related with heating emission, low temperature, weak solar radiation. It is concluded that the average SO₂ oxidation ratio (SOR) for the whole campaign is about 63%, with maximum (82%) in August and minimum in November. Both nitrate oxidation ratio (NOR) and the mean mass ratio (in $\mu\text{g}/\text{m}^3$) of NH₃/NH_x (NHR) were much lower than that of SOR, which was 15% in average, maximum in July and minimum in November. The same trend of NOR and NHR suggested that NH_x (NH₃+NH₄⁺) was also influenced by local sources and underwent the same transformation process at the atmosphere. Dramatic diurnal pattern of SO₄²⁻, NO₃⁻ and NH₄⁺ were monitored, but no obvious diurnal cycles for sodium, calcium and potassium were observed. The analysis of the equivalents of cations to anions revealed the existence of the acidic aerosols in PM_{2.5} at the urban site. Most of time, sulfate aerosol exists as NH₄HSO₄, large amount of anthropogenic emission and photo chemically aged result in the acidic aerosol.

Key words: PM_{2.5}, water-soluble aerosol, SOR, NOR, acidic aerosol

西安市 PM_{2.5} 中主要成分的质量浓度和数量浓度对比分析

(胡塔峰¹, 曹军骥^{1,2})

1 中国科学院地球环境研究所黄土与第四纪国家重点实验室, 西安, 710075;

2 西安交通大学全球变化研究院, 西安, 710049

摘 要: 本文于2010年冬季, 采集了不同天气状况下西安市城区的大气PM_{2.5}样品, 并借助配备有能谱的扫描电子显微镜 (SEM-EDX) 对样品进行了单颗粒分析。同时, 借助化学全分析手段获得了PM_{2.5}样品中主要化学组成的质量浓度, 包括水溶性无机离子、元素组成、有机碳(OC)和元素碳(EC)等。颗粒物的数量浓度显示, 样品中烟尘颗粒占绝大多数 (数量浓度介于74.7% ~ 82.7%), 而元素碳组分的质量浓度仅占了PM_{2.5}质量的很小部分 (<8 %)。相比PM_{2.5}样品中地壳来源物质的质量浓度, 单颗粒分析检测到矿物尘和燃煤飞灰颗粒具有较低的数量浓度。因此, 在进行大气气溶胶的精细表征时, 应结合使用气溶胶化学全分析手段和单颗粒分析技术。

关键词: 气溶胶, 化学组成, 单颗粒分析

Effect of NH₃ on the Formation of Indoor Secondary Pollutants from Ozone/Monoterpenes Reactions

(Yu Huang ^a, Shun Cheng Lee ^{a,*} Kin Fai Ho ^b, Jiaping Wang ^a, and Xinyi Niu ^a)

^a Department of Civil and Environmental Engineering,
Research Center for Environmental Technology and Management,
The Hong Kong Polytechnic University, Hung Hom, Hong Kong, China

^bSchool of Public Health and Primary Care, The Chinese University of Hong Kong

*Corresponding author tel.: 00-852-27666011; fax: 00-852-23346389.

E-mail address: ceslee@polyu.edu.hk (Prof. S.C. Lee)

Abstract: D-limonene is one of the dominant terpenoids in indoor environment, which can be emitted from cleaning products and air fresheners. D-limonene is prone to oxidation resulting in the formation of secondary pollutants including secondary organic aerosol (SOA), hydrogen peroxide and organic peroxide which can pose health risks on residents. In this study, we investigated the effect of ammonia (NH₃) on the formation of indoor SOA, hydrogen peroxide and organic peroxide from ozone/d-limonene reactions. The experimental results demonstrated that the presence of NH₃ (maximum concentration is 240 ppb) could significantly enhance the yields of SOA from the ozonolysis of d-limonene, but it had negligible effect on the production of hydrogen peroxide and organic peroxide. The maximum total particle number concentration generated from the oxidation reactions was up to $1.3 \times 10^5 \text{ \#cm}^{-3}$ in the presence of NH₃, while it was $5.7 \times 10^4 \text{ \#cm}^{-3}$ which was 43% lower without NH₃. The total peroxides concentration was approximately 0.9 ppb with and without NH₃ existence. The maximum concentrations of hydrogen peroxide and organic peroxide were 0.7 ppb and 0.2 ppb, respectively. The mechanism regarding to the NH₃ effect on the generation of indoor secondary pollutants from ozone/d-limonene reactions was further discussed.

Keywords: Indoor secondary pollutants; ozonolysis; ammonia effect; hydrogen peroxides and organic peroxides

利用多通道扫描式激光雷达监测大气污染物的 3D 分布

(黄忠伟^{1, 2}, 倪简白², 周天¹)

¹ 兰州大学大气科学学院 半干旱气候变化教育部重点实验室, 甘肃, 兰州 730000

² 台湾中央大学, 台湾, 中坜 32001

摘 要: 随着社会经济的快速发展, 与人类生存和发展密切相关的环境污染和生态恶化已经成为各国政府和公众不可避免的重要问题。大气污染一方面严重影响人们的生活品质, 另一方面通过改变大气辐射水平影响辐射收支平衡, 从而影响到区域乃至全球的气候。因此, 治理环境污染与遏制生态恶化已成为人类二十一世纪刻不容缓的责任和使命。

作为先进的主动遥感技术, 激光雷达具有以高时空分辨率对大范围的大气污染进行实时、快速、连续、长期的遥感监测等优势。它不仅可以对污染物的时空分布及其扩散进行跟踪监测, 而且能够对污染物的相对浓度进行很好的反演。早在 1997 年国际上就有学者开始利用激光雷达对大气污染物进行探测; 我国相关单位也在北京奥运会期间利用激光雷达为空气质量保障提供了及时准确的预测和风险评估数据。因此, 由于激光雷达技术具有的独特优势, 逐渐成为近年来大气遥感和环境监测的主要手段之一。

台湾中央大学近几年来在利用激光雷达监测大气污染物 3D 分布方面已经开展了许多工作。已开发的激光雷达系统具有可立体扫描、多通道、低成本等特点, 本文将从系统的设计思路、主要功能、系统的优势、数据结果分析、下一步工作计划等几个方面介绍主要的最新研究进展。

关键词: 激光雷达, 立体扫描, 大气污染物, 3D 分布

評估堆肥場生物危害特性

(黃筱茜¹、楊心豪^{1*}、王嗣涵²、洪柏宸³、羅金翔²)

1 稻江科技暨管理學院通識教育中心、臺灣

2 弘光科技大學環境工程研究所、臺灣

3 勞工安全研究所、臺灣

摘 要：堆肥作業其環境具有侷限性，且內部具有土壤及廢棄物等各類型微生物來源，可能包括了細菌、真菌及病毒等。本研究之目標主要建立我國堆肥作業設施之生物氣膠種類與濃度分佈、內毒素與真菌毒素特性及堆肥作業環境背景資料庫，本研究選定台中市及南投縣各一個廚餘類堆肥作業環境與屏東縣及嘉義縣各一個農業廢棄物類堆肥作業環境進行調查。生物氣膠對人體之危害則包括過敏性疾病、感染性疾病及中毒等。可能之感染性疾病，例如退伍軍人症、肺結核病等；過敏性疾病，例如氣喘、過敏性肺炎及鼻炎等，另一部份則是革蘭氏陰性細菌之內毒素和真菌所產生之真菌毒素均可能造成人類呼吸道之健康症狀與衛生問題，因此本計畫即針對堆肥作業環境之生物氣膠中之內毒素與真菌毒素進行調查。在各類的堆肥作業場所中，利用個人採樣幫浦配合濾紙針對內毒素的調查結果顯示，內毒素濃度在 45-724 EU/m³。內毒素濃度最高區域則是在堆肥成品包裝區，黃麴毒素濃度在 0.141-315.65 ng/m³。黃麴毒素濃度最高區域則是在堆肥成品包裝區，赭麴毒素濃度在 0.076-163.14 ng/m³。赭麴毒素濃度最高區域則是在堆肥成品包裝區。

關鍵字：生物氣膠、內毒素、真菌毒素

抗菌沸石去除室內空氣中生物性氣膠之研究

(黃于珊¹, 謝祝欽¹, 翁郁絮¹)

¹ 雲林科技大學環境與安全衛生工程系(所), 台灣

摘要：醫療院所室內空氣品質 (Indoor air quality, IAQ) 中超標的細菌及真菌等生物性氣膠 (Bioaerosol) 的問題已受到關注，為改善其問題，本文發表研製抗菌觸媒材料，可有效控制 IAQ 中 Bioaerosol 問題。本研究依結構分別發展顆粒狀及蜂巢狀沸石 (Zeolite) 為載體，含浸抗菌劑 (銀及碘) 以改質抗菌材料，並組裝抗菌設備應用於醫療院所內。抗菌材料並進行微結構特性分析包括：SEM、EDS、XRD、TGA 等。五種抗菌材料經八小時連續測試評估其抗菌效能，結果顯示顆粒狀與蜂巢狀結構對細菌皆有良好的抗菌效果，真菌部分以顆粒狀為優，推測與菌種本身繁殖方式及其構造不同所致。抗細菌率以蜂巢銀沸石 618 ± 111 (CFU/g-hr) 為佳，其次為蜂巢碘沸石 598 ± 90 (CFU/g-hr)，而抗真菌率中以顆粒銀沸石及碘沸石較佳分別為 715 ± 148 (CFU/g-hr) 及 550 ± 123 (CFU/g-hr)。測試結果顯示銀及碘皆有良好的抗菌效能，其中以銀為佳。另經兩個月長效性抗菌效能測試，得知長期抗細菌率為 336 ± 180 (CFU/g-hr)、抗真菌率為 623 ± 389 (CFU/g-hr)，本研究顯示研製抗菌材料具有良好的長效性能，可有效應用於控制醫療院所室內空氣中 Bioaerosol 問題。

关键字：多孔性材料，蜂巢狀，抗菌劑

应用颗粒物化学组分监测仪 (ACSM) 实时快速在线测定致霾细粒子化学组分和有机组分

(江琪^{1,2}, 孙业乐^{2*}, 王自发², 银燕¹, 王飞³)

¹南京信息工程大学, 中国气象局气溶胶与云降水重点开放实验室, 江苏南京, 210044;

²中国科学院大气物理研究所, 大气边界层物理与大气化学国家重点实验室, 北京 100029

³中国气象科学研究院, 北京 100081

摘要:灰霾频频袭击北京在内的我国广大中东部地区, 不仅造成大范围的空气污染, 还严重危害人体健康。灰霾的形成与细颗粒物化学组分密切相关。本文详细报道了颗粒物化学组分监测仪 (ACSM) 在表征致霾细粒子化学组分, 包括有机物、硫酸盐、硝酸盐、铵盐和氯化物, 以及快速估算大气一次和二次有机组分中的应用。通过对 2012 年 9 月亚微米细颗粒物 (PM₁) 观测研究发现, 北京秋季灰霾重污染天和清洁天的化学组分存在显著差异。有机物是 PM₁ 的主要化学组分, 在清洁天平均贡献 PM₁ 的 70%, 而在重霾污染天, 二次无机组分贡献量则显著增加, 超过 50%。

关键词:长江三角洲, 灰霾, 干消光系数, 能见度, API

Applying Aerosol Chemical Speciation Monitor (ACSM) real-time online fast monitoring of the Chemical and organic Composition of inducing haze fine particles

Jiang qi^{1,2}, Sun yele^{2*}, Wang zifa², Yin yan¹, Wang fei³

¹Key Laboratory for Aerosol-Cloud-Precipitation of China Meteorological Administration, Nanjing University of Information Science & Technology, Nanjing 210044, China

²State Key Laboratory of Atmospheric Boundary Layer Physics and Atmospheric Chemistry, Institute of Atmospheric Physics, Chinese Academy of Sciences, Beijing 100029, China

³Chinese academy of meteorological sciences, Beijing 100081, China

Abstract: The haze attacked our country in the vast areas of eastern region including Beijing frequently, not only resulted in a wide range of air pollution, but also seriously harm to human health. The haze formation is closely related to the chemical composition of fine particulate matter. This paper reports the application of Aerosol Chemical Speciation Monitor (ACSM) in characterization of induced haze chemical composition of fine particles including organic matter, sulfate, nitrate, ammonium, chloride and rapidly estimating of atmospheric primary and secondary organic components in detail. The observational studies of submicron aerosol species (PM₁) in September, 2012 have found that the chemical composition of the haze heavy pollution days and the cleaning days exhibiting significant differences. The organic is the main chemical component of the PM₁, the average contribution to PM₁ is ~70% in Cleaning days, but in heavy haze pollution days, the contribution of secondary inorganic species increasing significantly, more than 50%.

Observation and Analysis of Optical Properties of Atmospheric Aerosols in Beijing Urban Area

(Jing Junshan^{1,2}, Zhang Renjian¹, Che Huizheng³, Wu Yunfei¹, Xia Xiangao⁴, Yan Peng⁵, Zhao Deming¹)

¹ Key Laboratory of Regional Climate-Environment Research for Temperate East Asia, Institute of Atmospheric Physics, Chinese Academy of Sciences, Beijing

² University of Chinese Academy of Sciences, Beijing

³ Key Laboratory of Atmospheric Chemistry, Centre for Atmosphere Watch and Services, Chinese Academy of Meteorological Sciences, China

⁴ LAGEO, Institute of Atmospheric Physics, Chinese Academy of Sciences, Beijing

⁵ Meteorological Observation Center of CMA, Beijing

Abstract: One year (from June 2009 to May 2010) measurements of PM_{2.5}, aerosol absorption coefficient and scattering coefficient were analysed at an urban site in Beijing. Annual averages of PM_{2.5}, absorption coefficient, scattering coefficient, single scattering albedo, mass absorption efficiency and scattering efficiency were $67.39 \pm 66.23 \mu\text{g m}^{-3}$, $63.73 \pm 62.06 \text{ Mm}^{-1}$ and $360.45 \pm 404.96 \text{ Mm}^{-1}$, 0.82, 0.78 m² g⁻¹ and 5.55 m² g⁻¹, respectively. With maximum during the night and minimum in the afternoon, absorption coefficient and scattering coefficient showed the same diurnal characteristics while SSA displayed contrary tendency. Wind reduced the impact of the aerosol optical properties on atmospheric visibility, but sometimes airflow derived from the southeast of Beijing could cause absorption coefficient and scattering coefficient increase in the summer and autumn. It was the accumulation of pollutants that resulting in the rise of absorption coefficient and scattering coefficient and the visibility deterioration in summer, autumn and winter while in spring, the airflows from the dust sources elevated the particulate concentrations several times, but had limited effect on absorption coefficient and scattering coefficient. The frequencies of haze in autumn was higher than other seasons and visibility exponentially decayed with increasing PM_{2.5} concentration, which should be controlled lower than $64 \mu\text{g m}^{-3}$ to preserve the visibility more than 10 km.

Keywords: Aerosol absorption coefficient, Aerosol scattering coefficient, Haze

Gas-particle Concentrations and Distribution of Polycyclic Aromatic Hydrocarbon at Tropical Region of Southern Taiwan

多環芳香烴在台灣南部熱帶地區空氣氣態-顆粒態之濃度及分布

FUNG-CHI KO^{1, 2}, JING-O CHENG^{1, 3}, CHON-LIN LEE

(柯風溪, 鄭金娥, 李宗霖)

¹ National Museum of Marine Biology and Aquarium, Pingtung, Taiwan

² Institute of Marine Biodiversity and Evolutionary Biology, National Dong-Hwa University, Pingtung, Taiwan

³ Department of Marine Environment and Engineering, National Sun Yat-Sen University, Kaohsiung, Taiwan

Abstract: The atmospheric concentrations and gas-particle partitioning of polycyclic aromatic hydrocarbons (PAHs) were determined in the tropical region of southern Taiwan. The concentrations of total suspended particulates (TSP) and total PAH (t-PAH; gas+particulate) ranged from 1.6 to 78.8 $\mu\text{g m}^{-3}$ and 400 to 4400 pg m^{-3} , respectively. A seasonal variability in t-PAH concentrations was observed, with the highest levels of particle-associated PAHs found in winter/cold season. Diagnostic ratios showed that PAHs in the atmosphere predominantly come from vehicle emissions and biomass burning. The result of principal component analysis (PCA) indicated that due to long-range transport, PAHs in the southern Taiwan may originate from neighboring areas, such as the Kaohsiung metropolis during wintertime. In all samples, gas-particle partition coefficients (K_p) of PAHs correlated with sub-cooled liquid vapor pressures (P_L^0) and octanol-air partition coefficients (K_{oa}). The regression slopes of $\log K_p$ versus $\log P_L^0$ of all the sample were greater than -0.6, which was shallower than other studies conducted in temperate and subtropical zones, and reflected a non-exchangeable PAH fraction in the aerosols, likely associated to the soot carbon phase. This phenomenon might be caused by the significant photolysis of gaseous PAHs by light intensity in tropic southern Taiwan and the slow depuration of particulate phase. Experimental gas-particle partition coefficients (K_p) were compared to the predictions of octanol-air (K_{oa}) and soot-air (K_{sa}) partition coefficient models, showing that both K_{oa} and K_{sa} models underestimated the K_p values in this study. The preliminary observation of gas-particle partitioning of PAHs indicates the presence of a strong absorbent in the atmospheric aerosol, most likely soot carbon, in the tropic southern Taiwan.

Keywords: PAHs, tropical area, gas-particle partitioning, soot carbon

Similarities and diversities of PM_{2.5}, PM₁₀ and TSP profiles for fugitive dust in a coastal oilfield city, China

(Shaofei Kong¹, Yaqin Ji², Bing Lu², Xueyan Zhao², Zhipeng Bai^{2, 3*})

1. Key Laboratory for Aerosol-Cloud-Precipitation of China Meteorological Administration, Nanjing University of Information Science and Technology, Ningliu Road 219, Nanjing, China

2. College of Environmental Science and Engineering, Nankai University, Weijin Road 94 #, Tianjin, China;

3. Chinese Research Academy of Environmental Sciences, Beijing, 100012, China

Abstract: PM_{2.5}, PM₁₀ and TSP source profiles for road dust, soil dust and re-suspended dust were established by adopting a re-suspension chamber in a coastal oilfield city-Dongying in 11/2009-4/2010. Thirty-nine elements, nine ions, organic and elemental carbon were analyzed by multiple methods. Results indicated that Ca, Si, OC, Ca²⁺, Al, Fe and SO₄²⁻ were the most abundant species for all the three types of dust within the three fractions. OC/TC ratios were highest for dusts in Dongying when compared with literatures which may be related to the large amounts of oil exploited and consumed. Na, Mg and Na⁺ in soil and road dust from Dongying also exhibited higher mass percentages than others indicating the influence of sea salt as the city was more adjacent to coastal line. Enrichment factors analysis showed that Cd, Ca, Cu, Zn, Ba, Ni, Pb, Cr, Mg and As were enriched and these elements were tended to concentrate in finer fraction. Similarities of the profiles for different size fractions and different types of dust were compared by coefficient of divergence (CD). The profiles for different types of dust were different to each other with the CD values mostly higher than 0.30; while the profiles for different size fractions of each dust were similar to each other with the CD values mostly lower or near to 0.30.

Keyword: Source profile, fugitive dust, size-differentiated, particle, oilfield city

固定源排放 PM₁₀ 和 PM_{2.5} 无机组分特征研究

(孔少飞^{1,2}, 姬亚芹², 李志勇², 白志鹏^{2,3*})

1. 中国气象局气溶胶与云降水重点开放实验室/南京信息工程大学大气物理学院, 南京, 210044

2. 南开大学环境科学与工程学院, 天津, 300071

3. 中国环境科学研究院, 北京, 100012

摘要: 受体模型判断颗粒物来源的基础在于对各种可能的大气污染源排放颗粒物的化学组成或物理特征有详尽的了解。当前国内源排放颗粒物成分谱资料缺乏且陈旧, 源特征标识组分等相关信息匮乏, 尤其是受采样条件的限制, 现有的燃烧源排放颗粒物成分谱大多不能代表其真实排放。本研究采用稀释通道采样法采集了济南和东营 6 类 11 个固定源点位排放 PM₁₀ 和 PM_{2.5} 样品, 分析了其中 39 种元素、9 种离子、元素碳 (EC) 和有机碳 (OC) 组分, 获得了其组分浓度、百分含量、标识组分、特征元素比值, 讨论了成分谱的相似性; 并结合现场实测和资料搜集, 建立了 PM₁₀ 和 PM_{2.5} 上受关注化学组分的排放因子。结果表明, 不同类型固定源排放 PM_{2.5} 和 PM₁₀ 的质量浓度变化范围分别为 8.2-79.4 mg/m³ 和 23.3-156.7 mg/m³。浓度较高的几种组分为 Al、Ca、Fe、Si、NO₃⁻、SO₄²⁻、OC 和 EC。

本次实验所得不同类型固定燃烧源排放 PM_{2.5} 和 PM₁₀ 中阴阳离子的当量浓度比值变化范围分别为 0.90-2.84 和 0.49-2.76, 表明大多数固定燃烧源排放出的颗粒为酸性, 仅水泥窑炉排放颗粒中该比值小于 1, 尤其是粗颗粒上该值仅为 0.49, 由此表明水泥窑炉排放出的颗粒物为碱性。电厂、工业锅炉、烧结机、焦炉等固定源排放出的颗粒越细, 酸性越高。固定燃烧源排放 PM_{2.5} 和 PM₁₀ 中 NO₃⁻/SO₄²⁻ 比值变化范围分别为 0.03-0.66 和 0.14-0.85, 所有状况下该比值均小于 1。不同类型固定燃烧源排放 PM_{2.5} 和 PM₁₀ 中 OC/EC 比值的变化范围分别为 2.5-13.1 和 1.1-17.2。两种粒径颗粒中 OC/EC 的值表现出一致的变化规律, 即供暖锅炉>燃煤电厂>水泥窑炉>焦炉>工业锅炉>烧结机, 从有机碳气溶胶控制的角度考虑, 应按照上述顺序有所侧重。而从控制黑碳气溶胶的角度, 则应按相反的顺序优先考虑。不同类型固定燃烧源排放 PM_{2.5} 中 Cu/Sb、As/V、Ni/V、Zn/Pb 和 Zn/Cd 的比值变化范围分别为 15.6-182.3、0.4-8.1、2.3-7.6、2.0-4.6 和 159-6927, PM₁₀ 中 Cu/Sb、As/V、Ni/V、Zn/Pb 和 Zn/Cd 的变化范围分别为 11.2-71.6、0.4-2.3、0.4-5.5、1.9-5.2 和 160-2643。成分谱中含量丰富的物种为 SO₄²⁻、OC、EC、NO₃⁻、NH₄⁺、Al、Si 和 Ca, 其在 PM_{2.5} 中的百分含量范围分别为 4.79%-30.31%、1.71%-11.15%、0.32%-4.18%、0.36%-5.14%、0.11%-3.81%、1.07%-6.65%、3.31%-10.48% 和 0.90%-7.28%; 在 PM₁₀ 中的百分含量范围分别为 6.55%-27.39%、8.09%-11.43%、0.40%-7.37%、2.56%-6.07%、0.72%-4.36%、2.20%-5.71%、4.98%-13.01% 和 1.11%-5.34%。

对于固定源排放 PM_{2.5} 成分谱而言, 除水泥窑炉和工业锅炉两者的成分谱存在相似性外, 其余各种组合分歧系数均高于 0.30, 表明存在较大的差异。供暖锅炉排放细颗粒物与其余五种固定源排放颗粒物的分歧系数大于 0.50, 表明该种类型锅炉排放细颗粒物与其他几种固定源排放细颗粒存在显著的差异。对于固定源排放 PM₁₀ 成分谱而言, 大部分组合的分歧系数值高于 0.3, 但总得来看, 每种组合的分歧系数值比相应的细颗粒分歧系数值要低, 表明不同类型固定源排放颗粒物的差异主要体现在细颗粒上。

本研究建立了固定源排放 PM₁₀ 和 PM_{2.5} 中 OC、EC、10 种重金属 (V、Cr、Mn、Co、Ni、Cu、Zn、As、Cd 和 Pb) 和离子组分的排放因子。得出结论认为我国固定燃煤源排放 PM₁₀ 和 PM_{2.5} 及其上载带的化学组分排放因子由于除尘方式、除尘效率、锅炉类型和负荷、燃料组成等因素影响差异较大。因而, 基于稀释通道采样的固定源排放颗粒物中化学组分排放因子库需不断更新和完善。

关键字：固定源，稀释通道，PM₁₀，PM_{2.5}，成分谱，排放因子

台灣中南部地區大氣垂直剖面臭氧濃度及光化指標特性之調查

(賴進興¹, 吳義林², 林清和¹, 葉淑杏³, 葉旗福⁴)

¹ 輔英科技大學環境工程與科學系, 高雄;

² 成功大學環境工程學系, 台南;

³ 輔英科技大學休閒與遊憩事業管理系, 高雄;

⁴ 中山大學海洋環境工程學系, 高雄

摘 要：本研究針對台灣中南部區域選擇具代表性之觀測地點，規劃春秋兩季進行實場密集之調查，調查項目包括大氣垂直剖面空氣污染物臭氧濃度之量測及光化指標物種特性之量測，探討觀測區域境內之污染物濃度與形成原因。研究結果發現：觀測區域受來自西北方之污染相當顯著，而臭氧逐時濃度出現峰值春秋兩季有不同之現象，春季常有雙峰現象，秋季主要以單峰狀態為主，顯示光化反應為秋季臭氧之主要來源，與春季觀測則有傳輸造成現象不同。垂直剖面臭氧濃度之量測結果，海風層對於近地面臭氧濃度影響相當明顯，層內濃度約為 80 ppb，但層外可達 140 ppb；且於春季觀測時夜間與清晨皆可發現受到點源排放 NO_x 的影響，有臭氧消耗之現象。另外，光化採樣分析結果顯示：NO₂ 光解係數 (J_{NO_2}) 秋季最大值為 4.8×10^{-3} (1/s)，此區域於秋季光化反應比春季更為強烈，使得臭氧形成多以光化反應為主。H₂O₂ 量測結果顯示：秋季明顯高於春季，且當區域性臭氧污染較為嚴重時，同時可以發現夜間濃度大都在 2~3 ppb；再由光化指標分析結果顯示：春季主要為 VOCs-limited，而秋季則為 NO_x-limited，顯示在台灣中南部區域之臭氧管制策略，應依季節考量 NO_x 與 VOCs 之控制。

關鍵字：臭氧，光解係數，光化反應，垂直剖面，VOCs

Aqueous-phase photochemical oxidation and direct photolysis of vanillin as a model compound of methoxy-phenols from biomass burning

(Yong Jie LI^{1, #}, Heidi H.Y. CHEUNG¹, Dan Dan HUANG², Wei Hong FAN³, Liya E. YU³, and Chak K. CHAN^{1, 2, *})

¹Division of Environment, Hong Kong University of Science and Technology, Clear Water Bay, Hong Kong

²Dept. Chem. & Biomole. Eng., Hong Kong University of Science and Technology, Clear Water Bay, Hong Kong

³Division of Environmental Science and Engineering, National University of Singapore, Singapore

Keywords: aqueous-phase, SOA, vanillin, biomass.

[#]Presenting author email: lakeli@ust.hk; ^{*}Corresponding author email: keckchan@ust.hk

Abstract: Aqueous-phase reactions of organic compounds are an important source of secondary organic aerosol (SOA) (Ervens 2011). Laboratory studies focused mostly on small aldehydes such as glyoxal (De Haan 2009; Tan 2009) as precursors, and on pinene oxidation products (Lee 2011).

We showed experimental results of aqueous-phase reactions of a semi-volatile and slightly water soluble methoxy-phenol from biomass burning, vanillin (C₈H₈O₃). Reactions were performed in a vessel (Lee 2011) with UV (254 nm) irradiation under two conditions: (1) photochemical oxidation with H₂O₂ as an OH radical source; and (2) direct photolysis without H₂O₂ added. Solution of the resulted products, as well as the ammonium sulfate added (Lee 2011), was atomized continuously and dried before on-line analyses. An Aerodyne High-resolution Time-of-Flight Aerosol Mass Spectrometer (HR-ToF-AMS) was used to measure the dried particle compositions, and a Hygroscopic Tandem Differential Mobility Analyzer (HTDMA) and a Cloud Condensation Nuclei counter (CCNc) were used to determine the particle growth factor and CCN activity respectively.

Without UV irradiation, most of vanillin evaporated to the gas phase during drying and gave negligible organic mass in particles (Figure 1, before time < 0 min). A large amount of SOA was formed and retained after reactions under both conditions, although products might be different under these two conditions according to HR-ToF-AMS characterization (Figure 1). Off-line analyses by liquid chromatography-mass spectrometry (LC-MS) and gas chromatography-mass spectrometry (GC-MS) also confirmed that the product identities from these two conditions are different. Organic mass first increased rapidly and then decreased under condition (1), but kept increasing slowly under condition (2), as shown in Figure 1A and 1C, respectively. It was found that the degree of oxygenation of products from condition (1) first increased and then decreased, suggesting a competition between functionalization and fragmentation (Kroll 2009; Lee 2011), while it kept decreasing under condition (2). Hygroscopic behavior and CCN activity of ammonium sulfate decreased substantially with the organic products retained in the particles. The resolved growth factor of organics correlated with the increase of degree of oxygenation (O:C ratio) of organics formed.

Our results suggest that aqueous-phase reactions of methoxy-phenolic compounds from biomass burning can retain this portion of carbon mass in the particle phase even after extensive drying/dilution processes. This portion of carbon mass, once retained, significantly alters the particle hygroscopicity and CCN activity.

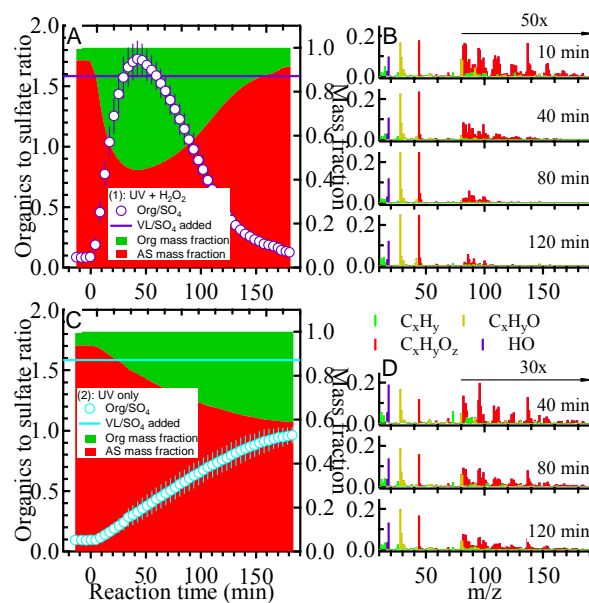


Figure 1. Changes of organic to sulfate ratio, organic mass fraction, and mass spectral feature during reactions under conditions (1) (A and B) and (2) (C and D).

This work was supported by the Research Grants Council (610909), the University Grants Committee (SEG-HKUST07) and the Environmental Conservation Funds (ECF) of Hong Kong (ECWW09EG04).

De Haan, Corrigan, Smith, Stroik, Turley, Lee, Tolbert, Jimenez, Cordova, and Ferrell, *Environ. Sci. Technol.*, 43, 2818-2824, 2009.

Ervens, Turpin, and Weber, *Atmos. Chem. Phys.*, 11, 11069-11102, 2011.

Kroll, Smith, Che, Kessler, Worsnop, and Wilson, *Phys. Chem. Chem. Phys.*, 11, 8005-8014, 2009.

Lee, Herckes, Leaitch, Macdonald, and Abbatt, *Geophys. Res. Lett.*, 38, L11805, doi: 11810.11029/12011gl047439, 2011.

Tan, Perri, Seitzinger, and Turpin, *Environ. Sci. Technol.*, 43, 8105-8112, 2009.

Aerosol radiative effects on the meteorology and concentrations of pollutants in Mega-Cities

(Guohui Li^{1,2}, Naifang Bei^{3,2}, and Luisa T. Molina²)

¹*Institute of Earth Environment, Chinese Academy of Sciences, Xi'an, China*

²*Molina Center for the Energy and the Environment, La Jolla, CA, USA*

³*School of Human Settlements and Civil Engineering, Xi'an Jiaotong University, Xi'an, China*

Abstract: Aerosols scatter or absorb incoming solar radiation, perturb the temperature structure of the atmosphere, and impact meteorological fields and further the distribution of gas phase species and aerosols. In the present study, the aerosol radiative effects on the meteorology and photochemistry in Mexico City are first investigated using the WRF-CHEM model during the period from March 24th to 29th associated with the MILAGRO-2006 campaign. Aerosols decrease incoming solar radiation by up to 20% and reduce the surface temperature by up to 0.5 °C due to scattering and absorbing the incoming solar radiation in Mexico City. The absorption of black carbon aerosols can also enhance slightly the temperature in the planet boundary layer (PBL). Generally, the change of the PBL height in the city is less than 200 m during daytime due to the aerosol-induced perturbation of temperature profile. Wind fields are also adjusted with the variation of temperatures, but all the aerosol-induced meteorological changes cannot significantly influence the distribution of pollutants in the city. In addition, when convective events occur in the city, the aerosol radiative effects reduce the convective available potential energy (CAPE) and the convective precipitation is generally decreased. Further studies are also performed to evaluate the aerosol direct effect on the meteorology and concentrations in Mega-Cities in China under the heavy haze condition.

Influences of Fireworks Display on Gaseous Ambient Air Pollutants and Titration Effects during the Taiwanese Lantern Festival

(Chung-Shin Yuan¹, Chang-Gai Lee²)

1 台灣中山大學環境工程研究所, 高雄 80424

2 大仁科技大學觀光事業系, 屏東, 90741;

摘 要: The display of fireworks is a traditional way to celebrate very important Chinese festivals such as New Year and Lantern Festival. This study investigated the influences of firework displays on ambient air quality during the Taiwanese Lantern Festival in Kaohsiung City. Both of the organic (methane, NMHC, THC, benzene and toluene) and inorganic (NO, NO₂, SO₂, CO, and O₃) gaseous pollutants were measured to fulfill the investigation. For organic gaseous pollutants, an increasing of THC concentration due to the firework displays was found. The concentration peaks of THC were caused mainly by the obvious increase of NMHC. The concentrations of NMHC were approximately 2.3 times higher than those during the non-firework periods. Moreover, the concentration peak of toluene during the firework periods was approximately 2.2~4.1 times higher than those during the non-firework periods, while benzene remained almost the same level as usual. For the inorganic gaseous pollutants, the concentration peaks of NO, NO₂ and CO were observed during the firework displays periods. The concentrations of NO and NO₂ was approximately twice and 3 times higher than those during the non-firework periods, respectively. This study further revealed that, even at nighttime, ambient O₃ could be reduced dramatically during the firework periods, when as NO₂ concentration increased concurrently, due to titration effects resulting from the prompt reaction of NO with O₃ to form NO₂ and O₂. This study revealed that firework displays for celebrating the Taiwanese Lantern Festival contributes significantly high amount of gaseous pollutants to the atmosphere of Kaohsiung City.

冬季兰州城市大气 PM_{2.5} 中碳气溶胶的污染特征与来源

(李刚¹, 石广玉², 李宏宇^{1,3}, 邓祖琴¹)

(1、中国气象局兰州干旱气象研究所, 兰州, 730020

甘肃省干旱气候变化与减灾重点实验室, 兰州, 730020

中国气象局干旱气候变化与减灾重点开放实验室, 兰州, 730020

2、中国科学院大气物理研究所LASG 国家重点实验室, 北京, 100029

3、南京大学气候与全球变化研究院, 大气科学学院, 江苏 南京 210008)

摘要: 利用 DRI-2001A 热/光碳分析仪测量 PM_{2.5} 中的元素碳 (EC) 和有机碳 (OC)。结果显示: EC、OC 和总碳 (TC) 的平均浓度分别为 7.48 $\mu\text{g}/\text{m}^3$, 22.71 $\mu\text{g}/\text{m}^3$ 和 30.19 $\mu\text{g}/\text{m}^3$ 。碳气溶胶占 PM_{2.5} 的 38.8%, OC 和 EC 的相关系数为 97.6%, 表明兰州冬季城市大气 PM_{2.5} 中碳气溶胶的污染来源相对简单, 主要是燃煤以及机动车尾气排放。二次有机碳 (SOC) 的浓度是 2.95 $\mu\text{g}/\text{m}^3$, 占 OC 含量的 14.35%, 表明冬季 OC 的主要来源是直接污染源。因子分析结果也表明, 冬季的燃煤和机动车尾气排放对碳气溶胶有最主要的贡献。

关键词: 大气细粒子, 元素碳, 有机碳, 二次有机碳, 因子分析

Pollution Characteristics and Sources of Carbonaceous Aerosols in PM_{2.5} During Winter in Lanzhou

Li gang¹ Shi guang-yu² Li hong-yu^{1,3} Deng zu-qin¹

(1、Institute of Arid Meteorology, china, Key Laboratory of Arid Climatic Change and Reducing Disaster of Gansu Province, Key Open Laboratory of Arid Climate Change and Disaster Reduction of CMA, Lanzhou 730020, china

2、LASG, Insitute of Atmospheric Physics, CAS, Beijing 100029, china

3、Institute for Climate and Global Change Research, School of Atmospheric Sciences, Nanjing University, Jiangsu Nanjing, 210008, China,)

Abstract: The Purpose of this study was to investigate the concentration characteristics and sources of carbonaceous aerosols in PM_{2.5} during winter in Lanzhou. Organic carbon(OC) and elemental carbon(EC) were measured by thermal/optical method using DRI-2001A. The average mass concentrations of OC、EC and TC were 7.48 $\mu\text{g}/\text{m}^3$, 22.71 $\mu\text{g}/\text{m}^3$ and 30.19 $\mu\text{g}/\text{m}^3$. Carbonaceous aerosol account for 38.8% of PM_{2.5}. The correlation coefficient of OC and EC was 97.6%. Mass concentration of SOC is 2.95 $\mu\text{g}/\text{m}^3$, Factor analysis on the eight carbon fraction indicated that coal combustion and vehicle emissions were the major sources for carbonaceous aerosol.

Key words: PM_{2.5}, OC, EC, SOC, Factor analysis

2011 年夏季新疆天山大气 PM_{2.5} 中碳气溶胶特征与来源分析

(李刚^{1, 2} 周军² 石广玉³ 李忠勤⁴ 王文彬⁴ 李宏宇^{1, 5} 邓祖琴¹)

1、中国气象局兰州干旱气象研究所, 甘肃省干旱气候变化与减灾重点实验中国气象局干旱气候变化与减灾重点开放实验室, 甘肃 兰州, 730020

2、中国科学院大气成分与光学重点实验室, 安徽 合肥, 230031

3、中国科学院大气物理研究所 LASG 国家重点实验室, 北京, 100029

4、中国科学院寒区旱区环境与工程研究所冰冻圈科学国家重点实验室/天山冰川观测试验站, 甘肃 兰州 730000

5、南京大学气候与全球变化研究院, 大气科学学院, 江苏 南京, 210008

摘 要: 2011 年 7 月 1-22 日于中国科学院天山冰川观测站采样点连续采集 PM_{2.5} 气溶胶样品。利用 DRI-2001A 热/光碳分析仪测定了其中元素碳 (EC) 和有机碳 (OC) 的浓度, 结果显示: EC 平均浓度、OC 平均浓度和 TC (总碳) 平均浓度分别为 1.38 $\mu\text{g}/\text{m}^3$, 5.05 $\mu\text{g}/\text{m}^3$ 和 6.43 $\mu\text{g}/\text{m}^3$ 。PM_{2.5} 中 OC 和 EC 的相关系数为 0.33, 表明夏季新疆天山大气 PM_{2.5} 中碳气溶胶的污染源相对复杂, 呈现多样性。OC/EC 的平均值是 3.86, 表明夏季新疆天山大气 PM_{2.5} 中导致二次污染的光化学反应比较活跃, 二次有机碳 (SOC) 的浓度为 2.35 $\mu\text{g}/\text{m}^3$, 约占 OC 含量的 46.5%。对碳气溶胶的 8 种组分因子分析结果表明, 人类活动对夏季新疆天山碳气溶胶的变化起着最大的贡献, 森林作用也不容忽视。

关键词: 大气细粒子, 元素碳, 有机碳, 二次有机碳

Preliminary study of the influence of OH radical source on the formation process of secondary organic aerosol in smog chamber experiment*

(Hong LI^{1#}, Kei SATO², Akinori TAKAMI², Xuezhong WANG¹)

1 State Key Laboratory of Environmental Criteria and Assessment, Chinese Research Academy of Environmental Sciences, Beijing 10012, China

2 National Institute for Environmental Sciences, Tsukuba 305-8506, Japan

Abstract: The isoprene/NO_x, isoprene/NO_x/CH₃ONO and isoprene/NO_x/H₂O₂ mixtures were irradiated separately to simulate the formation of secondary organic aerosol (SOA) from the OH-initiated isoprene photo-oxidation reaction in a 6-m³, teflon-coated, stainless steel indoor smog chamber; An in-situ Long-path FTIR, a SMPS and a AMS were used to measure the concentrations of reactants and gaseous products, the size distribution and volume concentrations of SOA and mass concentration of organic aerosol and inorganic components of aerosols. Oxidation process of isoprene, the product yields of main gaseous reaction products, and the SOA formation process were investigated and compared among the three mixtures irradiation systems to study the effects of OH radical sources on the formation process of secondary organic aerosols.

Key words: Secondary organic aerosol, OH radical sources, Isoprene photo-oxidation reaction, Indoor smog chamber

操作電壓對靜電集塵器收集微粒效率之影響

(李嘉塗, 莊崇賢)

摘 要:工業時代崛起, 各類空氣汙染物質、量濃度日益劇增, 雖當今有相當多類型集塵器, 皆能有效去除分佈於空氣粒、氣物質, 其中靜電集塵器收集效率最高, 亦可以達到 99%以上, 為達最佳效果, 關鍵則在於操作電壓值與流量大小。本研究探討六種圓球粒徑大小粒子運動度、粒子帶電荷數, 並以外徑 1.5 英吋、內徑 0.05 英吋管柱電極管在不同操作電壓下探討軸心線所帶電情況, 得知最大電場強度, 並可對不同操做電壓值估計其電流量值, 之後將六種粒徑大小探討每立方公分在六種不同電壓操作下可攜帶飽和電荷, 並計算其顆粒帶電所可飄移速度, 最後再利用長 5 英吋之電極管. 考慮六種操作電壓下及流量 $0.5\text{ft}^3/\text{min}$ 參數條件下, 探討收集效率。研究結果顯示, 當操作電壓值越高、氣流流量越小且所收集到顆粒粒徑越大情況下, 則越符合靜電集塵器收集效率指標。

關鍵字: 靜電集塵器, 電暈放電, 微米粒狀物, 電壓, 電流

二維噴管內氣流流動數值模擬研究

(李嘉塗,邱怡樺)

屏東科技大學環境工程與科學系, 屏東, 91201;

摘 要：實驗測量方法是理論分析和數值方法的基礎，然而，實現往往受到模型尺寸、流場環境、人為因素和測量精準度的限制，且還需投入相對較多的經費、人力和物力。CFD 方法克服了理論分析與實驗研究的弱點，利用電腦計算，方便快速的展現氣體流動情形。在自然環境中和工程裝置中的流動通常是湍流流動，根據所建立的模型所需要的微分方程式的數目，可以分為零方程式模型(代數方程式模型)、單方程式模型和雙方程式模型。本模擬研究使用 FLUENT-2D 求解器計算，是以一個二維漏斗型噴管，利用兩端高低壓力差，採用 Spalart-Allmaras 單方程式湍流模型，藉以觀察噴管內氣體流動的各種狀態，並以馬赫數等數值方法呈現。

关键字：FLUENT、CFD、湍流模型

2010年春季东亚地区气溶胶的模拟研究

(李嘉伟, 韩志伟*, 张仁健)

中国科学院大气物理研究所, 东亚区域气候-环境重点实验室, 北京 100029

摘 要: 利用区域空气质量模式系统 RAQMS, 模拟研究 2010 年 3 月东亚地区 PM_{10} 气溶胶和沙尘气溶胶的空间分布和时间变化, 着重研究 19-23 日爆发的特大沙尘暴过程。3 月 19 日, 沙尘气溶胶主要在戈壁地区产生, 随后横扫东亚大部分地区。模式模拟结果与中国 17 个城市的地面空气污染指数(API)观测数据、卫星反演数据、日本的激光雷达观测资料进行了对比验证。检验结果证明, RAQMS 模式能够很好地反映东亚地区 PM_{10} 气溶胶的时空分布, 能够模拟沙尘暴的主要特征和演变过程。总体上, 模式在中国东部地区表现优于西部地区。近地面月平均 PM_{10} 浓度在中国西部地区超过 $400 \mu\text{g m}^{-3}$, 在华北和华中地区为 $200\text{-}400 \mu\text{g m}^{-3}$, 在中国及东亚其余地方则低于 $100 \mu\text{g m}^{-3}$ 。在研究时段内, 沙尘气溶胶是 PM_{10} 质量浓度的最主要成分, 占中国西部地区 PM_{10} 质量浓度的 80%以上, 在华北和华中沙尘气溶胶所占比例为 30%-60%, 在华南和西太平洋地区, 该比例为 20%-40%。2010 年 3 月爆发的沙尘暴在其影响范围和输送路径上都具有独特性, 因为此次沙尘暴的影响最远到达华南珠江三角洲地区(如香港)。沙尘含量年际变化分析显示, 2010 年 3 月东亚地区沙尘气溶胶的起沙量、沉降量及其在大气中的含量均高于沙尘活动同样活跃的 2002 年和 2006 年同期。2010 年 3 月东亚沙尘总起沙量约为 110.4Mt, 其中大约 68%通过干沉降和湿清除过程重新沉降到地表, 剩余的 32%则悬浮于大气中, 参与长距离输送过程。

基于 CMAQ 模式的珠三角地区碳气溶胶排放研究

(李楠^{1,2} 傅宗政³ 曹军骥^{1,4})

1 中科院地球环境研究所, 西安, 710075

2 中国科学院大学, 北京, 100049

3 北京大学物理学院大气与海洋科学系, 北京, 100871

4 西安交通大学全球变化研究院, 西安, 710049

摘 要: 碳气溶胶是大气细颗粒物的重要组成, 主要包括元素碳和有机碳。燃烧过程可以直接向大气中排放碳气溶胶。有机碳气溶胶也可以通过挥发性有机化合物经过氧化反应而生成, 此类有机碳气溶胶称为二次有机气溶胶。本研究利用区域化学传输模式 CMAQ 对珠三角地区的碳气溶胶进行模拟研究, 并将模拟结果与观测进行比较。我们的研究目的是为了更好地区量化珠三角地区一次和二次碳气溶胶来源。我们利用目前最为先进的源排放清单做模式模拟基础, 结合观测资料, 对源排放清单进行 top-down 估算。并耦合加入液相二羰基类二次有机气溶胶生成机制, 进一步研究珠三角地区二次有机气溶胶的来源。研究表明: 1) 利用优化的 top-down 排放清单, 模式对于碳气溶胶的模拟能力大幅提高; 2) 二羰基类二次有机气溶胶是珠三角地区二次有机气溶胶的主要组成部分。

关键词: 碳气溶胶, 二次有机气溶胶, 源排放, CMAQ

人类黑碳气溶胶与东亚夏季气候年代际变化

(李双林、*Rashed Mahmood*, 万江华)

(中国科学院大气物理研究所; 中国科学院气候变化研究中心; 北京 100029.

Email: shuanglin.li@mail.iap.ac.cn)

Abstract: Two inter-decadal shifts in East China summer rainfall during the last three decades of the 20th century have been identified. One shift occurred in the late 1970s and featured more rainfall in the Yangtze River valley and prolonged drought in North China, along with the substantial weakening of East Asian summer monsoon (EASM). The other shift occurred in the early 1990s and featured increased rainfall in South China, in accompany with the further weakening of EASM. In this study, the authors used Geophysical Fluid Dynamics Laboratory's (GFDL's) atmospheric general circulation model known as Atmosphere and Land Model (AM2.1), which has been shown to capture East Asian climate variability well, to investigate the influence of anthropogenic black carbon (BC) aerosols by conducting sensitive experiments with or without historical BC. The results suggest that the model with the prescribed BC over East Asia reproduces the first shift well, including intensified rainfall in the Yangtze River and weakened monsoonal circulation. However, the model captures only a fraction of the observed variations for the second shift event. Further experiments with prescribed remote upstream BC are conducted, and the results suggest that the decreased BC over Europe around the early 1990s may have contributed to the second shift of EASM. Thus, the role of BC in modulating the two shift events is different. The local BC's impact is relatively less important for the early 1990s event, while the interdecadal decrease of European BC around the early 1990s may have played an important role.

Reduction of both NO_x and PM emission by using water containing diesel fuels

(Yu-Cheng Chang¹, Wen-Jhy Lee¹)

¹ Department of Environmental Engineering, National Cheng Kung University, Tainan 70101, Taiwan

Abstract Diesel engines are widely employed in both heavy-duty vehicles and generators, due to its high thermal efficiency, high power output and low emissions of regulated pollutants, such as carbon monoxide (CO) and hydrocarbon (HC). However, the International Agency for Research on Cancer (IARC) has classified diesel engine exhaust as carcinogenic to humans (Group 1), and research has shown that there is a significantly increased risk of mortality from lung cancer with increased exposure to diesel exhaust. Cleaner and more efficient diesel engines have been developed over the past few decades. For example, the exhaust gas recirculation (EGR) process was developed to reduce NO_x emissions. However, due to the trade-off relationship between NO_x and PM, the EGR is not effective for simultaneously removing NO_x and PM. Now the focus of pollutant reduction techniques is mainly on cleaner alternative fuels. Numerous studies have investigated the emission and energy performance of diesel engines that are fueled with biodiesel. Their findings show that the related particulate matter (PM), carbon monoxide (CO), total hydrocarbons, sulfur dioxide, and polycyclic aromatic hydrocarbon (PAH) emissions are lower than those of regular diesel. In addition, these fuels improved the engine performance. However, many of these studies also indicated that the use of biodiesel and related diesel blends lead to higher NO_x emissions, which are strictly controlled by emissions standards in many countries. Thus, NO_x emissions are a critical barrier for the adoption of biodiesel.

Alcohol additives, such as ethanol and butanol can reduce NO_x formation, while reducing PM and CO emissions and improving energy performance. These types of alcohol could be produced by fermenting biomass feedstocks; however, high water content in the fermentation products make it difficult to use without dehydration. The removal of water during product fermentation will require additional energy and increase production costs.

Recently, several studies have reported that water-containing alcohol-diesel blends improve the energy efficiency of diesel engines and reduce pollutant emissions (NO_x, PM, Total-PAHs and Total-BaP_{eq}). The addition of water-containing alcohol-diesel blends is beneficial in terms of saving energy and reducing pollution. The high oxygen concentrations of the alcohol-diesel blends could result in more complete combustion, which would increase energy efficiency and lower PM, CO and PAH emissions. In addition,

the oxygenated additives and the small amount of water could result in a cooling effect that reduces the combustion temperature. This process would also reduce the NO_x emissions. However, previous studies have only considered individual oxygenated fuels rather than the typical compounds that are produced from the biomass feedstock fermentation process. These compounds include acetone, butanol and ethanol at volume percentages of approximately 22-33, 62-74 and 1-6%, respectively.

Here, a water-containing acetone-butanol-ethanol (ABE) solution, which simulates products that are produced from biomass fermentation without dehydration processing, was investigated as a biodiesel-diesel blend additive to lower NO_x emissions from diesel engines. Although biodiesel had a greater NO_x emission, the blends that contained 25% of the water containing ABE solution had significantly lower NO_x (4.30-30.7 %), PM (10.9-63.1 %), and PAH emissions (26.7-67.6 %) than the biodiesel-diesel blends and regular diesel, respectively. In addition, the thermal energy efficiency of this new blend was 0.372-7.88 % higher with respect to both the biodiesel-diesel blends and regular diesel. Because dehydration and surfactant additions are not necessary, the application of water containing ABE-biodiesel-diesel blends can simplify fuel production processes, reduce energy consumption, and lower pollutant emissions. Thus, the water containing ABE-biodiesel-diesel blend is a highly potential green fuel in the future.

Keyword: water-containing ABE, diesel engine, PM, NO_x

气溶胶标准化发展概况及对策

(李兆军¹ 李劲松²)

1 中国科学院过程工程研究所, 北京 100190

2 军事医学科学院微生物流行病学研究所, 北京 100071

摘 要: 本文在分析了国内外, 包括美国标准学会、ASTM、英国、德国、法国、欧洲标准学会等发达国家有关气溶胶标准的基础上, 提出了, 要适应我国经济和社会飞速发展, 以及人们对环境 and 安全关注度与日俱增的现实, 如气溶胶与人体健康、周边大气的质量、人员聚集区域空气微生物超标应急相应等, 应特别重视气溶胶的标准化研究, 包括气溶胶的采集、观测、特性分析等方面的标准, 使得气溶胶的科研成果尽快形成相应的标准, 进而指导气溶胶科研仪器的自主创新, 进一步推动气溶胶的科研开发工作, 使气溶胶的研发走向良性循环的道路。

关键字: 气溶胶, 标准化, 发展, 概况

閩江口大氣懸浮微粒濃度季節變化趨勢及污染源貢獻量分析

(廖建欽¹、李宗璋¹、張正馳¹、陳光暉²、袁中新¹、張章堂²、江士豪)

1 國立中山大學環境工程研究所, 高雄 80424

2 國立宜蘭大學環境工程學系, 宜蘭 26041

3 連江縣東引鄉公所, 連江 21241

摘要：馬祖列島位於台灣海峽西北方，四面環海，東距基隆 114 哩，西與福建閩江口僅一水之隔。近年來，大陸東南沿海地區經濟及工業快速發展，石化燃料消耗量及人為污染物的排放量均大幅增加，再加上區域性生質燃燒等影響，將東南亞地區所排放的空氣污染物在西南季風引導下經由長程傳輸，對馬祖地區的空气品質產生一定程度的影響。有鑒於此，本研究自 2012 年 7 月 1 日至 12 月 31 日於閩江口附近陸地及海島設置六處懸浮微粒採樣站，同步進行 PM₁₀ 懸浮微粒採樣，將所採集之懸浮微粒進行離子成份(F⁻、Cl⁻、NO₃⁻、SO₄²⁻、Na⁺、NH₄⁺、K⁺、Mg²⁺、Ca²⁺等九種)、金屬元素(Mg、Ca、Ti、Cr、Mn、Fe、Ni、Zn、Al、As、Pb、K、Cd)及碳成份(OC、EC)分析，再利用化學分析結果進行主成份分析(PCA)及化學質量平衡受體模式(CMB receptor model)模擬，解析大氣懸浮微粒之污染源種類及貢獻量。採樣結果顯示馬祖地區秋季空氣品質尚佳(55±24 µg/m³)，但秋末及冬初則有高濃度懸浮微粒情形發生(102±25 µg/m³)。就整體空間分佈而言，懸浮微粒濃度大致呈現西高東低的趨勢，夏季期間 PM₁₀ 濃度最高值常發生於黃岐中學採樣站，秋季過後 PM₁₀ 濃度最高值常發生於梅花中學採樣站，而東引鄉鄉民代表會在不同季節 PM₁₀ 濃度皆屬最低。就懸浮微粒污染源種類及貢獻量而言，馬祖及福州地區主要以逸散性揚塵(12.5~38.5%)、二次衍生性氣膠(13.1~29.8%)、交通污染源(9.1~27.7%)、海鹽飛沫(6.4~28.3%)、農廢燃燒(2.87~11.28%)為主；而秋季過後及空氣品質劣化期間，工業污染源貢獻量呈明顯上升趨勢(17.8~33%)，然而連江縣轄內並無大型相關工業，因此推測工業性污染主要由境外輸入。

关键字：馬祖列島；大氣懸浮微粒；長程傳輸；主成份分析；化學質量平衡受體模式

大氣中 VOC 垂直層化分佈觀測及其對臭氧空氣品質之影響探討

(廖思婷¹ 高英暉¹ 林啟燦¹ 洪崇軒² 袁中新³)

1 高雄海洋科技大學海洋環境工程系

2 高雄第一科技大學環境與安全衛生工程系

3 中山大學環境工程研究所

摘要：空氣污染物水平傳輸與垂直擴散之速率截然不同，以往大多數空氣污染物的監測及研究也多在地面上進行，垂直高空之空氣污染分佈，則較少被探討。如今化學工業區製程漸多，高煙囪數量也急遽增加，污染物在高空的排放也相對較多；且污染物容易經光化學反應衍生出二次污染物，如臭氧、過氧醯基硝酸酯(PAN)及光化學煙霧等問題，也是當前所關注的重要議題。但當前臭氧空氣品質推估模式，皆假設前驅污染物之垂直高度範圍是均勻混合的。近年來，陸續有文獻指出大氣 VOCs 濃度會受氣象條件、季節、時間等因素影響，而產生層化現象；此層化現象是否存在？是否會影響臭氧空氣品質之推估？仍未被清楚的研究。為印證層化現象是否存在！本研究以繫留氣球採樣法，於 2011 年在北高雄地區高海科大及文府國小兩測站，夏冬兩季各採一天連續 24 小時，每間隔 6 小時採集一組層化分佈之樣品(由地面至 800 公尺，每 100 公尺採一樣)，再進行氣樣 VOCs 之分析，共計 64 個樣品(16 組垂直濃度變化)，以觀察北高雄地區 VOCs 垂直層化現象。研究結果顯示，16 組數據中，有 14 組呈現層化現象；對於大氣垂直分佈而言，日夜間污染平均濃度多半呈現「高空」大於「地面」的趨勢，而此情況發生機率高達 87.5%之多；顯示大氣中 VOC 垂直濃度分佈，確實有層化現象存在。層化所造成 VOCs 容易累積的高度會因季節有所不同，夏季高度約為 700 公尺，而到了冬季則下降至 100 及 400 公尺。就不同高層光化學反應性而言，夏季高海科大及文府國小最大 MIR，分別出現在 400 公尺及地面，其貢獻物種為甲苯及丙酮；冬季高海科大及文府國小最大 MIR，則分別出現在 500 及 800 公尺，其主要貢獻物種為 BTEX 及十二烷。MIR 為影響臭氧空氣品質模式之重要指標；前述結果顯示，MIR 估算值亦隨不同高度而有差異；因此，合理推論，臭氧前驅物在大氣中所呈現之層化分佈，極可能會影響空氣品質模式之推估結果，值得相關研究學者持續深入探討。

关键字：揮發性有機化合物 (VOCs)、臭氧空氣品質、垂直分佈、層化現象、MIR

Study of long-range transport air pollutants to Taiwan during Southeast Asia biomass burning events

(Chuan-Yao Lin¹, Chun Zhao², Xiaohong Liu², Neng-Huei Lin³, Kai-Hsien Chi⁴)

1. Research Center for Environmental Changes, Academia Sinica, Taipei, Taiwan

2. Atmospheric Science and global change division, Pacific Northwest National Laboratory, Richland, WA, USA

3. Department of Atmospheric Science, National Central University, Taiwan

4. Institute of Environmental and Occupational Health Sciences

Abstract: Biomass burning in the Indochina Peninsula (Indochina) is one of the important ozone sources in the low troposphere over East Asia in springtime. Moderate Resolution Imaging Spectroradiometer (MODIS) data show that 20,000 or more active fire detections occurred annually in spring only from 2000 to 2011. In this study, WRF-Chem model was employed to evaluate the biomass burning products transport from Indochina during the episodes between 15 and 19 March, 2008. Hourly Data at background Liulin mountain station (2862 m elevation) shows that CO, O₃ and PM₁₀ are ranging about 200-300 ppb, 30-60 ppb and 50-80 ug/m³, respectively. It was estimated that the concentrations of those species are about factor of 2-3 higher than other seasons during study period. Simulation results demonstrate that the leeside troughs over Indochina play a dominant role in the uplift of the air pollutants below 3 km. Furthermore, the impact of biomass burning from Indochina on downward shortwave flux could as high as around 20- 30 Wm⁻² in northern Taiwan during study period.

高雄市都會區大氣細懸浮微粒濃度時空變異特徵

(林銳敏¹, 李瑞龍¹)

1 臺灣高雄第一科技大學環境與安全衛生工程系, 高雄, 811

摘要：本研究以高雄市境內 11 處空氣品質監測站為評估對象，針對 2010 年細懸浮微粒(PM_{2.5})逐時濃度進行統計評析，探討 PM_{2.5} 濃度之時間/空間分佈及變異特徵。各測站 PM_{2.5} 監測濃度之相關性分析結果顯示，各測站之 PM_{2.5} 濃度變化，短期時間(1-hr)內，不同測站易受測站周邊鄰近污染源影響；隨著大氣擴散，各測站長時間(24-hr)濃度變化趨勢較相近，因此各測站間 24-hr 濃度相關係數較高於各測站間 1-hr 濃度相關係數。然而以配對統計(paired t-test)檢定，發現測站間仍有顯著差異(p<0.05)，表示各測站濃度變化雖可能因區域環境影響而趨勢相近(高相關係數)，但各測站受其周邊污染源的影響而造成各測站間濃度水準有顯著的差異。高雄市 PM_{2.5} 年平均濃度為 41 µg/m³，全年超過預警值(65 µg/m³)百分比為 13.08 %，其中以大寮及林園測站超標比例最高，主要原因可能因為林園及小港區為工業區所在地，當盛行風向為西南風時，位於下風處之大寮站則發生高濃度；反之，美濃測站超標比例最低，可能因為位置靠近山區且人口數較少，整體環境型態與市中心之型態明顯不同。四季中 PM_{2.5} 日平均濃度的季節變化以夏季濃度最低(平均 23 µg/m³)；冬季濃度最高(平均 62 µg/m³)且濃度變化大，且冬季將近 40%時間濃度超過預警值(65 µg/m³)。研究結果亦顯示較高的 PM_{2.5} 濃度值主要發生於冬季盛行風向(北風)及夏季盛行風向(西南風)低風速條件，且高雄市主要以大寮及林園測站為高濃度熱點地區。本研究的成果可以提供環保單位進一步的進行 PM_{2.5} 高濃度熱點地區民眾的暴露評估，及規劃有效的污染源排放管制策略。

关键字：細懸浮微粒，PM_{2.5}，污染熱點，時空變化，都會區

Development of an optimal method for ^{14}C -based source apportionment of $\text{PM}_{2.5}$ carbonaceous aerosols at a background site in East China

(Di Liu^{1,4}, Jun Li¹✉*, Yanlin Zhang¹, Yue Xu¹, Xiang Liu¹, Ping Ding², Chengde Shen², Yingjun Chen³, Chongguo Tian³, and Gan Zhang¹)

1 State Key Laboratory of Organic Geochemistry, Guangzhou Institute of Geochemistry, Chinese Academy of Sciences, Guangzhou 510640, China

2 State Key Laboratory of Isotope Geochemistry, Guangzhou Institute of Geochemistry, Chinese Academy of Sciences, Guangzhou 510640, China

3 Yantai Institute of Coastal Zone Research, Chinese Academy of Sciences, Yantai 264003, China

4 Graduate University of the Chinese Academy of Sciences, Beijing 100039, China

Abstract: Carbonaceous aerosol is one of the most abundant components (20-80%) of atmospheric fine particulates ($\text{PM}_{2.5}$) [1] and substantially affects both climate and human health. Based on their optical properties, carbonaceous aerosols can be classified as organic carbon (OC) or elemental carbon (EC). In general, EC is a primary pollutant derived exclusively from the incomplete combustion of fossil fuels and biomass burning, whereas OC is a complex mixture of primary and secondary organic aerosols (POA and SOA, respectively).

Compared with other methods, such as the use of the OC/EC ratio only, radiocarbon (^{14}C) analysis facilitates the direct differentiation of modern carbon sources from fossil fuel sources [2, 3]. To date, many ^{14}C studies have focused on the amount of total carbon (TC) in aerosols [4-6], and only a few studies have separately analyzed both OC and EC due to limitations of the technique, the bulk samples required, and the high cost for ^{14}C measurement. Furthermore, due to their ambiguous artificial boundary, the identification of the individual OC and EC fractions in carbonaceous aerosols is depends significantly on the method [7]. Because EC is emitted into the atmosphere solely from either fossil fuel combustion or biomass burning as primary particles, a clear distinction of the EC source between these two sources can be achieved [8, 9]. As a result, the use of a combination of OC/EC separation and ^{14}C analysis for the identification of the source, regardless of whether its origin is fossil or non-fossil, is more effective than the analysis of the ^{14}C in the TC.

Due to the rapid economic growth and high population density in China, the aerosols and their precursor emissions have drawn significant attention in recent decades. As one of the three largest economic hubs in China, the Yangtze River Delta (YRD) experiences serious air pollution but few

* Corresponding author. Phone: +86-20-85291508; fax: +86-20-85290706; email: junli@gig.ac.cn

monitoring station of ^{14}C -related studies. Ningbo Atmospheric Environmental Observatory (NAEO) , where close to the East China Sea and in the southern part of the YRD, was established since it is a key site or outlet for the aerosol transport routes from the Chinese sub-continent to the Pacific Ocean.

The objectives of this study were the following: 1) set up an off-line EC separation method and system for ^{14}C determination and 2) quantitatively apportion the contemporary and fossil sources of OC and EC using this method and clarify their source seasonality at a regional background site in East China. In addition, the concentrations and seasonal variations of OC, EC, and levoglucosan (an indicator of biomass burning) in $\text{PM}_{2.5}$ were also investigated to substantiate the ^{14}C -based source apportionment results.

重庆城市灰霾特征与数值模拟研究

(刘红年¹ 吕梦瑶^{1,2})

¹ 南京大学大气科学学院, 南京, 210093

² 中国气象局国家气象中心, 北京, 100081

摘要: 近年来, 随着我国国民经济的迅速发展及城市化进程的加剧, 城市空气污染问题越来越突出, 尤其是灰霾天气日趋严重。低能见度与灰霾天气已成为当前国内外许多城市面临的重要环境问题。本文利用重庆 2007 年污染物浓度监测资料及南京大学空气质量预报系统 (NJU-CAQPS2.0), 对重庆地区的灰霾特征进行了统计分析和数值模拟研究, 得出了以下一些主要结论: (1) 2007 年重庆主城区年平均能见度为 5.63km; 无论是季节平均还是年平均, 每日 4 个时次的能见度都小于 10km, 冬季能见度最低, 在 08、14、20、02 四个时次的气象观测记录中, 08 时能见度最低, 14 时和 20 时能见度较高。(2) 2007 全年, 重庆市主城区有 162 天是灰霾天, 占全年的 44.4%, 其中干霾天气有 125 天, 湿霾天气有 37 天, 分别占总灰霾天数的 77.2% 和 22.8%。春季和冬季发生灰霾的天数最多, 冬季湿霾天气发生频率较高。从灰霾污染的等级来看, 轻微灰霾发生次数较多, 一共有 80 天, 占总灰霾天数的 49.4%, 重度灰霾发生的次数最少, 只有 20 天, 占总灰霾天数的 12.3%; 春季、夏季和秋季都以轻微灰霾天气为主; 冬季灰霾天以重度、中度灰霾天气为主。重度灰霾和中度灰霾多由湿霾天气造成, 而轻度灰霾和轻微灰霾多由干霾天气引起。(3) 数值模拟结果显示, 夜间 02: 00 至清晨 08: 00 左右出现贴地逆温, 与重污染出现的时间基本一致。各个时次的 BC、POC、PM₁₀、PM_{2.5} 和能见度的水平分布与排放源及气象条件密切相关, 08 时左右的污染物浓度最高。各污染物的日平均浓度具有显著的空间分布特征, 与排放源的位置关系密切, 污染源排放较大的区域相应污染物浓度值也较高; 各污染物的浓度值均是城区高于郊区, 而能见度城区低于郊区。(4) 颗粒物对消光系数的贡献率超过 80%, 春夏两季, 有机物和黑碳气溶胶是能见度下降的最重要的贡献者, 春季二者所占比例可达 45.8% (城区) 和 59.3% (郊区), 夏季二者所占比例可达 51.8% (城区) 和 64.5% (郊区); 秋季, 城区硫酸盐 (21.3%)、硝酸盐 (16%)、有机物 (27.1%)、黑碳 (16.2%) 所占比例大致相同, 是能见度下降的最重要贡献者, 但是在郊区硫酸盐 (24.8%) 和硝酸盐 (41.4%) 的贡献率最高, 二者之和超过了 65%。各成分对消光系数的贡献率受源排放和相对湿度等气象条件的影响。

关键字: 灰霾, 能见度, 重庆, 南京大学城市空气质量模式

全球沙尘气溶胶源汇分布及其变化特征的模拟分析

(刘建慧¹, 赵天良^{1,*}, 韩永翔¹, S.L.Gong², 熊洁¹)

(1.南京信息工程大学 大气物理学院, 江苏 南京;2.Air Quality Research Technology Branch, Environment Canada, Toronto, Ontario M310044H 5T4, Canada)h Division, Science &

摘要: 根据全球沙尘气溶胶气候模式 GEM-AQ/EC 模拟的 1995-2004 年的沙尘起沙量和干湿沉降量, 分析了沙尘气溶胶源汇的全球时空变化特征。全球沙尘起沙量集中在各个主要沙漠地区, 北非对全球沙尘气溶胶贡献最大为 66.6%。沙尘气溶胶沉降的高值区分布在沙漠源区及其紧临的下风地区。最大净沙尘气溶胶接收主要分布在沙漠周围地区并形成净接收量大于 $10 \text{ tkm}^{-2}\text{yr}^{-1}$ 的位于 0°N ~ 60°N 之间的北非、欧亚大陆、西太平洋, 北印度洋, 北美和大西洋的带状分布。在北非、阿拉伯半岛、中亚、东亚和澳洲 5 个主要沙漠地区中, 起沙量和沉降量都存在明显的季节变化, 除中亚其他 4 个区域干湿沉降量和起沙的季节变化基本一致; 东亚地区沙尘气溶胶起沙量和总沉降量的季节变化最为明显, 而北非沙漠起沙量和总沉降量的季节变化最小, 其它三个区域的季节变化幅度基本相同。中亚起沙峰值和阿拉伯半岛起沙次峰值出现在夏季, 其他区域的峰值均出现在春季。10 年间全球陆地年平均起沙量为 $1500 \pm 94 \text{ MT}$, 保持略微上升趋势。以北非沙漠起沙量年际变化率最低 (6.3%), 而以东亚 (28.3%) 和澳洲 (45.0%) 起沙量年际变化最为明显; 全球陆地的沙尘气溶胶沉降量以约 9.9 MT/yr 的速率递减, 全球海洋的沙尘气溶胶沉降递增。

关键字: 沙尘气溶胶, 起沙量, 干湿沉降量

Modeling study on distributions and variations of global dust aerosol sources and sinks

LIU Jianhui¹, ZHAO Tianliang¹, HAN Yongxiang¹, S.L.Gong², XIONG Jie¹

(1.School of Atmospheric Physics, Nanjing University Information & Technology, Nanjing 210044;2.Air Quality Research Division, Science & Technology Branch, Environment Canada, Toronto, Ontario M3H 5T4, Canada)

Abstract: Based on a 10-yr(1995-2004) simulation of dust emission and dry and wet deposition with the global air quality model system GEM-AQ/EC, the global spatial and temporal variation of the dust aerosol sources and sinks were characterized. Global dust emissions are centered in major deserts region, North African deserts contributed up to 66.6% to the global dust aerosol. The high values of the dust aerosol deposition spread desert sources and their nearly downwind regions. The maximum net dust aerosol sinks are mainly distributed around the desert regions and form the net receptor with greater $10 \text{ tkm}^{-2}\text{yr}^{-1}$ in a zonal pattern between 0°N and 60°N from North Africa, Eurasia, west Pacific Ocean, the north Indian

Ocean, North America to the Atlantic ocean. In five major deserts of North Africa, Arabian Peninsula, Central Asia, East Asia and Australia, the dust emissions and depositions present the significant seasonal variations, The regional depositions expecting Central Asia are in almost the same seasonal cycle with the emission; the seasonal variations of dust aerosol emissions and depositions are most obvious in East Asia, while they are weakest in the North Africa and basically similar in three other regions. Central Asia peak and the Arabian Peninsula peak appear in the summer, but the other regions peak appear in the spring. Over the 10 years, the global annual average emissions are estimated with 1500 ± 94 MT in a slightly rising trend. The interannual variability rate of dust emission in North Africa is lowest (6.3%) and highest in East Asia (28.3%) and Australia (45.0%); The dust aerosol depositions over global land decrease at a rate of around 9.9 MT/yr, while they increase year to year over the oceans.

Key words: Dust aerosol, Emission, Dry and wet deposition

武汉光谷地区春季大气颗粒物的粒径分布特征

(刘珏 胡辉 刘立)

华中科技大学环境科学与工程学院 湖北武汉 430074

摘 要：2013 年 2 月~4 月间在武汉市光谷地区使用粒径谱仪对粒径范围在 $0.25\mu\text{m}$ 至 $32\mu\text{m}$ 之间共 31 个通道的大气颗粒物的数浓度以及 PM_{10} 、 $\text{PM}_{2.5}$ 、 PM_1 的质量浓度进行监测。监测结果说明，大气颗粒物个数中，粒径在 $0.25\mu\text{m}$ 至 $0.58\mu\text{m}$ 之间的颗粒物占绝大部分，其中灰霾天时占约 92.6%，非灰霾天时占约 96.5%。粒径在 $0.25\mu\text{m}$ 至 $32\mu\text{m}$ 之间的颗粒物数浓度变化趋势与质量浓度的变化趋势大体相同。灰霾天颗粒物数浓度明显高于非灰霾天，而且无论是灰霾天还是非灰霾天，趋势大致都是颗粒物的数浓度随着时间由白天到傍晚逐渐降低。

关键词：亚微米粒子, 数浓度, 粒径分布, 灰霾天, 非灰霾天

The PAH concentrations and compositions in aerosol over Marginal and Open sea in the North Pacific Ocean

(Junwen Liu^{a,b}, Yue, Xu^a, Jun Li^{a*}, Gan Zhang^a)

^aState Key Laboratory of Organic Geochemistry, Guangzhou Institute of Geochemistry, Chinese Academy of Sciences, Guangzhou 510640, China

^bUniversity of Chinese Academy of Sciences, Beijing 100049, China

*Telephone + 86 20 8529 1508; Fax: +86 20 8529 0706

E-mail address: junli@gig.ac.cn

Abstract: As a group of ubiquitous contaminants in environment, polycyclic aromatic hydrocarbons (PAHs) in atmosphere can be formed and emitted by natural and anthropogenic combustion processes. In this paper, we selected some filter samples collected aboard the R/V DayangYihao in the year of 2007 and analyzed 15 USEPA priority control PAHs over Asian marginal seas and remote North Pacific Ocean, respectively. The results showed that particulate PAHs over marginal sea were higher than that over the remote North Pacific Ocean by a factor of ~ 5 -10. The PAH composition profile over marginal Sea was in agreement with that emitted by the continental emission sources, however, different pattern was observed for the PAHs over the remote North Pacific Ocean.

Keywords: polycyclic aromatic; hydrocarbons (PAHs); ocean; composition; profile

东莞市不同区域气溶胶细粒子 PM_{10} 及其中重金属元素的污染特征

(刘立¹, 胡辉^{1,*}, 李娴², 黄免彦³, 蔡勋江³, 张国斐³)

¹ 华中科技大学环境科学与工程学院, 湖北武汉 430074

² 东莞市环境保护监察分局, 广东东莞 523000

³ 东莞市环境监测中心站, 广东东莞 523000

摘 要: 2011 年 8 月到 2012 年 7 月期间使用中流量大气采样器在东莞市两点(生活区 A 点和工业区 B 点)进行 PM_{10} 、 $PM_{2.5}$ 和 PM_1 的采集, 并用 ICP-MS 分析颗粒物中的 Pb、Cu、Zn、As、Cd、V、Mn、Cr、Mn、Hg 和 Al 等 10 种元素。分析结果显示, 工业区 B 点气溶胶细粒子及其中重金属污染明显较生活区 A 点严重, PM_1 及其中 Zn、Pb、Mn、Cu、V、Hg、As、Cr、Cd 等元素的浓度年均值分别是 A 点的 1.20 倍、1.21 倍、1.17 倍、1.11 倍、1.12 倍、1.22 倍、1.16 倍、1.20 倍、1.20 倍、1.22 倍和 1.15 倍。各重金属元素及其富集因子(EF)具有明显的季节分布特征, 均为冬季>秋季>春季>夏季。富集因子法的分析结果表明, 东莞市无论生活区 A 还是工业区 B 点, 其气溶胶细粒子 PM_1 中重金属元素主要受人为源影响。

关键词: PM_1 ; 不同区域; 重金属元素; 富集因子

南京城市群区大气污染对地表气象要素及能量收支的影响研究

(刘丽霞¹, 凌肖露^{1*}, 郭维栋¹)

1 南京大学气候与全球变化研究院, 南京大学大气科学学院, 南京 210093

摘 要: 利用 2012 年 4-6 月南京溧水野外观测站近地层微气象、地表辐射和通量交换数据, 结合南京大学地球系统区域过程综合观测研究站 (SORPES-NJU) 的 $\text{PM}_{2.5}$ 质量浓度及环境保护部发布的空气污染指数 (API), 使用聚类分析和合成分析的方法, 定量分析了南京地区不同大气污染程度下地表能量收支和气象要素的变化及响应特征。进而针对 2012 年 6 月上旬一次因作物秸秆燃烧导致的严重空气污染事件, 开展了细致的典型个例分析。从日变化的角度分析了污染演化过程中微气象学特征量和辐射量的响应特性。结果表明, 南京地区污染天日均气压比清洁天气低约 4hPa, 盛行南风 and 偏南风, 且风速比清洁天气低约 13.5%。气溶胶污染物导致地面接收的净辐射通量减小, 最大净辐射差值高达 $120 \text{ W}\cdot\text{m}^{-2}$; 污染天、清洁天的最大感热通量分别占净辐射的 30 % 和 36 %, 而潜热通量的变化并不明显。个例分析表明, 污染过程爆发前期, 气压降低, 风速迅速减弱; 气溶胶浓度维持高值期间, 气压与地面风速较低, 污染物的扩散受到抑制, 同时气温明显降低, 日最低相对湿度升高; 之后伴随着风速增大、气压回升、气温升高, 气溶胶扩散条件较为有利, $\text{PM}_{2.5}$ 浓度逐渐回落。

关键词: 城市群区, 气溶胶, 气象要素, 地表能量收支

Is formation of NH_4NO_3 a critical factor for the growth of > 10 nm new particles to cloud condensation nuclei size in marine boundary layer?

(Xiaohuan Liu, Yujiao Zhu, Huiwang Gao, Tianran Zhang, Yao Xiaohong^{*})

Key Laboratory of Marine Environment and Ecology, Ministry of Education of China, Ocean University of China, Qingdao 266100, China

Abstract: In the last three decades, huge efforts have been taken to improve understanding of the relationship between ambient nucleation of new particles and its impact on the climate in marine boundary layer (MBL), e.g., CLAW hypothesis and studies related. However, only >40-50 nm new particles could be activated as cloud condensation nuclei (CCN) under typical range of water supersaturations occurring in MBL. The knowledge gap still existed, i.e., which chemicals are critical factors in growing nucleated particles to CCN size in MBL. In this study, we found that nucleated particles in MBL cannot grow over 40 nm in absence of strong formation of NH_4NO_3 . However, the strong formation of NH_4NO_3 together with organics can grow nucleated particles close to or over 50 nm in MBL. These indicate that the strong formation of NH_4NO_3 is a critical factor to grow nucleated particles to CCN size in MBL. However, the strong formation of NH_4NO_3 occurred only in polluted air mass in MBL. Thus, ambient nucleation of new particles in clear and remote MBL is probably not a source of CCN due to lack of a strong formation of NH_4NO_3 and the nucleation may have no impact on the climate.

Keywords: new particle formation, NH_4NO_3 , secondary organics, China Seas, CMAQ model

长江三角洲地区 1980-2009 年灰霾分布特征及影响因子研究

(刘晓慧, 朱彬*, 王红磊, 张恩红)

(南京信息工程大学, 中国气象局气溶胶与云降水重点开放实验室, 江苏, 南京 210044)

摘要: 本文选取中国长江三角洲地区 38 个观测站 1980~2009 年的地面观测资料和 2001~2009 年国家环境保护总局公布的 API 数据, 统计分析了长三角地区近 30 年灰霾分布情况. 计算了观测站点的消光系数并进行了两次订正, 给出了其季均值和年均值分布情况, 对比了 1 个背景站(黄山光明顶观测站)和 3 个典型站(南京、杭州和合肥)的能见度与灰霾日数、干消光系数和 API 之间的关系. 结果表明, 近 30 年来, 长三角地区的灰霾日数整体呈增长趋势, 有 72% 的站点灰霾日数的年平均增长率大于零. 订正后的消光系数冬季高, 夏季低. 南京、杭州和合肥灰霾日数与干消光系数的增长趋势一致, 在霾日, 南京、杭州和合肥三地, 能见度与 API 呈负相关, 其相关性随相对湿度的增加而增强.

关键词: 长江三角洲, 灰霾, 干消光系数, 能见度, API

Haze trends and its factor influencing over the Yangtze River Delta Region of China, 1980–2009.

LIU Xiao-hui, ZHU Bin*, WANG Hong-lei, ZHANG En-hong

(Key Laboratory for Aerosol-Cloud-Precipitation of China Meteorological Administration, Nanjing University of Information Science and Technology, Nanjing 210044, China)

Abstract: Based on the meteorological data from 38 observation stations, haze variations over the Yangtze River Delta region for the period of 1980~2009 are presented. The extinction coefficient of each observation was also modified and analyzed. The corrected extinction coefficient for each station was highest in winter, lowest in summer. Over the past 30 years, there has been a significant increase in haze days. Horizontal visibility, haze days, dry coefficient and air quality index (API) of the three typical pollution station (Nanjing, Hangzhou, Hefei) and one background station (Huangshan) were analyzed. It was discovered that in haze days, visibility was anti-related with API, and the correlation gradually increased with relative humidity.

Keywords: the Yangtze River Delta Region; haze; dry extinction coefficient; visual range; API

基金项目: 国家自然科学基金项目(41275143); 江苏省高校自然科学研究重大基础研究项目(12KJA170003); 江苏省“333”高层次人才培养工程项目; 江苏省“六大人才高峰”计划; 江苏省江苏高校优势学科建设工程项目(PAPD); 江苏高校研究生创新计划项目(NO782002146)

* 责任作者, 教授, binzhu@nuist.edu.cn

臺中市政府清潔隊柴油車輛裝置濾煙器試範運行成果

(劉邦裕¹)

1 臺中市政府環境保護局，臺中市，40301

摘要：臺中縣市合併後成為臺灣新興都會區，發展時間僅次於臺北市與高雄市，人口達 2,675,939 人，由於車輛眾多污染排放嚴重，因此臺中市政府環境保護局於 2009 年執行『臺中市清潔隊車輛裝置濾煙器示範運行計畫』，選擇 15 輛柴油車輛進行清潔隊柴油車輛裝置濾煙器的示範運行，評估柴油車輛裝置濾煙器對於柴油車輛污染減量的效益，特別是粒狀污染物的減量效益。為延續 2009 年示範運行計畫的成果，於 2010 年執行「清潔車輛裝置濾煙器設備採購暨 2009 年濾煙器維修再生計畫」，再選擇 15 輛柴油車輛進行清潔隊柴油車輛裝置濾煙器的示範運行，並於 2012 年持續進行柴油車輛已裝置濾煙器之維護保養相關工作。2009 年執行『臺中市清潔隊車輛裝置濾煙器示範運行計畫』，選擇出廠年份介於 1997 年至 2003 年的 15 輛柴油車輛進行清潔隊柴油車輛裝置濾煙器的示範運行，評估柴油車輛裝置濾煙器對於柴油車輛污染減量的效益，該計畫進行柴油車輛於安裝濾煙器前後粒狀污染物（PM）、氣狀污染物（CO 及 HC）及多環芳香烴化合物（PAHs）的污染減量效益。其中該年度粒狀污染物（PM）平均去除效益為 90%，一氧化碳（CO）及碳氫化合物（HC）則無明顯去除效益，而多環芳香烴化合物（PAHs）的濃度平均去除效益為 24%。而 2010 年執行「清潔車輛裝置濾煙器設備採購暨 2009 年濾煙器維修再生計畫」，選擇出廠年份介於 2001 年至 2005 年的 15 輛柴油車輛進行清潔隊柴油車輛裝置濾煙器的示範運行，該年度則針對粒狀污染物（PM）進行濾煙器安裝前後及該柴油車輛行駛 1 年後之效益評估，其中安裝前後之粒狀污染物（PM）平均去除效益為 86%，而行駛 1 年後之粒狀污染物（PM）平均去除效益為 60%。由於 2009 年執行『臺中市清潔隊車輛裝置濾煙器示範運行計畫』所選擇的清潔隊柴油車輛皆為較為老舊之車輛，經過臺中市政府環境保護局針對清潔隊車輛進行汰舊換新的過程後，都已經報廢並將濾煙器拆下待安裝至其他清潔隊車輛，而 2010 年所安裝濾煙器之 15 輛柴油車輛也有 3 輛已經報廢。因此於 2012 年重新選擇 4 輛出廠年份於 2001 年至 2005 年之柴油車輛安裝自報廢車輛拆卸下來之濾煙器，其安裝前後之粒狀污染物（PM）平均去除效益為 98%。臺中市政府環境保護局自 2009 年開始，進行清潔隊柴油車輛安裝濾煙器之污染減量效益評估，在粒狀污染物（PM）的污染減量效益良好，未來亦可針對老舊清潔隊柴油車輛在屆齡報廢前 3 至 5 年安裝濾煙器，以達到污染減量效益，也可以讓市民感受到環保局對所屬柴油車輛管理的用心。

关键字：濾煙器，狀污染物，氣狀污染物，多環芳香烴化合物排放量

二行程機車青白煙檢測與改善成效探討

(劉邦裕¹, 江嘉凌², 鐘文舜², 姜禹丞³, 盧昭暉³)

1 臺中市政府環境保護局, 臺中

2 思維環境科技有限公司, 臺中

3 國立中興大學機械工程研究所, 臺中

摘 要:二行程機車的機油經由曲軸箱隨燃料進入燃燒室中一起燃燒, 因為機油不易揮發, 油滴顆粒較大, 在引擎燃燒室內無法迅速燃燒, 經由排氣系統排放出來, 即形成青白煙。這種青白煙是粒狀污染物的一種, 由於可用肉眼明顯的分辨出來, 為一般民眾所厭惡, 環保署自1999年實施「鼓勵民眾檢舉高污染烏賊車」活動以來, 各地環保局的檢舉信件都以機車為主, 可見機車所排放的青白煙最為一般民眾所關切。

臺中市二行程機車約有 38 萬輛, 佔機車總數 22%, 本研究針對 2011 年曾遭民眾檢舉至少 1 次以上, 且經目測判煙判定為有污染之虞之機車, 列為青白煙通知檢測對象。本研究採實驗方式進行, 直接以惰轉急加速的方式來執行檢測, 並以 Berkeley 300 型不透光率分析儀來進行量測, 機車轉速控制條件為 $5,500 \pm 500 \text{rpm}$, 主要是量測排氣中的不透光率。本研究共檢測 543 輛遭檢舉烏賊車, 其中粒狀污染物檢驗不合格共 154 輛, 占 28.4%, 平均不透光率為 21.5%。更換排氣管、機油泵等老舊零件對二行程機車的不透光率有較明顯的改善, 可使平均不透光率降為 15%。

關鍵字: 二行程機車、不透光率、Berkeley 300

臺中市清潔隊柴油車輛加裝濾煙器試範運行成效探討

(劉邦裕¹，余忠賢²，游雲欽²，陳以松³，盧昭暉³)

1 臺中市政府環境保護局，臺中市，403

2 瑩諮科技股份有限公司，臺中市，407

3 國立中興大學機械工程研究所，臺中市，402

摘要：清潔隊柴油車輛是指垃圾車與資源回收車，這些車輛每天在大街小巷中穿梭往返，負責收集市民所產生的生活垃圾，集中載運至焚化廠處理。由於這些車輛每天都與民眾進行近距離的接觸，其污染排放對民眾的健康影響非常大。臺中市政府環境保護局為減少垃圾車的排煙污染，已擬定計畫，針對污染嚴重的車輛加裝濾煙器。本研究即是進行此做法的成效評估，以引擎動力計檢測及車輛排煙檢測兩種方式進行。

引擎動力計檢測是以一具 6000c.c. 的重型柴油引擎進行，依據五種不同的轉速與負載組合，比較加裝濾煙器後的粒狀污染物排放量以及排氣中的不透光率變化，測試結果發現粒狀污染物排放量可達到 80% 的減量效果，而不透光率則由 30% 降為 2%。

車輛排煙檢測是在臺中市柴油車動力站進行，以全負載定轉速及無負載急加速測試來進行檢測，量測排氣中的黑煙污染度，同時量測後軸輸出馬力。測試結果顯示，加裝濾煙器後煙度可減量 90%。但隨著濾煙器使用時數增加，效率會逐漸下降。馬力測試結果顯示安裝濾煙器後，後輪輸出馬力無明顯差異。但在排氣量較大的車輛，持續使用車輛馬力呈現下降趨勢。

但因使用者須在使用一段期間後將濾煙器再生，否則會影響車輛性能，造成使用者負擔，進而降低使用意願。故如何降低再生的不便利性，是未來推廣濾煙器的關鍵。

關鍵字：柴油車，濾煙器，再生技術，黑煙污染度。

自動貝他計和手動採樣器之 $PM_{2.5}$ 量測結果差異探討

(劉俊男¹, 亞瓦希 阿米¹, 洪毅弘¹, 蔡春進^{1,*}, 巫月春², 陳重方²)

1 國立交通大學環境工程研究所, 臺灣, 30010;

2 行政院環境保護署環境檢驗所, 臺灣, 32024

摘 要: 本研究以一部雙通道採樣器(Dichotomous sampler, Dichot, Model SA241, Andersen Inc., Georgia, USA)及一部貝他計(beta attenuation monitor, BAM, Model 1020, Met One Instruments Inc., Washington, USA)在台灣北部的新莊及竹東空氣品質監測站進行大氣 $PM_{2.5}$ 質量濃度的比對採樣。採樣結果顯示, 貝他計在新莊及竹東測站的 $PM_{2.5}$ 濃度監測值($PM_{2.5,B}$)會分別較雙通道採樣器所量測到的 $PM_{2.5}$ 濃度($PM_{2.5,D}$)高出 29.78 及 28.42 %。本研究另外以兩部分別放置玻璃纖維及鐵氟龍濾紙的 Dichots 在交通大學校園進行採樣比對, 結果顯示前者所測得的 $PM_{2.5}$ 濃度($PM_{2.5,DG}$)高出後者($PM_{2.5,DT}$)約 24.3 %, 此誤差也和上述在新莊及竹東測站 $PM_{2.5,B}$ 和 $PM_{2.5,D}$ 之間的誤差相近。 $PM_{2.5,DG}$ 和 $PM_{2.5,DT}$ 樣本的化學分析結果則顯示, $PM_{2.5,DG}$ 較 $PM_{2.5,DT}$ 高出的總無機離子濃度和兩者之間的質量濃度差異相近, 且這些額外多出的離子中又以硫酸根及硝酸根為主。由上述實驗結果可知, BAM 和 Dichot 之間的採樣誤差主要係由 BAM 所使用之玻璃纖維濾紙吸附酸性氣體所造成, 其中又以二氧化硫及硝酸為主要的吸附氣體。本研究也另外估算了採樣期間的大氣含水量以及 BAM 和 Dichot 於採樣過程中樣本上揮發性硝酸銨的揮發量, 結果顯示兩者對 $PM_{2.5,B}$ 和 $PM_{2.5,D}$ 之間採樣誤差並無顯著的影響。

關鍵字: 貝他計, 雙通道採樣器, $PM_{2.5}$ 採樣誤差, 玻璃纖維濾紙。

福建省大气污染物排放清单的初步估算研究

(鲁斯唯¹, 吴水平¹, 陈晓秋²)

1 厦门大学环境与生态学院, 厦门, 361102;

2 福建省环境监测中心站, 福州, 350003

摘 要: 本研究在 2007 年污染源普查数据基础上, 结合统计年鉴中工业消耗数据进行动态更新, 以 2009 年为基准年, 从工业活动、居民生活等多个方面对福建省大气污染物 SO_2 、 NO_x 、 $\text{PM}_{2.5}$ 、 VOC_s 和 NH_3 在内的大气污染物的排放量进行估算, 建立了福建省大气污染物排放清单。结果显示, 污染物排放较高的地区主要集中在沿海区域, 如福州、泉州和漳州, 而植被覆盖率高南平和三明的 VOC_s 排放量也较高。工业排放是 SO_2 的主要污染源, 占 SO_2 排放总量的 63.6%, 电厂排放是 NO_x 和 $\text{PM}_{2.5}$ 的主要排放源, 机动车是 NO_x 最主要污染源, 占排放总量的 34.11%, 机动车污染应引起重视。

近 50 年中国气溶胶光学厚度反演及长期变化特征的分析

(罗建国 吴润)

(云南大学资源环境和地球科学学院, 昆明, 650091)

摘 要: 本文选用了中国 1960-2009 年的逐日平均水汽压和水平能见度资料, 在已有的利用能见度反演光学厚度方法的基础上, 以 2001-2009 年卫星资料 MISR level3 逐月气溶胶光学厚度为标准, 利用多元非线性回归方法订正了反演方案中的参数, 对比了订正参数后与原方案的反演结果。此后, 利用订正后的参数反演了 1960-2009 年中国地区逐日气溶胶光学厚度, 分析了我国气溶胶光学厚度时空分布与季节特征。结果表明: 2001-2009 年间订正参数后的反演方案在空间分布与气溶胶光学厚度值的大小上更加接近 MISR 观测值, 同时能够较好的反映光学厚度的极值情况, 改进后反演方案平均相对误差均在 20%以内。中国地区气溶胶光学厚度近 50 年总体呈增加趋势, 其中 1960-1978 年增加率较 1978-1999 年快, 而 2000-2007 年增加率更快, 2008 年后气溶胶光学厚度开始下降。近 50 年夏季气溶胶光学厚度最高, 最高值出现在 2003 年, 年平均值为 0.32-0.34。春秋两季次之, 最低的是冬季。春秋两季气溶胶光学厚度空间分布相似, 大值区出现在四川盆地、长江中下游、两广地区以及新疆南部, 夏季大值区出现在北方、冬季大值区出现在南方。2000 年前大城市气溶胶光学厚度增长速度较小城市快, 2000 年后相反。

关键词 能见度, 气溶胶, 光学厚度, 反演

利用影像處理技術評估大氣能見度與 PM2.5 之關係

(羅金翔¹、楊心豪^{2*}、黃筱茜²、王嗣涵¹)

1 弘光科技大學環境工程研究所、臺灣

2 稻江科技暨管理學院通識教育中心、臺灣

摘 要：本研究建立能見度與影像監測之中尺度即時測系統，同時評估懸浮微粒 PM2.5、能見度與大氣影像指標之關係。分別於中科四期二林園區及沙鹿地區進行手動 PM2.5 採樣、擷取能見度及影像指標數值，並將手動 PM2.5 採樣數據與鄰近環保署測站 PM2.5 數值進行回歸分析，研究成果發現，懸浮微粒 PM2.5 與能見為負相關之關係，與影像指標值呈現正相關，顯示當能見度越高時懸浮微粒濃度為越低的，影像指標之處理結果亦同；梧棲氣象站之能見度與沙鹿監測站資料分析之結果，顯示能見度與 PM2.5 呈現負相關趨勢，顯示當能見度越高時 PM2.5 為越低的；手動採樣與自動測站採樣資料之關係，其結果為兩地區懸浮微粒濃度，都為自動測站值較手動採樣值為高。

關鍵字：能見度，PM2.5，影像處理

混合气溶胶吸湿性研究

(马庆鑫¹, 刘畅², 马金珠¹, 贺泓¹)

1 中国科学院生态环境研究中心, 北京, 100085;

2 中国气象科学研究院, 北京, 100081

摘 要: 气溶胶颗粒物在大气中广泛存在, 对人体健康具有负面影响, 也是全球气候变化模式预测最不确定的因素之一¹。因此, 研究气溶胶颗粒在大气传输过程中的各种物理化学性质变化, 尤其是对吸湿性的研究, 对于进一步认识气溶胶颗粒的健康效应和气候效应具有重要的意义。

大气颗粒物通常是多种组分以外混或者内混状态存在。以往关于颗粒物的吸湿性研究, 通常只研究水蒸气在单一组分颗粒物表面的吸附和脱附过程; 在混合组分吸湿性的研究中, 也很少涉及颗粒物中不同组分在吸湿过程中的相互影响。

二元羧酸是大气气溶胶中有机酸的主要成分, 也是大气有机气溶胶的重要组成部分。二元羧酸被认为是有效的云凝结核, 能够参与成云过程, 影响大气辐射平衡^[2]。外场观结果表明, 二元羧酸在大气中常常与矿质颗粒物或者海盐气溶胶混合^[3,4]。虽然对于二元羧酸、矿质颗粒物或海盐气溶胶的单一组分的吸湿性已经有很多研究, 但是对于这些组分的混合颗粒物的吸湿性还少见报道。在本研究中, 我们采用拉曼光谱仪和水蒸气吸附仪研究了二元羧酸与矿质颗粒物以及海盐颗粒物的混合物的吸湿性。

研究表明, 乙二酸与 $\text{Ca}(\text{NO}_3)_2$ 的混合物在吸湿过程中能够发生反应, 使得酸性较弱的乙二酸能够置换酸性较强的硝酸, 从而极大地改变混合物的吸湿性^[5]。而 NaCl 与二元羧酸在吸湿过程中的反应可能性取决于二元酸的酸性。 NaCl 与乙二酸混合物在吸湿过程中发生化学反应, 形成乙二酸钠, 明显的降低颗粒物在高相对湿度下的吸水量; NaCl 与丙二酸混合物在吸湿过程中反应较弱, 对混合颗粒物在高相对湿度下的吸水量影响不明显, 但是混合物的潮解点明显降低; NaCl 与丁二酸混合物在吸湿过程中没有反应发生, 对吸湿性也没有明显影响。本研究结果对于认识矿质气溶胶、海盐气溶胶与有机气溶胶混合物的吸湿性具有重要意义。

关键字: 海盐; 二元羧酸; 混合物; 吸湿性; 复合效应

参考文献

1. IPCC, Climate Change 2007
2. Yu, S., *Atmos. Res.*, 2000, 53, 185-217.
3. Sullivan, R. C.; Prather, K. A., *Environ. Sci. Technol.* 2007, 41 (23), 8062-8069.
4. Alexander Laskin, R. C. M., Mary K. Gilles, Jerome D. Fast, Rahul A. Zaveri, Bingbing Wang, Pascal Nigge, Janani Shutthanandan, *J. Geophys. Res.* **2012**, 117, D15302.
5. Ma, Q., and He, H., *Atmos. Environ.*, 2012, 50, 97-102.

雾化液滴对湿法采集纳米 TiO₂ 气溶胶的影响研究

(茆平¹², 冯曙艳¹, 杨毅^{12*}, 刘梦楚¹, 周阳¹, 陈守文¹², 王正萍¹²)

1 南京理工大学环境与生物工程学院, 南京, 210094

2 南京理工大学连云港研究院, 连云港, 222006

摘要: 为掌握雾化液滴对提高湿法采样器对纳米气溶胶采集效率的影响作用, 考察了不同喷雾流量和雾化室尺寸对采集效率的影响, 并通过 Fluent 软件仿真模拟不同尺寸雾化室内雾化液滴的运动状况, 了解液滴对湿法采集的影响机理。研究表明, 雾化室中的液滴作用以润湿包覆为主, 而储液腔中的液滴主要以碰撞凝并实现对气溶胶粒子的捕获, 润湿包覆对纳米 TiO₂ 气溶胶粒子的采集效果大于碰撞凝并的捕获效果。当雾化室和储液腔的喷雾流量均控制为 40ml/min 时, 湿法采样器的采集效率可达到最高(92%)。仿真和实验结论均表明, 雾化室的最佳尺寸是高度 170mm、内径 60mm。

关键词: 湿法采样器, 雾化液滴, 采集效率, 仿真模拟

***基金项目:** 江苏省环保厅环保科研项目 (No.2012015)、连云港社会发展科技项目 (No.SH1203)、连云港科技基础建设项目 (No.JC1203) 南京理工大学连云港研究院自主科研项目 (No.NUSTLYG-2012-001)

作者简介: 茆平, 男, 1987.10, 博士研究生。

通讯作者: 杨毅, 男, 1973.10, 副研究员, 博士生导师。主要从事微纳米气溶胶检测技术研究。E-mail: yyi301@163.com

Water-soluble secondary organic aerosol in Qinghai Lake: implication for sources, formation, and degradation during long-range transport

(Jingjing Meng¹, Gehui Wang^{1,2,*}, Jianjun Li¹, Chunlei Cheng¹, Junji Cao¹)

¹ State Key Laboratory of Loess and Quaternary Geology, Institute of Earth Environment, Chinese Academy of Sciences, Xi'an 710075, China

² School of Human Settlements and Civil Engineering, Xi'an Jiaotong University, Xi'an 710049, China

Abstract: PM_{2.5} aerosol sampling for collection of 24 h samples was carried out every day from Qinghai Lake (3200m a.s.l.), a remote continental site in the northeastern part of Tibetan Plateau from July to August 2010. To better understand the production of water-soluble organic aerosols, the samples were analyzed for water-soluble dicarboxylic acids (C₂-C₁₁) and related compounds (ketocarboxylic acids and α -dicarbonyls), as well as organic carbon (OC), elemental carbon (EC), water-soluble organic carbon (WSOC), and water-soluble inorganic ions. Distributions of dicarboxylic acids and related compounds were characterized by a predominance of oxalic acid (29.3 – 347.6 ng m⁻³, 148.2 \pm 83.9 ng m⁻³) followed by malonic (9.3 – 77.6 ng m⁻³, 27.2 \pm 15.5 ng m⁻³) and succinic (3.6 – 29.3 ng m⁻³, 14.5 \pm 8.0 ng m⁻³) acids. The average contributions of diacids, ketoacids and dicarbonyls to WSOC were 44.1%, 1.3%, and 0.4 %, respectively. They were several times higher than those reported in north-western cities from which air masses were transported to the Qinghai Lake, indicating an importance of photochemical processing of aerosols during a long-range transport. The diacids/WSOC and C₉/diacids ratios were higher than those reported previously in different atmosphere aerosols, which may indicate that the local aerosols were chiefly influenced by the biomass burning (herbages and dung) and photochemical oxidations were enhanced because of the stronger solar radiation. This study demonstrated that diacids were primarily produced by the secondary photochemical oxidation of organic pollutants and ω -oxoacids were likely intermediates to the production of dicarboxylic acids.

Keywords: Oxalic acid; secondary organic aerosols; PM_{2.5}; Qinghai Lake

Particle size distribution and characteristics of Polycyclic Aromatic Hydrocarbons during an autumn haze episode in Nanjing, China

(Qingzi Meng¹, Shuxian Fan^{1,2}, Fan Zu¹, Jiabao He¹, Jian Zhang¹, Yu Sun¹)

1. Department of Atmospheric Physics, Nanjing University of Information Science and Technology, Nanjing 210044, China

2. Key Laboratory for Meteorological Disaster, Ministry of Education, Nanjing University of Information Science and Technology, Nanjing 210044, China

Abstract: The purpose of this study is to understand the characteristics of pollution and distribution of polycyclic aromatic hydrocarbons (PAHs) in fine (PM_{2.1}) and coarse (PM_{2.1-10}) particles at suburban and city site during an autumn haze episode in Nanjing. PM₁₀ samples were collected from Nov. 1, 2009 to Nov. 14, 2009. Filter samples were extracted by using Soxhlet and analyzed by using a gaseous chromatograph/mass spectrometer (GC-MS). Sixteen PAHs were measured at day and night of suburban and city site in this study. The results show that the concentrations of particles could be as high as 579.55 and 573.43 μg/m³ at suburban and city site during the haze episode, it was 3-4 times higher than normal days and the proportion of fine particles in the haze episode was also higher than normal days; the varies of concentration of PAHs were in accord with the concentration of particles. The concentrations of particles and PAHs at night were higher than in the daytime both at city and suburban site during the haze episode; the main kinds of PAHs in particles were the high-molecular-weight PAHs which make up approximately 80% of the total PAHs no matter in normal days or haze episode. It also turns out that wet removal mechanism has strong scavenging ability for pollutants, especially for the fine fraction; the spectral distribution of PAHs was the transfer of coarse fraction to fine fraction and this phenomenon was most obvious at night at city site, which indicates that the emission sources and the condition of boundary layer play important roles in the distribution and concentration of PAHs; the concentration of CAN-PAHs is relatively higher at both sampling sites and periods, the highest proportion of CAN-PAHs appear at the night of city site, it was as high as 52% of total PAHs, it is higher risk exposures for the people in Nanjing.

Keywords: Polycyclic aromatic hydrocarbons; Haze episode; Particle size distribution; Meteorological conditions; Nanjing

Ambient Ammonia and Ammonium Observed at a Remote Mountain Site in Western China

(Zhaoyang Meng¹, Xiaofang Jia², Jianzhong Ma¹, JianQiong Wang³, Xiaolan Yu¹, YiAn Jiang⁴)

¹ Key Laboratory for Atmospheric Chemistry of CMA, Institute of Atmospheric Composition, Chinese Academy of Meteorological Sciences, Beijing 100081, China.

² CMA Meteorological Observation Centre, Beijing 100081, China

³ Qinghai Province Meteorological Bureaus, Xining 810001, China

⁴ Department of Logistic Service, Ministry of Railways of China, Beijing 100844, China

Abstract: Ammonia is a very reactive gas and plays a major role in the neutralization of atmospheric sulfuric and nitric acid to form ammonium salts, thereby affecting the acidity of cloud water and aerosols.¹⁻⁴ Some studies show that the spatial variability of the NH₃ concentration was large in China, with higher levels in North, Southwest and East China.⁵⁻⁶ The measurements of NH₃ and PM_{2.5}, particularly those from the background sites, are highly needed but have been scarcely reported. It is important to create databases suitable for the proper validation of models used to predict global or regional distributions of ammonia and ammonium aerosol, and their present and future influences on climate, human health, and ecosystems. The data of NH₃ and PM_{2.5} may also be useful in the validation of satellite measurements.

With an average altitude of over 4000 m, the Qinghai-Tibetan Plateau is the highest landmass on Earth, and plays a key role in atmospheric circulation. The atmosphere lying over the Plateau is probably the least affected by human activities in the Asian continent because of the sparse population and minimal industrial activities in western China.⁷ In this paper, we present the measurements of NH₃, SO₂, NO₂ and PM_{2.5} at a site in the northeastern edge of Plateau during 2009-2011 in order to better understand the sources of ammonia and ammonium aerosol over the remote highlands of western China. The levels and variations of these species are reported and the relative contributions of NH₃ to NH_x deposition are also investigated.

Keywords: Ammonia, ammonium, a remote mountain site in China

西安水溶性类腐殖质气溶胶 (HULIS) 的污染特征及其来源

(倪海燕¹, 韩永明^{2*}, 曹军骥²)

1 西安交通大学, 西安, 710049;

2 中国科学院地球环境研究所, 西安, 710075

摘 要: 类腐殖质气溶胶 (HULIS) 是大气有机气溶胶的主要组成部分, 对云凝结核的形成和气溶胶吸湿性增长至起着重要作用, 但是 HULIS 的性质和来源在很大程度上仍是未知的。本文使用固相萃取法获得了 2008 年 7 月至 2009 年 8 月间西安 PM_{2.5} 中的 HULIS, 并采用热光法获得 HULIS 的碳含量 (HULIS-C)。HULIS-C 年均质量浓度为 $3.1 \pm 3.0 \mu\text{gC m}^{-3}$ 。HULIS 含量冬季最高 ($6.2 \mu\text{gC m}^{-3}$), 秋季次之 ($3.3 \mu\text{gC m}^{-3}$)、夏季 ($1.5 \mu\text{gC m}^{-3}$) 和春季较低 ($1.2 \mu\text{gC m}^{-3}$)。冬季高浓度的主要原因是冬季能源消耗量大, 比如燃煤和生物质燃烧; 而春夏季低浓度主要是由于较少的能源消耗和较丰富的降水。HULIS 是水溶性有机碳 (WSOC) 的重要组分, 占 WSOC 的 34.5%, 表明其是影响 WSOC 吸湿性的重要组分; 相关性分析表明, HULIS 与左旋葡聚糖 ($r=0.84$) 和 K^+ ($r=0.81$) 呈显著相关, 说明 HULIS 主要来源于生物质燃烧; 此外, HULIS 与二次有机碳 (SOC) 相关性良好 ($r=0.83$), 表明 HULIS 同时有二次来源。

关键字: 类腐殖质气溶胶, HULIS, PM_{2.5}, 西安

乌鲁木齐市大气 PM_{2.5} 和 PM_{2.5-10} 中有机碳、元素碳的粒径分布及季节性分布

(热比古力·达木拉¹, 迪丽努尔·塔力甫¹, 王新明², 丁翔², 阿不力孜¹·伊米提¹)

¹ 新疆大学化学化工学院, 新疆 乌鲁木齐 830046; 2. 中国科学院广州地球化学研究所, 广东 广州 510640

摘要: 采用 NL20 型级式采样器, 于 2011 年 1 月至 2011 年 12 月, 在乌鲁木齐市新疆科学院院内设置采样点, 采集 PM_{2.5} 和 PM_{2.5-10} 样品。并用碳分析仪测定样品中有机碳(OC)和元素碳(EC)的含量, 考察了有机碳和元素碳的季节变化特征及粒径分布特征。研究表明: PM_{2.5} 中的 OC 和 EC 浓度变化范围为 3.3~61.8, 0.7~4.9 (μg/m³), PM_{2.5-10} 为 1.1~7.3, 0.1~2.5 (μg/m³), 其中冬季 PM_{2.5} 的质量浓度(299.3 μg/m³)、PM_{2.5} 中的 OC 浓度(29.3 μg/m³)、PM_{2.5-10} 的质量浓度(116.5 μg/m³)、PM_{2.5-10} 中 OC 浓度(3.9 μg/m³)均为四个季节中最高, 即 PM_{2.5} 和 PM_{2.5-10} 中的 OC 和 PM_{2.5-10} 中的 EC 浓度相同地呈现出冬季>秋季 > 春季>夏季的季节变化特征, 而 PM_{2.5} 中 EC 则有冬季>秋季 >夏季 >春季的季节变化特征; 在乌鲁木齐市冬季, 采暖燃烧的煤是 OC 和 EC 的主要贡献源, 造成 OC 大大高于 EC, 从而使 OC / EC 比值增大。各种气象条件对 PM_{2.5}、PM_{2.5-10}、OC、EC 和 OC/EC 比值的变化都有不同程度的影响, 特别是大雾天气、相对湿度、风速和降雪是影响碳气溶胶浓度变化的重要因素。

关键词: PM_{2.5}, PM_{2.5-10}, 有机碳; 元素碳, 乌鲁木齐

Characterization on Carbonaceous Aerosols in PM_{2.5} and PM_{2.5-10} in Urumqi, China

Rabigul Damulla¹, Dilnur talip¹, wang xin ming²

(¹ College Of Chemistry And Chemical Engineering, Xinjiang University, Analysis Chemistry 830046, china)

(² State Key Laboratory of Organic Geochemistry, Guangzhou Institute of Geochemistry Chinese Academy of Sciences, Guangzhou 510640, China)

Abstract: Chemical characteristics and possible sources of fine particular matter (PM_{2.5}, PM_{2.5-10}) was investigated for 1 year in Urumqi. PM_{2.5} and PM_{2.5-10} was collected from January 2011 to December 2011. which carbonaceous species, organic carbon (OC) and elemental carbon (EC), in the samples were analyzed. Seasonal variations of OC and EC concentrations were investigated; results showed that carbonaceous concentrations varied in wide ranges with 10.3 ~ 559.0 (μg/m³) for PM_{2.5}, 16.7 ~ 218.8 (μg/m³) for PM_{2.5-10}. carbonaceous concentrations varied in wide ranges with 3.3~61.8 and 0.7~4.9 (μg/m³) for OC and EC in the PM_{2.5}; Carbonaceous concentrations varied in wide ranges with 1.1~7.3 and 0.1~2.5 (μg/m³) for OC and EC in the PM_{2.5-10}. On seasonal average, the highest PM_{2.5} (299.3 μg/m³) and OC (29.3 μg/m³) levels; PM_{2.5-10} (116.5 μg/m³) and OC (3.9 μg/m³) levels occurred during winter. The seasonal average concentrations of PM_{2.5} and PM_{2.5-10} organic carbon levels ranked by the order of winter > autumn > summer > spring, while the seasonal

average concentrations of EC(PM_{2.5-10}) were in the order of winter >autumn >spring > summer. The average OC/EC ratio 6.1 for PM_{2.5} or PM_{2.5-10} was comparable with most urban cities in the world .the stronger correlation between OC and EC ($R>0.8$) ,showed that there were similar OC and EC emissions in Urumqi .

Key words : PM_{2.5}; PM_{2.5-10}; Organic Carbon ; Elemental Carbon ;Urumqi

武汉市雾霾期间 $\text{PM}_{2.5}$ 浓度和气象因子对能见度影响分析

(沈龙娇¹, 王建民², 胡珂³)

武汉市环境监测中心站, 武汉 430015;

摘要: 为了研究颗粒物、气象因子对武汉市大气能见度的影响, 于 2013 年 1 月 1 日~2013 年 1 月 31 日对武汉市大气能见度、 $\text{PM}_{2.5}$ 、相对湿度、温度、大气压、风速进行监测。结果表明, $\text{PM}_{2.5}$ 对能见度的影响最大, 相对湿度次之, 再次是风速, 而气温对能见度的影响较小。不同的相对湿度下, 武汉市 $\text{PM}_{2.5}$ 对能见度的影响不同。研究认为, 提高武汉地区大气能见度, 重点在于减少武汉市大气中气溶胶的形成。

关键字: 能见度, $\text{PM}_{2.5}$, 相对湿度, 相关性, 武汉市

Abstract: In order to study the effects of particles and meteorological factor on visibility in Wuhan. Visibility, $\text{PM}_{2.5}$, RH, Temperature, Atmospheric pressure and wind speed were measured during 1st~31st January, 2013 in Wuhan. The results show that: The $\text{PM}_{2.5}$ mass concentration has a significant relationship with visibility, relative humidity, wind speed is once again, and the temperature effect on visibility. The effect of $\text{PM}_{2.5}$ on visibility was different in several visibility sections in Wuhan. Therefore, The emphasis which should be reduced is the formation of aerosols in the atmosphere to increase the visibility in Wuhan.

Key words: visibility, $\text{PM}_{2.5}$, relative humidity, correlation, Wuhan

Seasonal and day-night variations of chemical species in PM₁₀ over Xi'an, China: Implications of water-soluble organic carbon (WSOC) sources

(Zhenxing Shen^{a,b,*}, Junji Cao^b, Qian Zhang^a, Jianjun Li^b, Suixin Liu^b)

^aDepartment of Environmental Science and Engineering, Xi'an Jiaotong University, Xi'an 710049, China

^bKey Laboratory of Aerosol, SKLLQG, Institute of Earth Environment, Chinese Academy of Sciences, Xi'an 710075, China

^cAir Quality Research Division, Science and Technology Branch, Environment Canada, Toronto, Canada

*Author to whom correspondence should be addressed. E-mail: zxshen@mail.xjtu.edu.cn (Zhenxing Shen)

Abstract: To investigate the seasonal and day-night variation of PM₁₀ chemical species, daytime and nighttime PM₁₀ mass, water-soluble ions (Na⁺, NH₄⁺, K⁺, Mg²⁺, Ca²⁺, F⁻, Cl⁻, NO₃⁻, and SO₄²⁻), organic carbon (OC), elemental carbon (EC), and water-soluble carbon (WSOC) were acquired at a urban site of Xi'an from 20 December 2006 to 12 November 2007. No dramatic differences were found in PM₁₀ or chemical species loadings between daytime and nighttime. In general, PM₁₀ concentrations were in excess of 1.5 times to China Ambient Air Quality Standard (CAAQS) for 24-h average PM₁₀ (150 µg m⁻³). Carbonaceous fractions and water-soluble ions accounted for nearly one-third and 12.4% of the PM₁₀ mass. Relative Low NO₃⁻/SO₄²⁻ ratio suggested that stationary source emissions were more important than the vehicle emissions in the source areas in Xi'an, China. Good correlation between WSOC and OC were observed, which indicated that they might derive from the similar origin, such as primary emission sources or secondary processes. Moreover, a strong relationship between WSOC and K⁺ was observed in winter, which implies winter WSOC were mainly from biomass burning. This was also highlighted by the chemical components results of biomass burning events. In contrast, poor correlation between WSOC and K⁺ in summer indicated WSOC was mainly of Secondary organic carbon contribution from strong photochemical activity.

Keywords: PM₁₀, water-soluble ions, WSOC

Aerosol Variations in Boundary Atmospheres: Review and Prospect

(Shi Guangyu and Chen Bin)

Institute of Atmospheric Physics, Chinese Academy of Sciences, Beijing 100029, China

Abstract: Atmospheric aerosols play important roles in climate and atmospheric chemistry: They scatter sunlight, provide condensation nuclei for cloud droplets, and participate in heterogeneous chemical reactions. To enable better understanding of the vertical physical, chemical and optical features of the aerosols in East Asia, using some atmospheric and aerosol measurement instruments on board a kind of tethered-balloon system, a series of measurements were operated in some typical areas of East Asia, including Dunhuang, which is located in the source origin district of Asian dust and Beijing, which is the representative of large inland city during the years of 2007-2011. Mineral composition and microbial components carried by the airborne particles were both analyzed. Moreover, the simultaneous observations over the districts of China, Japan and Korea supported by an international cooperative project are highly expected.

References:

CHEN Bin, YAMADA Maromu, SHI Guangyu, ZHANG Daizhou MATSUKI Atsushi and IWASAKA Yasunobu, Vertical Changes in Mixing State of Aerosol Particles in the Boundary Layer in Beijing, China: Balloon-borne Measurements in Summer and Spring: *Journal of Ecotechnology Research*, 17(1),1-9(2013)

Daizhou Zhang, Bin Chen, Maromu Yamada, Hongya Niu, Biao Wang, Yasunobu Iwasaka and Guangyu Shi, Elevated Soot Layer in Polluted Urban Atmosphere: a Case Study in Beijing. *Journal of the Meteorological Society of Japan*, Vol. 90, No. 3, pp. 361–375, 2012

G. Shi, D. Zhang, B. Wang, B. Chen, M. Yamada, and H. Niu. Elevated aerosol layer embedded with aged soot particles in a polluted urban atmosphere. *Atmos. Chem. Phys. Discuss.*, Vol. 11(2011), p1641-1669.

Bin Chen, Fumihisa Kobayashi, Maromu Yamada, Yang-Hoon Kim, Yasunobu Iwasaka and Guang-Yu Shi, Identification of Culturable Bioaerosols Collected over Dryland in Northwest China: Observation using a Tethered Balloon. *Asian Journal of Atmospheric Environment*, Vol. 5-3, pp.172-180, September 2011

Bin Chen, Guang-Yu Shi, Maromu Yamada, Dai-Zhou Zhang, Masahiko Hayashi and Yasunobu Iwasaka Dependence of Visibility on Particle Sizes in Different Boundary Layers over Beijing. *Asian Journal of Atmospheric Environment*, Vol. 4-3, pp.141-149, December 2010

青岛市区春、夏季生物气溶胶浓度及影响因子分析

(宋志文^{**}, 吴等等, 钱生财, 徐爱玲, 夏岩)

青岛理工大学环境与市政工程学院, 青岛, 266033

摘要: 为了解青岛市生物气溶胶分布特征和影响因子, 采用 SAS ISO100 空气浮游菌采样仪和安德森 FA-I 型六级空气微生物取样器, 分析青岛市市区街道春、夏季空气细菌和空气真菌浓度、粒径分布及环境因子对空气微生物浓度的影响。结果表明, 青岛市区春季空气细菌和空气真菌浓度分别为 $596.6 \text{ cfu}\cdot\text{m}^{-3}$ 、 $797.4 \text{ cfu}\cdot\text{m}^{-3}$, 夏季分别为 $280.9 \text{ cfu}\cdot\text{m}^{-3}$ 、 $250.9 \text{ cfu}\cdot\text{m}^{-3}$, 春季空气细菌和空气真菌浓度均高于夏季; 春季和夏季空气细菌粒径均呈偏态分布, 空气真菌粒径呈对数正态分布; 春季空气细菌、空气真菌粒子中值直径分别为 $4.6\mu\text{m}$ 和 $2.2\mu\text{m}$, 夏季分别为 $4.1\mu\text{m}$ 和 $1.9\mu\text{m}$, 春季空气细菌和空气真菌中值直径均大于夏季。空气细菌浓度与温度呈正相关, 空气真菌浓度随着温度升高而增加, 温度到达 25°C , 随温度增加有下降趋势; 空气细菌浓度与湿度正相关, 空气真菌浓度与湿度负相关; 一定范围内, 空气细菌、空气真菌浓度随风速增大而升高, 达到一定程度后, 随风速增加开始降低。

关键词: 空气细菌, 空气真菌, 浓度, 粒径分布, 环境因子, 青岛

Concentration and Influence Factors Analysis of Airborne Microbes in Spring and Summer in Qingdao.

SONG Zhi-wen^{**}, WU Deng-deng, QIAN Sheng-cai, XU Ai-ling, XIA Yan

(Institute of Environment and Municipal Engineering, Qingdao Technological University, Qingdao 266033, China).

Abstract: To determine the concentrations and influencing factors of bioaerosol in Qingdao, airborne microbes were collected by SAS ISO100 and Andersen Six Stage Sampler in city streets. Concentrations of airborne bacteria and airborne fungi, size distributions, and influence of environmental factors on airborne microbe concentrations were studied systematically. The results showed that the average concentrations of airborne bacteria and airborne fungi were $596.6 \text{ cfu}\cdot\text{m}^{-3}$, $797.4 \text{ cfu}\cdot\text{m}^{-3}$ in spring, and $280.9 \text{ cfu}\cdot\text{m}^{-3}$, $250.9 \text{ cfu}\cdot\text{m}^{-3}$ in summer, respectively. The average concentrations of airborne bacteria and airborne fungi were higher in spring than those in summer. The particle sizes of airborne bacteria were plotted with skew distribution, and those of airborne fungi with normal logarithmic distribution. The median diameters of airborne bacteria and airborne fungi were $4.6\mu\text{m}$ and $2.2\mu\text{m}$ in spring and $4.1\mu\text{m}$ and $1.9\mu\text{m}$ in summer. The median diameters of airborne bacteria and airborne fungi were larger in spring than in summer. The concentration of airborne bacteria was positively correlated with temperature. Concentration of airborne fungi increased with temperature, but when temperature reached 25°C , began to decrease with temperature. The concentration of airborne bacteria and humidity had a positive correlation while the concentration of airborne fungi and humidity had a negative correlation. Within a certain range, the airborne bacteria and airborne fungi concentrations increased with wind velocity but upon reaching a certain level, begun to decrease.

Key words: airborne bacteria; airborne fungi; concentration; size distribution; environmental factor; Qingdao

Column-integrated aerosol optical properties over Xi'an, China

(Xiaoli Su¹, Junji Cao^{1,2}, Zhengqiang Li³, Meijing Lin⁴, Gehui Wang¹)

¹ Key Laboratory of Aerosol Science & Technology, SKLLQG, Institute of Earth Environment, Chinese Academy of Sciences, Xi'an 710075, China,

² Department of Environmental Science and Engineering, Xi'an Jiaotong University, Xi'an 710049, China,

³ Institute of Remote Sensing and Digital Earth, Chinese Academy of Sciences, Beijing 100101, China,

⁴ Zhongshan Bureau of Meteorology, Zhongshan 528400, China.

Abstract: Column-integrated aerosol optical properties were derived systematically for the first time from the measurements of a ground-based CIMEL sun photometer in Xi'an from May to November, 2012. Aerosol Optical Depth (AOD), Angstrom exponent, water vapor content and inversed aerosol optical and micro-physical properties, including aerosol volume size distribution, complex refractive indices and single scattering albedo (SSA), were analyzed in this study. Evolution of daily AOD at 440 nm (τ_{440}) was compared with that of 24-hr mean concentrations of PM_{2.5}. Statistics of monthly means calculated from quality-assured daily AOD, Angstrom exponent ($\alpha_{440-870}$) and water vapor content (C_w) were presented and discussed. August showed the highest monthly τ_{440} with the value of 1.13, while the largest monthly $\alpha_{440-870}$ (1.30) and C_w (4.28) appeared both in July. Monthly variations of size distribution were investigated and indicated the domination of coarse mode aerosols in most of the studied months, except July and August, when the contribution of accumulation and coarse mode were fairly comparable. Monthly variability of complex refractive index (including both real and imaginary parts) and single scattering albedo was also studied, along with their wavelength dependence, which implied the variance in aerosol types for different months. Finally, an episode, involving urban and dust aerosols, was analyzed using aerosol retrievals from sun photometer, while MODIS images captured by Aqua satellite and average wind vectors from the NCEP operational global analyses were considered in the case study.

Keywords: Aerosol Optical Depth; Angstrom Exponent; water vapor content, aerosol optical properties, sun photometer

The molecular composition and mass-size distribution of biogenic secondary organic aerosol from Xi'an

(SUN Tao, WANG Ge-hui, LI Jian-jun)

State Key Laboratory of Loess and Quaternary Geology, Institute of Earth and Environment, Chinese Academy of Sciences, Xi'an 710075, China.

Abstract: In this study, concentration and size distribution of biogenic secondary organic aerosols (i.e., isoprene, pinene and sesquiterpene photooxidation products) in the summertime atmosphere of Xi'an city, China was characterized using a GC/MS technique after a conversion to TMS derivatives. Our results showed that BSOA in Xi'an are dominated by isoprene oxidation products, which accounted for around 80% of the total quantified BSOA. Biogenic secondary organic carbon derived from isoprene, α - β -pinene and sesquiterpene were $0.39\mu\text{g C/m}^3$, $0.13\mu\text{g C/m}^3$, $0.10\mu\text{g C/m}^3$, respectively. Size distributions of the nine determined compounds suggest that BSOA in the city are enriched in fine particles. Compared to that in other cities and mountain areas the relatively lower ratio of MBTCA/CPA ratio of Xi'an BSOA indicates that BSOA in the city are mostly derived from local sources and more fresh.

Key words: biogenic secondary organic aerosol; isoprene; α - β -pinene; sesquiterpene; molecular composition; size distribution

An Observational Study of the Hygroscopic Properties of Aerosols over the Pearl River Delta Region

(Haobo Tan^{a,b}, Yan Yin^a, Xuesong Gu^a, Fei Li^b, P.W. Chan^d, Hanbing Xu^c, Xuejiao Deng^b)

^a Institute of Tropical and Marine Meteorology, China Meteorological Administration, Guangzhou, Guangdong 510080, China

^b Key Laboratory for Aerosol-cloud-precipitation of China Meteorological Administration, Nanjing University of Information Science and Technology, Nanjing 210044, China;

^c Experimental Teaching Center, Sun Yat-sen University, Guangzhou 510275, China

^d Hong Kong Observatory, Hong Kong, China

Abstract :Hygroscopic growth can significantly affect size distribution and activation of aerosol particles, as well as their effects on human health, atmospheric visibility, and climate. In this study, a H-TDMA (Hygroscopic Tandem Differential Mobility Analyzer) was utilized to measure hygroscopic growth factor and mixing state of aerosol particles at the CAWNET station in Panyu, Guangzhou, China. A statistical analysis of the results show that, at relative humidity (RH) of 90%, for less-hygroscopic particles of 40-200 nm in diameter, the growth factor (g_{LH}) was around 1.13, while the number fraction (NF_{LH}) varied between 0.41 ± 0.136 and 0.26 ± 0.078 ; for more-hygroscopic particles, the growth factor (g_{MH}) varied between 1.46 and 1.55 with the average equivalent ammonium sulfate ratio ranging from 0.63 to 0.68. The differences in AS among particle of different sizes reveal that more-hygroscopic inorganic salts, such as ammonium sulfate and ammonium nitrate, are of more effective condensation growth for Aitken mode particles. A combined analysis of the probability density function of growth factor (Gf-PDF) and simultaneous meteorological data shows that during clean periods with air masses moving from the north, the particles are more likely to have homogeneous chemical composition, while during polluted or pollution accumulation periods, variations in mean number weighted growth factor (g_{mean}) and NF_{MH} become more pronounced, indicating that locally-emitted aerosol particles tend to be in an externally mixed state and contain a certain proportion of less-hygroscopic particles. This study can help improve our understanding of aerosol hygroscopicity and its impact on the atmospheric visibility and environment.

Keywords: H-TDMA, aerosol hygroscopicity, urban aerosol, haze, Pearl River Delta

东南极大陆沿岸黑碳气溶胶的本底特征研究

(汤洁 卞林根 逯昌贵)

中国气象局气象探测中心, 北京 100081

中国气象科学研究院, 北京 100081

摘 要: 利用 2010 年 2 月 18 日-2011 年 3 月 31 日南极中山站的黑碳(BC)浓度及气象资料, 对 BC 本底浓度、季节变化、来源等进行了初步研究. 结果显示, BC 浓度在偏东南风影响下, BC 浓度异常偏高, 该方向是站区发电和人为活动污染扩散方向, 对本底浓度影响较大. 当风速小于 $3 \text{ m}\cdot\text{s}^{-1}$ 时, BC 浓度也偏高且不稳定. 在计算本底浓度时, 剔除了东偏南风方向和小于 $3 \text{ m}\cdot\text{s}^{-1}$ 的 BC 浓度资料. 东南极大陆沿岸秋季和冬季逐月平均 BC 浓度较低, 最小出现在 5 月; 为 $3.3 \text{ ng}\cdot\text{m}^{-3}$, 春季和夏季较大, 最大出现在 2 月; 为 $10.0 \text{ ng}\cdot\text{m}^{-3}$, 次大出现在 10 月; 为 $8.7 \text{ ng}\cdot\text{m}^{-3}$. BC 本底浓度的变化除了局部方向人为活动的影响, 主要来源是由对流层气流从低层向南极的输送. BC 浓度季节变化特征与其它南极站基本相似。

关键词: 东南极大陆沿岸, 黑碳, 本底特征, 季节变化

北京一次持续雾霾天气过程的气象特征分析

(唐宜西^{1,2}, 张小玲², 熊亚军³)

1 成都信息工程学院, 成都, 610225;

2 中国气象局北京城市气象研究所, 北京, 100089;

3. 北京市气象台, 北京, 100089

摘要: 2013年1月10日至14日, 北京平原地区出现了水平能见度一度在2km以下, 以PM_{2.5}为首要污染物, 空气质量持续5天维持在重度以上污染水平的雾-霾天气。综合分析雾-霾期间的天气形势、北京地区常规和加密气象资料以及城郊连续观测的PM_{2.5}浓度资料, 结果表明: 此雾-霾过程期间, 北京高空以平直纬向环流为主, 受西北偏西气流控制, 没有明显冷空气南下影响北京地区, 地面一直处于均压场, 高压底部, 低压带等不利于污染物扩散和稀释的弱气压场控制; 大气层结稳定、地面风速偏小(观象台日平均风速均在2.0m/s以下, 2分钟平均风速在0~3.5m/s内波动, 并且1~2m/s的风频率为75%, 1m/s以下的风频率为11%)、相对湿度较大(日平均相对湿度在70%以上)、逆温频率高强度大(除每日的正午时段外, 其余大部分时间均存在强近地逆温层), 边界层内污染物的水平和垂直扩散能力差, 静稳的气象条件相互配合导致污染物的持续积累和雾-霾的形成; PM_{2.5}浓度与地面气象因子存在密切的联系, PM_{2.5}质量浓度较高的时段对应着低能见度、较低的风速、较高的相对湿度以及以偏南风为主导风向; 12日午后北京地面风场显示南部地区为西南风, 此后西南风势力逐渐向北推进, 至20时覆盖了北京东南部的平原地区, 对西北及东北部的山区没有显著影响, 由此得出12日午后至13日凌晨出现的城区重污染现象与偏南风的输送有关; 北京城区及南部的京津冀地区人类活动排放污染物强度大, 在相对稳定和高湿的天气背景下, 受地形和城市局地环流的影响, 北京本地污染物累积和受西南风影响区域污染物的输送以及PM_{2.5}细粒子在高温高湿条件下的物理化学转化等过程共同作用造成此次北京城区及平原地区污染物浓度快速增长并持续偏高。高浓度PM_{2.5}对大气消光有显著影响, 造成低能见度和严重的雾-霾天气。

关键字: 雾霾天气, 重污染, 气象条件, 污染物输送

参考文献

- [1] 胡亚旦, 周自江. 中国霾天气的气候特征分析[J]. 气象, 2009, 35(7): 73-78.
- [2] 赵普生, 徐晓峰, 孟伟, 等. 京津冀区域霾天气特征[J]. 中国环境科学, 2012, 32(1): 31-36.
- [3] Duan F K, He K B, Ma Y L, et al. Concentration and chemical characteristics of PM_{2.5} in Beijing, China: 2001-2002[J]. Science of the Total Environment, 2006, 355(1-3): 264-275.
- [4] Li L, Wang W, Feng J, et al. Composition, source, mass closure of PM_{2.5} aerosols for four forests in eastern China[J]. Journal of Environmental Sciences, 2010, 31(3): 405-412.
- [5] Grazia M Marazzan, Stefano Vaccaro, et al. Characteristics of PM₁₀ and PM_{2.5} particulate matter in the ambient air of Milan [J]. Atmospheric Environment, 2001, 35: 4639-4650.
- [6] Nilson E D, Patero J, Boy M. 2001. Effects of air masses and synoptic weather on aerosol formation in the continental boundary layer[J]. Tellus Series B-Chemical and Physical Meteorology, 53(4): 462-478.
- [7] 郭利, 张艳昆, 刘树华, 等. 北京地区PM₁₀质量浓度与边界层气象要素相关性分析[J]. 北京大学学报, 2011, 47(4): 607-612.
- [8] 徐晓峰, 李青春, 张小玲. 北京一次局地重污染过程气象条件分析[J]. 气象科技, 2005, 33(6): 543-547.
- [9] 王淑英, 张小玲. 北京地区PM₁₀污染的气象特征[J]. 应用气象学报, 2002, 13(特刊): 177-184.
- [10] 任阵海, 苏福庆, 高庆先, 等. 边界层内大气排放物形成重污染背景解析[J]. 大气科学, 2005, 29(1): 57-63.
- [11] 颜鹏, 刘桂清, 周秀骥, 等. 上甸子秋冬季雾霾期间气溶胶光学特性[J]. 应用气象学报, 2010, 21(3): 257-265.

- [12] 吴兑, 毕雪岩, 邓雪娇, 等. 2006. 珠江三角洲大气灰霾导致能见度下降问题研究[J]. 气象学报, 64 (4): 510-517.
- [13] 宋宇, 唐孝炎, 方晨, 等. 2003. 北京市能见度下降与颗粒物污染的关系[J]. 环境科学学报, 23 (4): 468-471.
- [14] Qiu J H, Yang L Q. Variation characteristics of atmospheric aerosol optical depths and visibility in North China during 1980-1994[J]. Atmospheric Environment, 2000, 34: 603-609.
- [15] Wu D, Tie X X, Li C C, et al. An extremely low visibility event over the Guangzhou region: A case study[J]. Atmospheric Environment, 2005, 39: 6568-6577.
- [16] 程从兰, 李青春, 刘伟东, 等. 北京地区一次典型大雾天气的空气污染过程物理量分布特征[J]. 气象科技, 2003, 31 (6): 345-349.
- [17] 樊文雁, 胡波, 王跃思, 等. 北京雾、霾天细粒子质量浓度垂直梯度变化的观测[J]. 气候与环境研究, 2009, 14 (6): 631-637.
- [18] 贺克斌, 贾英韬, 马永亮, 等. 北京大气颗粒物污染的区域性本质[J]. 环境科学学报, 2009, 29 (3): 482-487.
- [19] Zhao, X. J., P. S. Zhao, J. Xu, W. Meng, W. W. Pu, F. Dong, D. He, and Q. F. Shi, 2013. Analysis of a winter regional haze event and its formation mechanism in the North China Plain, Atmos. Chem. Phys. Discuss., 13, 903-933.
- [20] Huang W, Tan J G, Kan H D, et al. Visibility, air quality and daily mortality in Shanghai, China[J]. Science of The Total Environment, 2009, 407: 3295-3300.
- [21] 白志鹏, 蔡斌彬, 董海燕, 等. 灰霾的健康效应[J]. 环境污染与防治, 2006, 28 (3): 198-201.
- [22] 孟燕军, 程从兰. 影响北京大气污染物变化的地面天气形势分析. 气象, 2002, 28 (4): 42-46.
- [23] 李德平, 程兴宏, 等. 北京地区三级以上污染日的气象因子初步分析[J]. 气象与环境学报, 2010, 26 (3): 7-13.
- [24] 陈媛, 岑况, 等. 北京市区大气气溶胶 $PM_{2.5}$ 污染特征及颗粒物溯源追踪分析[J]. 现代地质, 2010, 24 (2): 345-354.

CARSNET 太阳光度计室内积分球标定方法研究

(陶然^{1, 2, *}, 车慧正², 鲁赛³)

¹ 成都信息工程学院大气科学学院, 中国 成都, 610225

² 中国气象科学研究院大气成分研究所, 中国 北京, 100081

³ 中国气象局气象探测中心大气成分服务于观测中心, 中国 北京, 100081

*Email: taoran616@sina.com

摘 要: 基于溯源于美国 NIST 机构标准的 Labsphere 公司生产的积分球光源系统, 利用积分球辐亮度标定方法, 对四台新型 Ce-318 太阳光度计(T914, T984, T985 和 T986)的天空散射通道进行了室内标定, 建立了一套应用于中国气溶胶遥感监测网(CARSNET)内 Ce-318 太阳光度计的室内标定方法和流程, 并且对这四台经此方法标定的新型太阳光度计进行了室外观测验证。标定结果显示, 2012 年 6 月利用西安光学精密机械研究所 ASD 分光光度计传递对积分球辐射源进行过标定, 积分球辐亮度除了在 1 个灯的光度级别下 440nm 处十次测量的相对误差达到 0.12%, 在其余波段和其余光强下相对标准偏差在 0.40%以内, 说明此积分球光源输出稳定, 用其作为标准光源可靠, 结果可信度较高。计算得到的一起标定系数在可见光波段与 Cimel 公司提供的出厂数据相比, 偏差均在合理范围内, 红外波段偏差稍大, 其中 T914 的 1020nm 波段、T984 的 870nm 波段、T985 的 1020nm 波段和 T986 的 870nm 以及 670nm 波段的标定结果与出厂值的相对偏差在 3.12%~5.24%之间, 其余波段的标定结果与出厂值相对偏差不超过 3%。利用完成标定的仪器(T985 和 T986)在室外进行观测验证, 获得的数据显示, 在太阳等高度角天空扫描(ALMUC)和太阳主平面扫描(PPLAN)两种扫描模式下, 各扫描模式在 $\pm 6^\circ$ 处, 由 AUR 通道和 SKY 通道各自测量的太阳辐照度在所有观测波段(1020nm, 1640nm, 870nm, 675nm, 440nm 和 500nm)处, 其辐照度数值是基本一致的, 相差在 1%以内, 表明本文介绍的标定方法适用于 CARSNET 仪器的大规模标定, 并对站网观测的精确度和数据质量的提高有帮助。

Development of an integrating sphere calibration method for China Aerosol Remote Sensing NETwork Cimel sunphotometer

(Ran Tao^{1, 2}, Huizheng Che^{2*}, Quanliang Chen¹, Yaqiang Wang², Junying Sun², Xiaochun Zhang³, Sai Lu³, Jianping Guo², Hong Wang², Xiaoye Zhang²)

¹College of Atmospheric Sciences, Chengdu University of Information Technology

*²Key Laboratory of Atmospheric Chemistry (LAC), Chinese Academy of Meteorological Sciences (CAMS),
CMA, Beijing, 100081*

³Meteorological Observation Center, CMA, Beijing, 100081

Address: 46 Zhong-Guan-Cun S. Ave., Beijing 100081, China

E-mail: chehz@cams.cma.gov.cn

Tel: 86-10-5899-3116

Fax: 86-10-6217-6414

Abstract:Based on the integrating sphere traced from NIST (U.S.A), a sphere calibration method and protocol for the China Aerosol Remote Sensing NETwork (CARSNET) Cimel sunphotometer was established. Four Ce-318 sunphotometers have been verified using the calibration method and operational protocol. The calibration results show the instruments' coefficients differ less than 3% (~5%) for visible (infrared) wavelengths from the original ones offered by Cimel Co. Ltd. In-situ validation experiments data showed the irradiances at $\pm 6^\circ$ measured by sun collimator (aureole) are consistent with those measured by sky collimator (sky) under both almucantar (ALMUC) and principal plane (PPLAN) scenarios. The differences at all wavelengths are less than 1%, which indicates the method and protocol are suitable for CARSNET field sunphotometer calibration and should benefit the improvement of data quality and accuracy of network observations.

Keywords: Ce-318 sunphotometer, integrating sphere calibration, CARSNET

大型燃烧腔的设计、特征与实验测试——生物质露天燃烧的室内模拟

(田杰¹, 韩永明^{1*}, 倪海燕², L.-W.A. Chen^{3,1}, 曹军骥¹)

1 中国科学院地球环境研究所, 西安, 710075

2 西安交通大学, 西安, 710049;

3 Desert Research Institute, 2215 Raggio Parkway, Reno, Nevada 89512, USA

摘 要: 生物质露天燃烧会直接向大气中排放各种气态和颗粒态污染物, 如有机污染物 (包括多环芳烃等)、重金属、二氧化碳、一氧化碳等, 是大气细颗粒物 ($\text{PM}_{2.5}$) 和含碳气溶胶 (如有机碳 OC 和元素碳 EC) 的一个主要来源, 不仅恶化区域空气质量, 降低大气能见度, 而且改变生态系统的循环, 产生不利的健康效应。为了获得生物质露天燃烧的排放因子, 中国科学院地球环境研究所 (IEECAS) 与美国沙漠研究所 (DRI) 合作建立了一套测量生物质露天燃烧排放因子的室内模拟平台, 包括稀释通道采样系统和大型燃烧腔。本文着重介绍了大型燃烧腔的结构组成、工作原理以及在模拟生物质露天燃烧真实状况时相较于其他燃烧腔的特点和优势, 并通过实验测试得到小麦秸秆的排放因子 $\text{EF}_{\text{PM}_{2.5}}=10.49\pm 3.43\text{g/kg}$, $\text{EF}_{\text{OC}}=3.94\pm 2.50\text{g/kg}$, $\text{EF}_{\text{EC}}=0.53\pm 0.19\text{g/kg}$, 通过文献数据对比, 证明大型燃烧腔系统设计科学合理, 在排放因子、排放清单、源谱分析及 $\text{PM}_{2.5}$ 来源解析研究中具有广阔的应用前景。

关键字: 大型燃烧腔, 生物质露天燃烧, 排放因子

Aerosol vertical distribution and seasonal variation over SACOL derived from CALIPSO lidar observations

(Pengfei Tian, Lei Zhang, Xianjie Cao)*

Key Laboratory for Semi-Arid Climate Change of the Ministry of Education, College of Atmospheric Sciences, Lanzhou University, Lanzhou, 730000, China

**Author to whom correspondence should be addressed. E-mail: zhanglei@lzu.edu.cn*

Abstract: Firstly, presents an assessment of CALIPSO observation by comparing to the ground based lidar CE 370-2. Then CALIPSO level 2 aerosol profile data from June 2006 to October 2011 is used to study the vertical distribution and seasonal variation of aerosols over SACOL. Four types of aerosols are observed over SACOL: dust (with an occurrence frequency of 55.3% among all subtypes of aerosols), polluted dust (27.3%), smoke (15.5%) and clean continental (1.8%). Aerosols are uniformly distributed from ground to 2 km above, anthropogenic aerosols decrease while natural aerosols relatively increase from 2 to 4 km, dust dominates in the heights of 4~6 km, while only polluted dust is observed in the layer of 6~8 km, no aerosol is observed above 8 km. In spring, dust occurs frequently over SACOL (90.6%); in summer, the occurrence frequency of smoke almost equals that of polluted dust and these two types of aerosols occur almost at the same height bin; in autumn, local dust and smoke are mixed from ground to 2 km; in winter, dust is observed in the height bin of 2~6 km. Dust is mostly observed in spring and winter within 6 km; smoke is mostly observed in summer and autumn within 4 km; polluted dust has much the same occurrence frequency in summer, autumn and winter, mostly below 2 km and can reach the height bin of 6~8 km.

Key words: atmospheric aerosol, CALIPSO, vertical distribution, seasonal variation

北京城区夏季大气气溶胶亲水性特征研究

(田平^{1,2}, 张仁健², 颜鹏³, 王广甫¹, 武云飞²)

1 北京师范大学核科学与技术学院, 北京, 100875;

2 中国科学院大气物理研究所, 北京, 100029;

3 中国气象局气象探测中心, 北京, 100081

摘 要: 为研究北京城区夏季气溶胶的光学特性及其亲水性特征, 2012 年 5 月 26 日至 2012 年 6 月 30 日在中国科学院大气物理研究所铁塔分部 (IAP, CAS) 进行了针对气溶胶散射系数 σ_s 、吸收系数 σ_a 、单次散射反照率 ω_0 以及 σ_s 亲水性增长因子 $f(\text{RH})$ 随相对湿度变化的实验。结果显示, 2012 年 6 月北京城区 525 nm 气溶胶 σ_s 、 σ_a 和 ω_0 的平均值分别为 $370.3 \pm 313.2 \text{ Mm}^{-1}$ 、 $42.4 \pm 28.4 \text{ Mm}^{-1}$ 、 0.85 ± 0.26 , 与其它在北京城区的测量结果相比偏低。当相对湿度从低到高变化的过程中, $f(\text{RH})$ 主要表现出平滑连续增长的特点。在“清洁”天气下, $f(\text{RH}=80\%)$ 亲水特性不显著; 而在“污染”情况下和“重污染”情况下, σ_s 体现出较强的吸湿特性。根据 $\text{PM}_{2.5}$ 和 PM_{10} 膜采样中化学成分的分析结果, 观测期间 $f(\text{RH}=80\%)$ 和 $\text{OMC}/\text{SO}_2\text{-4}$ 之比呈明显的负相关关系, 说明有机碳成分对气溶胶的亲水性有一定的抑制作用。本文同时研究了 σ_s 、 σ_a 和 ω_0 对亲水性增长因子的影响, 结果显示, 当 σ_s 大于 200 Mm^{-1} 或 ω_0 大于 0.9 时, $f(\text{RH}=80\%)$ 有剧烈增大的趋势。

关键字: 隔散射系数, 吸收系数, 亲水性增长因子

Impact of meteorological parameters and gaseous pollutants (SO₂ and NO₂) on PM_{2.5} and PM₁₀ mass concentrations during 2010 in Xi'an, China

(Ping Wang¹, JunJi Cao¹, Yongming Han¹, Yu Huang², Shuncheng Lee²)

¹ State Key Lab of Loess and Quaternary Geology, Institute of Earth Environment, Chinese Academy of Sciences, Xi'an 710075, China

² Department of Civil and Environmental Engineering, The Hong Kong Polytechnic University, Hong Kong

Abstract: PM_{2.5} and PM₁₀ mass from quartz-fiber weight were obtained in Xi'an for two weeks of every month corresponding to January, April, July and October during 2010 at upwind district of Gaoling county (GLC), downwind background station of Black river reservoir (BRR) and four urban sites. Annual average PM_{2.5} and PM₁₀ mass concentrations were $140.9 \pm 108.9 \mu\text{g m}^{-3}$, $257.8 \pm 194.7 \mu\text{g m}^{-3}$, respectively. Seasonally, high concentrations in wintertime and low ones during summertime were attributed to seasonal variations of meteorological parameters and cycle changes of precursors (SO₂ and NO₂). Stepwise Multiple Linear Regression (MLR) analysis indicated that relative humidity is the main factor influencing on meteorological parameter. Sulfate of SO₂ oxidation products are concentrated in fine mode of PM_{2.5} and nitrate of NO₂ oxidation in coarse mode of PM₁₀. Entry MLR analysis suggested that SO₂ and NO₂ contributed 48.6% and 33.9%, and 17.5% and 0.7% of the total PM_{2.5} and PM₁₀, respectively. Trajectory cluster results indicated long distance air mass from northwest in winter (82.1%) and in spring (67.9%), and short distance from surrounding provinces in summer (62.5%) and autumn (73.2%). Potential Source Contribution Function (PSCF) analysis showed three day Dust storm (DS) came from Taklimakan Desert in Xinjiang and Gobi Desert in Inner Mongolia in spring. Remote sensing retrieval (OMI UV Aerosol Index (AI), OMI tropospheric NO₂ column of Aura and Aerosol Optical Depth (AOD) of MODIS TERRA) from Giovanni online tools of NASA Goddard Earth Sciences Data and Information Services Center (GES DISC) were verified results of observation on the ground to some extents.

Key words: Xi'an, PM_{2.5} and PM₁₀, meteorological parameters, gaseous pollutants, MLR, PSCF.

青海湖地区单颗粒黑碳气溶胶的特性

(王启元¹, 曹军骥^{2*}, 胡塔峰²)

1 西安交通大学环境科学与工程系, 西安, 710049;

2 中国科学院地球环境研究所, 西安, 710075

摘 要: 2011 年 10 月在我青海湖畔使用单颗粒黑碳光度计(SP2)测量单颗粒黑碳气溶胶的质量、粒径分布及其混合状态。并使用黑碳仪测量黑碳的光学性质以及一氧化碳(CO)分析仪测量 CO 的浓度。测量结果表明黑碳平均质量浓度为 $0.36 \mu\text{g m}^{-3}$, 明显高于世界各地背景及偏远地区的质量浓度。黑碳浓度在夜间呈现出峰值而在下午呈现出低谷。这种日内变化与当地的混合层高度成反相关。黑碳的质量粒径分布峰值在~175nm, 且在~495nm 处有一个次峰值。采样期间, ~50%的黑碳颗粒物呈现出内部混合。黑碳仪与 SP2 的对比结果表明, 青海湖地区存在除黑碳以外的其他物质对光有吸收作用。黑碳浓度与 CO 具有很好的相关性 ($r=0.83$), 表明他们具有相同的来源, 此外黑碳与 CO 的比值为 $1.5 \pm 0.1 \mu\text{g m}^{-3} \text{ ppbv}^{-1}$ 代表了青海湖地区的混合排放源特征。

关键字: 黑碳, 单颗粒黑碳光度计, 青海湖

*通讯联系人, E-mail address: cao@loess.llqg.ac.cn

Investigation of NR-PM₁ Species and Effect on Visibility in Xi'an, China

(Yichen Wang^{1,2}, JunJiCao¹)

¹.State Key Laboratory of Loess and Quaternary Geology, Institute of Earth Environment, Chinese Academy of Sciences, Xi'an 710075, China.

².Graduate University of Chinese Academy of Sciences, Beijing 100049, China.

Abstract :With an Aerodyne Aerosol Chemical Speciation Monitor, we mainly focused on the variation of NR_PM1 species, its inorganic species formation and its effect on visibility impairment under a stable atmospheric condition (low wind speed period, from 1 September to 6 September, from 26 September to 1 October respectively). The NR_PM1 took up ~60% of PM_{2.5}. Organic contributes the most (58% on average) to the NR_PM1 mass loading, other species make ~40% contributions. Through Principle component analysis, we found NH₄⁺, SO₄²⁻ and NO₃⁻ played a stably significant role on visibility impairment within different period of the day. With the IMPROVE equation, Light scattering from NR_PM1 was ~ 80% of that from PM_{2.5}, illustrating the dominance of NR_PM1 in the light scattering process. Organics contributed the most to light scattering during this period whereas (NH₄)₂SO₄ and NH₄NO₃ played more important role on the visibility variation than Org did. Overall, it is the combination of organics, (NH₄)₂SO₄ and NH₄NO₃, not a single species that are responsible for the variation of visibility variation. Sulfate formation was dominated with gas phase reactions during daytime and droplet phase reactions at night. Nitrate particles, however, were not formed immediately after gas phase reactions in the afternoon. Two types of OA (HOA and OOA) were found in this study. The oxygenation level of organics was relatively high and photochemical reaction proceeded rapidly in the afternoon. BBOA(biomass burning organic aerosol) cannot be resolved though tracers of BBOA(m/z 60 and 73) have a prominent signal, illustrating the similar variation of time series between these two factors, which maybe resulted from the traditional energy consumption pattern in villages.

Key words: ACSM, NR_PM1, stable atmospheric condition, formation, visibility, HOA, OOA

台灣北部三個空氣品質測站之大氣微粒來源及特性研究

(危涵¹, 劉俊男¹, 蔡春進^{1,*}, 巫月春², 陳重方²)

1 台灣交通大學環境工程研究所, 臺灣, 30010;

2 行政院環境保護署環境檢驗所, 臺灣, 32024

摘要: 本研究利用正矩陣因子法(Positive Matrix Factorization, PMF)以及其他輔助來源分析之相關理論分析台灣北部都會地區三空氣品質測站: 中山、新莊及竹東測站, 三種微粒(PM_{10} 、 $PM_{2.5}$ 及 $PM_{0.1}$)之污染來源。本研究使用的數據為交大環工所蔡春進教授研究團隊的成果, 其微粒的採樣係利用雙道採樣器(Dichotomous PM_{10} samplers)、微孔均勻沉降微粒採樣器 (Micro-Orifice Uniform Deposit Impactor, MOUDI) 及半自動氣膠碳成份分析儀(Sunset Laboratory Model 4 Semi - Continuous OC/EC Field Analyzer)完成, 並分析了微粒中的元素(Al、Fe、Na、Mg、K、Ca、Ba、Ti、Mn、Cu、Zn、Pb、V 及 Cr 共 17 種)、離子(F^- 、 Cl^- 、 NO_3^- 、 SO_4^{2-} 及 NH_4^+ 五種)及元素碳和有機碳濃度。2011 年 5 月至 2012 年 9 月, 期間共進行 38 次(中山測站)、36 次(新莊測站)及 35 次(竹東測站) 24 小時的採樣。在元素、離子及有機碳和元素碳之來源特性研究中, 其相關性可幫助判別各物種與污染來源之間的關係。PMF 的分析結果中三個測站的 PM_{10} 及 $PM_{2.5}$ 中皆分別以地殼元素及汽機車排放為最大宗污染源, 而 $PM_{0.1}$ 中的主要污染源有二次氣膠或汽機車排放, 中山測站位於都市繁忙之市中心, 以汽機車排放為主, 竹東測站則在較小型的都市, 污染物容易受到光化學反應作用而以二次氣膠為主要來源, 新莊測站位於大都市邊陲地區, 二次氣膠及汽機車排放兩污染源貢獻比例相當。此初步結果顯示, 粗微粒的部分仍以自然界的來源貢獻為主, 但在交通繁忙的都會區, 細微粒及奈米微粒將受到人類活動極大的影響, 而以汽機車排放或二次氣膠為主。

关键字: 都會地區大氣微粒、正矩陣因子法、污染來源解析、條件機率函數、地殼富集值

同时测定大气中气态和颗粒态多环芳烃及其含氧/氮衍生物的新方法

(魏崇^{1,2,4}, Benjamin A. Musa Bandowe², Hannah Meusel², 何建辉¹, 韩永明^{1,*}, 曹军骥^{1,3}, Thorsten Hoffmann⁵, Wolfgang Wilcke²)

1 中国科学院地球环境研究所, 西安, 710075;

2 瑞士伯尔尼大学, 伯尔尼, CH 3012

3 西安交通大学全球变化研究院, 西安, 710049

4 中国科学院大学, 北京, 100049

5 德国美因兹大学, 美因兹, 55128

摘要: 多环芳烃 (PAHs) 及其含氧/氮衍生物 (OPAHs、NPAHs) 可由化石燃料不完全燃烧产生, 另外 OPAHs 和 NPAHs 还可以由 PAHs 经过光化学反应生成。他们都具有致癌、致畸、致突变等“三致效应”, 尤其是 OPAHs 和 NPAHs 的毒性比 PAHs 更强。本文的目的是为了测试和应用新的方法来同时测量大气中气态和颗粒态的 PAHs、OPAHs 和 NPAHs 的浓度。本文分别使用聚氨酯泡沫和石英滤膜来采集大气中气态和颗粒态物质。使用加速溶剂萃取仪来提取目标组分, 并应用不同极性的溶剂从硅胶层析柱中分离出 PAHs 和 OPAHs+NPAHs 组分。PAHs 和 OPAHs 组分由带有 EI 离子源的 GC/MS 来测量, 而 NPAHs 则是利用反向化学电离源 (NCI) 的 GC/MS 来测量。添加标准后的 PAHs, OPAHs 和 NPAHs 的回收率分别是 80% (60-150%), 70% (40-120%), 75% (40-120%)。线性度测试 (PAHs ($r^2 = 0.985 - 1.000$), OPAHs ($r^2 = 0.970 - 0.994$) 以及 NPAHs ($r^2 = 0.883 - 0.991$)) 以及标准参考物质的测量 (与标准值相比 <10%) 也表明我们的改进具有高的精确度和精密度。

关键字: 多环芳烃 (PAHs), OPAHs/NPAHs, 加速溶剂萃取法, 回收率

气溶胶中硫酸根离子的 FTIR 定量分析³

(魏秀丽⁴, 高闽光, 刘建国, 刘娜, 徐亮, 童晶晶, 金岭)

(中国科学院环境光学与技术重点实验室, 中国科学院安徽光学精密机械研究所 合肥 230031)

摘 要: 大气气溶胶是影响大气环境的三大污染物之一, 在大气污染过程中, 大气气溶胶粒子污染在其中占有重要的地位。本文通过对FTIR方法研究气溶胶硫酸根离子测量方法的改进, 使离子定量研究更精确。通过FTIR方法研究气溶胶水溶液中加入硫酸铵的特性, 分析气溶胶水溶液中硫酸氢加入前后的硫酸根拟合曲线, 对空气中硫酸根进行定量。表明硫酸根红外吸收峰是 615cm^{-1} 可以作为定量的吸收峰, 我们研究了这些红外吸收峰吸收面积和离子质量成线性关系, 溶剂对离子定量分析没有影响。Ge片上滴膜的均匀性没有影响到定量分析的结果。

关键词: 气溶胶, FTIR, 无机离子

³国家自然科学基金 (41105022);

⁴魏秀丽, 女, 助理研究员, E-mail:xlwei@aiofm.ac.cn.;

青岛市不同功能区冬季空气微生物群落代谢与多样性特征

(吴等等, 宋志文^{**}, 徐爱玲, 郑远, 夏岩)

(青岛理工大学, 山东青岛, 266033)

摘 要: 选取青岛市 5 个不同功能区(市区街道、海滨区域、饮用水源地、垃圾填埋场和人工湿地), 采用 SAS ISO100 空气浮游菌采样器于 2013 年 1 月采集空气微生物样品, 应用 Biolog 方法分析空气微生物群落碳源代谢特征、群落功能多样性, 阐明空气微生物群落代谢、多样性特征与环境相关性。结果表明, 不同功能区空气微生物群落碳源代谢强度存在差异, 海滨区域和饮用水源地空气微生物群落碳源代谢强度明显高于其他功能区; 不同功能区空气微生物群落 Shannon 指数和 Simpson 指数接近, 但海滨区域和饮用水源地 McIntosh 指数明显高于其他功能区; 海滨区域和饮用水源地空气微生物群落碳源代谢类型丰富, 代谢水平高, 而人工湿地、市区街道及垃圾填埋场碳源代谢类型单一, 代谢水平低, 5 个功能区空气微生物群落对羧酸类碳源代谢水平均较高; 功能区空气微生物群落碳源代谢特征差异呈现区域性, 其中分异代谢特征差异的主要碳源类型是羧酸类; 风速、温度、湿度等非生物因素对空气微生物群落碳源代谢特征具有不同程度影响, 且不同功能区主导非生物因素存在差异。

关键词: 青岛市, 城市功能区, 空气微生物, 代谢特征, 群落多样性, Biolog 方法

Metabolic Characteristics and Community Diversities of Airborne Microbes in Different Functional Regions in Qingdao in Winter

WU Deng-deng, SONG Zhi-wen^{**}, XU Ai-ling, ZHENG Yuan, XIA Yan (Institute of Environment and Municipal Engineering, Qingdao Technological University, Qingdao 266033, China).

Abstract: In order to determine the metabolic characteristics and community diversities of airborne microbes in different functional regions in Qingdao in winter, monitoring points were set up in five different functional regions (city streets, coastal area, source area of drinking water, municipal landfill site, and constructed wetlands for wastewater treatment). Airborne microbes were collected by SAS ISO100 in January 2013 and their carbon source metabolic characteristics, functional diversity of microbial community, and relationship with environmental factors were analyzed systematically through the Biolog method. The results showed that the differences of carbon metabolic profiles of air microbial communities from the five locations were significant. Among the five locations, levels of carbon metabolic profiles at coastal area and source area of drinking water were higher than those in other locations. The Shannon indexes and Simpson indexes in five different city functional regions were similar. However, the McIntosh indexes at coastal area and source area of drinking water were higher than that in other locations. Among the five locations, carbon catabolic types and levels at coastal area and source area of drinking water were richer and higher compared to those in the artificial wetland, urban streets, and refuse landfill. Utilization level of carboxylic acids was higher in the five air samples compared with other carbon sources. The characteristics of carbon metabolic profiles revealed regional features and the key carbon source was carboxylic acids which caused the differences in characteristics of carbon metabolic profiles. Environmental factors, such as wind speed, temperature, and humidity may have effects on carbon utilizations to certain degrees with the dominant factors different according to different environments.

Key words: Qingdao, city functional regions, airborne microbe community, metabolic characteristics, Microbial diversity, Biolog method

Characteristics of aerosol transport and distribution in East Asia

(Jian Wu¹ (吴涓), Jun Guo^{1,2} (郭俊), Deming Zhao³ (赵得明))

¹*Department of Atmospheric Science, Yunnan University, Kunming 650091, China*

²*School of Atmospheric Physics, Nanjing University of Information Science & Technology, Nanjing, 210044, China*

³*Key Laboratory of Regional Climate-Environment for Temperate East Asia, Institute of Atmospheric Physics, Chinese Academy of Sciences, Beijing, 100029, P. R. China*

Abstract: We used daily aerosol simulations for the period from 2001 to 2003 that were generated by the Goddard Chemistry Aerosol Radiation and Transport (GOCART) model to characterize aerosol transport and distributions in East Asia. In comparison with the AERONET, MODIS, and visibility observations, the model can capture the main distribution features of the aerosol optical depth (AOD) and its temporal changes with a correlation coefficient of 0.75 and 0.85, respectively. It was found that high AODs occur in Central China, the Sichuan basin, the Indo-China peninsula, the Indian subcontinent, and the Bay of Bengal because of black carbon, organic matter, and sulfate, whereas in the Taklimakan desert and its adjacent regions, high AODs occur because of dust. The potential effects of the hygroscopicity of aerosol particles on the AOD were mainly observed in the Sichuan basin, the Bay of Bengal, the Indo-China peninsula, and Central and Southern China. The East Asian aerosol transport was distinctly affected by the flux divergence induced by aerosol advection (AFD) and by the flux divergence induced by wind divergence/convergence (WFD). For black carbon, organic matter, and sulfate, the effect of AFD was a factor of 2 or 3 larger than that of WFD in the divergence region, whereas AFD dropped to 70% of WFD in the convergence region. The high AOD of black carbon, organic matter, and sulfate over the Sichuan basin related to the circulation characteristics of convergence in low altitudes and divergence in high altitudes, which can collect aerosol from adjacent regions at altitudes below 300 hPa and cause them to diverge easterly at higher altitudes.

Keywords: Aerosol; AOD; Transport; East Asia; GOCART model.

Corresponding author: Wu J. wujian@ynu.edu.cn

台灣柴油車 NO_x 排放管制成效探討

(吳容輝¹, 林文淵¹, 顏瑞瑩¹, 許仲景², 莊志偉², 盧昭暉³, 林建良³)

1 嘉義縣環境保護局, 嘉義

2 華門工程顧問股份有限公司, 台南

3 國立中興大學機械工程研究所, 台中

摘要: 本文主要目的是探討臺灣柴油車的 NO_x 排放, 以瞭解使用中車輛的排放情形。其中新車排放情況以環保署的柴油車審驗資料為主, 使用中車輛排放情況是以嘉義縣環境保護局在 2004~2011 年所執行的測試資料為主, 分別探討新車排放、全負載不同轉速、不同排氣量與不同管制期程對 NO_x 排放之影響。

本文發現三期重型柴油車的 NO_x 與 PM 都相當集中, 接近排放標準。NO_x 的新車審驗值都集中在 3~5 g/ bhp-hr 的區域內, 平均值為 3.74 g/ bhp-hr, 而 PM 的分佈則集中在 0.06~0.1 g/ bhp-hr 的區域內, 平均值為 0.09 g/ bhp-hr。

使用中柴油車的 NO_x 濃度分佈類似 γ 分佈。全負載 100%轉速時與全負載 60%轉速的 NO_x 濃度分佈較集中, 而全負載 40%轉速的 NO_x 濃度分佈則較分散。排氣量 3000cc 以下柴油車的 NO_x 排放濃度約 500ppm, 隨著測試轉速降低而上升; 3000cc 以上柴油車的 NO_x 排放濃度約 700~1150ppm, 隨著排氣量增加而上升, 也會隨著測試轉速降低而升高。自從全面實施第四期柴油車輛排放標準, 2007 年以後的 NO_x 平均排放濃度有明顯的降低趨勢。全負載 100%轉速下的 NO_x 平均排放濃度, 從 2004 年至 2011 年減少了 44%, 顯示加嚴排放法規, 控制 NO_x 污染排放有明顯的效果。平均 NO_x 排放濃度以 40%轉速最高, 為 844ppm, 其次為 60%轉速, 為 768ppm, 而 100%轉速的 NO_x 排放濃度最低, 為 643ppm。在全負載各轉速下的平均 NO_x 濃度以一期車排放最高。在全負載 40%轉速與 60%轉速下的三期車排放有稍微比二期車還多, 四期車所量測的排放濃度為最低。在全負載 100%轉速下的 NO_x 排放濃度隨著排氣法規所制定期程越嚴格而降低。

若考慮單位輸出功的排放量(g/bhp-hr)時, 平均 NO_x 排放量以 40%轉速最高, 為 9.03 g/bhp-hr, 其次為 100%轉速, 而 60%轉速的 NO_x 排放量最低。各轉速下的平均 NO_x 排放量, 皆高於各期程所規範的排放標準。在全負載各轉速下的 NO_x 排放量, 有隨著所制定期程越嚴格而降低。二期使用中車輛在全負載各轉速下的平均 NO_x 排放量都已超過新車法規標準; 三期與四期之使用中車輛在 60%與 100%轉速下都非常接近新車法規標準, 而在 40%轉速時, NO_x 排放量超過新車法規標準。

關鍵字: 柴油車, NO_x, 汙染排放

北京夏季大气气溶胶吸收特性——多仪器比对观测

(武云飞¹, 张仁健¹, 颜鹏², 田平¹, 张养梅², 陈聪³)

1 中国科学院大气物理研究所, 北京, 100029

2 中国气象科学研究院, 北京, 100081

3 南京信息工程大学, 南京, 210044

摘 要: 2012 年 6 月, 利用光声气溶胶消光仪 PAX、多角度吸收光度计 MAAP、黑碳仪 AE-31、炭黑吸收光度计 PSAP 对北京城区气溶胶吸收及黑碳浓度进行同步对比观测, 并参考经验订正方案对测量的吸收系数进行订正。结果表明几种气溶胶吸收仪器的测量结果具有较好的一致性, 订正后的不同仪器获得的吸收系数 (532 nm) 偏差小于 10%。实验期间气溶胶吸收系数 (532 nm) 均值 \pm 标准差为 $28.01 \pm 20.02 \text{ Mm}^{-1}$, 黑碳质量浓度及其质量吸收效率 (532 nm) 分别为 $4.63 \pm 3.04 \mu\text{g m}^{-3}$ 、 $5.60 \pm 1.00 \text{ m}^2 \text{ g}^{-1}$ 。订正后 AE-31 和 PSAP 的吸收波长依赖性 (吸收 Angstrom 指数) 均有一定程度的增大, 需进一步探讨经验订正方案在不同波段的订正效果。污染期间, 质量吸收效率及吸收 Angstrom 指数都略有增加, 表明污染期间可能存在少量非黑碳的吸收性成分 (如棕碳等) 的贡献。

关键字: 吸收系数, 比对观测, 波长依赖性

2000~2010 年中国地区人为排放源年际变化趋势研究

(谢祖欣, 韩志伟*)

中国科学院大气物理研究所, 东亚区域气候-环境重点实验室, 北京 100029

摘 要: 本文利用 TRACE-P, INTEX-B 和 MEIC 排放清单对 2000-2010 年中国地区人为排放源分布及其变化特征进行了分析研究, 得到如下结论: (1) 2000-2010 年, PM_{10} , $\text{PM}_{2.5}$ 和 SO_2 的排放量在 2006 年最大。2010 年 $\text{PM}_{2.5}$ 和 SO_2 的排放量略有降低, PM_{10} 的排放量大幅减少。 NO_x 的排放量一直处于上升状态, 2010 年比 2000 年的排放量高出约 80%, 超过了同年 SO_2 的排放量, 增长较快。 NO_x 的大幅增加与近年来机动车保有量的大量增加、能源结构的变化有关。此外, BC、OC 和 NMVOC 的排放量变化不大。(2) 排放量最大的区域依次为华东、华北和西南地区。2000 至 2006 年, 各地区污染物排放整体呈现上升趋势。2006 年后, 华东和西南地区污染物排放总体上有一定程度的减少, 尤其是 SO_2 和 NO_x 的减少较为显著, 2010 年 SO_2 和 NO_x 在华东地区排放比 2006 年分别减少了 1.8Tg 和 0.9Tg, 在西南地区的减少量分别为 1.8Tg 和 1.5Tg。而华北地区除 PM_{10} 大量减少外, $\text{PM}_{2.5}$ 、 SO_2 和 NMVOC 排放量基本不变, NO_x 的排放比 2006 年增加了 0.9Tg。(3) 各种成分排放强度的高值区集中于华北、长江中下游、四川和重庆地区、珠江三角洲等地。与 2000 年相比, 2006 年 SO_2 、 NO_x 和 BC 高值区的覆盖面积和排放强度均有所增加。2010 年各种成分排放强度高值区所覆盖的面积较 2006 年略有缩小, 而大中城市等人为活动最为密集的地区排放强度则有明显增加, 突显出我国快速城市化进程所带来的城市大气污染问题的加剧。

青藏高原沙漠化对东亚沙尘气溶胶贡献的敏感性模拟试验分析

(熊洁¹, 赵天良^{1*}, 刘煜², 韩永翔¹, Feng Liu³)

¹ 南京信息工程大学大气物理学院, 江苏南京

² 中国气象科学研究院大气成分研究所, 北京

³ Center for Atmospheric Science, Division of Illinois State Water Survey, Prairie Research Institute,

University of Illinois at Urban-Champaign, Champaign, Illinois, USA

基金项目: 南京信息工程大学科研启动基金资助项目 (20110304);

国家自然科学基金资助项目 (4107506; 41175093)

*责任作者, 教授, tlzhao@nuist.edu.cn

摘 要: 目前青藏高原沙尘气溶胶的研究主要在地面观测和卫星遥感分析方面, 而其沙尘模拟的缺陷在于目前无详尽的高原沙漠分布。为了认识青藏高原的严重沙漠化产生的沙尘气溶胶及其影响, 应用全球气溶胶气候模式 CAM3.1 针对高原沙漠对东亚大气气溶胶的最大可能贡献进行敏感性模拟试验。试验分析表明: 青藏高原上潜在的起沙源区主要分布在临近柴达木盆地的高原西部、藏南地区以及青南高原; 高原的起沙量春季最大, 秋季次之, 冬季第三, 夏季最小。沙漠化的高原除了显著地增加了高原上大气沙尘气溶胶的浓度, 近地面的大气边界层沙尘气溶胶显著增多区域的是中国中西部地区, 对流层中部沙尘气溶胶增多显著区域自中国中西部地区东伸到达中国东海岸、甚至朝鲜半岛、日本直至太平洋上空。青藏高原沙源在近源区即青藏高原及周边地区的高贡献率主要在低层, 而在远源区如日本岛南部海域及中太平洋区域, 其贡献率主要在高层。高原沙尘气溶胶极易被扬升到西风带, 成为全球最高效率的沙尘远程传输源地。青藏高原沙漠化可能使其成为全球重要的沙气溶胶源地。

关键词: 青藏高原, 沙尘气溶胶, 沙漠化, CAM3.1, 敏感性模拟试验

Sensitivity simulation of contribution of desertification over Tibetan Plateau to East Asian dust aerosols

ABSTRACT: By using the climate model CAM3.1, a sensitivity study of potential desertification over Tibetan Plateau (TP) has been conducted. The simulations show that the potential dust emission sources over the TP are mainly distributed in the western plateau near to Qaidam Basin, southern Tibet, southern Qinghai plateau; The sand emissions vary seasonally with the peak in spring, the low in summer. Besides the dust aerosol concentrations over the TP are greatly enhanced, the dust aerosols emitted from the TP could significantly increase dust aerosols in the lower troposphere over central-western China and in the mid-troposphere from central-western China, Korea, Japan to West Pacific. The contributions of the TP-desertification to East Asian dust aerosols are high mainly in the lower-troposphere near to the TP, while in the far-source region such as the south of Japan and the Middle Pacific region was highly in high-rise. Plateau dust aerosol could be easily ascended to westerlies, becoming the world's highest efficiency dust-distance transmission source.

Key words: Tibetan Plateau; Dust aerosol; Desertification; CAM3.1; Sensitivity simulation test

米散射微脉冲激光雷达应用的探讨

(徐赤东 纪玉峰 徐青山)

中国科学院合肥物质科学研究院

摘 要：微脉冲激光雷达是伴随着实际大气探测问题而产生的。该项技术相对比较成熟，由于雷达技术的特殊性和认知程度，在实际业务应用中还需要解决很多问题。尤其是对于非专业的使用者来说，仪器的硬件构成、系统数据质量问题、数据的深入分析等都是非常棘手的现状。这些问题恰恰是微脉冲激光雷达得以很好应用的障碍。本文通过硬件、算法和发展的介绍得出业务应用中需要解决的关键点。

关键字：大气气溶胶，微脉冲激光雷达，颗粒物

Inter-annual variability of wintertime PM_{2.5} chemical composition in Xi'an, China: Implications of Emission Changes

(H.M. Xu^{5,2}, J.J. Cao¹, K.F. Ho³)

1 Key Lab of Aerosol Science & Technology, SKLLQG, Institute of Earth Environment, Chinese Academy of Sciences, Xi'an, China

2 University of Chinese Academy of Sciences, Beijing, China

3 School of Public Health and Primary Care, The Chinese University of Hong Kong, Hong Kong, China

Abstract: The chemical characteristics of PM_{2.5} from Xi'an urban area in January and February 2006 and the same period of 2010 were determined in this study. Chemical mass closure analyses were carried out in PM_{2.5} samples, in order to illustrate the changes in PM_{2.5} chemical compositions in Xi'an winter time. Enrichment factors relative to earth crust abundances were evaluated and it was noted that most anthropogenic elements including Ni, Cd, As, and Pb had significant reductions. Correlation and multivariate analysis technique, such as Positive Matrix Factorization (PMF) were used for source apportionment to identify the possible sources of PM_{2.5} and to determine their contribution changes. Similar sources were identified between these two years. Secondary transformation, fugitive dust, coal combustion and vehicular emissions almost accounted for 80% of the mass concentrations of PM_{2.5}. Moreover, the abundances of these major sources were changed with different years: coal combustion contributed the most (28.9%) of PM_{2.5} mass concentrations in 2006, followed by vehicular emissions (28.0%) and secondary transformation (15.3%); but vehicular emissions was the most contributor (25.7%) in 2010 and the contribution of fugitive dust increased to 22.5% as well. Besides, industrial emissions and fireworks emissions + biomass burning were the minor sources for PM_{2.5} in Xi'an.

Keywords: Mass closure analysis, PM_{2.5}, Source apportionment, Xi'an

* Corresponding author. *Postal address: Institute of Earth Environment, Chinese Academy of Sciences (CAS), No. 10 Fenghui South Road, High-Tech Zone, Xi'an 710075, China. E-mail: cao@loess.llqg.ac.cn Tel: 86-29-8832-6488, Fax: 86-29-8832-0456*

上海市大气散射系数的季节变化特征

(徐薇¹, 修光利^{1,6}, 陶俊², 王丽娜¹, 朱梦雅¹, 冯玲¹, 张大年¹)

(1: 国家环境保护化工过程环境风险评价与控制重点实验室, 华东理工大学, 上海 200237;

2: 环保部华南环境科学研究所, 广州, 510655)

摘要: 为研究上海市大气颗粒物散射系数分布特征以及颗粒物化学组分贡献率, 用浊度仪对散射系数近一年监测, 同时采集 PM_{2.5}, 分析其主要化学成分浓度。观测发现, 散射系数秋冬季较高, 夏季最小。日变化有早晚两个峰, 秋冬较明显。PM_{2.5} 与散射系数有非常好的线性关系。春季影响大气能见度的关键组分是二次离子, 夏季是 EC, 秋季和冬季均没有明显的关键组分。

关键字: 散射系数, 能见度, PM_{2.5}

⁶基金项目: 中央高校基本科研业务费专项资金 (WB1113005)、国家自然科学基金 (21277044)、上海市教委科研创新基金 (12ZZ054); 博士点基金 (20120074140001); 国家环境保护公益性行业科研专项资助 (项目编号: 200809143) 联合资助。

第一作者, 徐薇 (1987-), 博士研究生, 研究方向: 大气污染化学。责任作者: 修光利 (1972-), 教授, xiugl@ecust.edu.cn

Estimation of aerosol refractive index and optical properties during summer and winter time at a regional background station in Yangtze River Delta Region of China

(Peng Yan^{1,2}, Xiuji Zhou²)

¹ Meteorological Observation Center of China Meteorological Administration, Beijing, China

² Chinese Academy of Meteorological Sciences, Beijing, China

Abstract: Using the data of size resolved aerosol mass concentration and chemical composition obtained at Lin'An regional background air pollution monitoring station in Yangtze River delta region of eastern china, the size resolved aerosol effective refractive index was estimated for a summer and winter period. The real part of the estimated effective refractive index ranged from 1.55 to 1.60 if assumed dry aerosols in both summer and winter samples and ranged from 1.44-1.48 in summer samples if liquid water was include in the aerosol mass budget. The imaginary part of refractive index for submicron particles had significantly higher values in winter than in summer, and had much higher values for dry aerosols than if liquid water was included. Based on the estimated aerosol effective refractive index and measured aerosol size distributions, aerosol scattering and absorption coefficients were calculated. The calculated scattering coefficients assuming dry aerosols were 30% ~ 50% lower than those measured using Nephelometer instrument, and the calculated aerosol absorption coefficients were 10% ~ 40% lower than the measured values. When including the liquid water in the aerosol mass budget, the estimated scattering and absorption coefficients were closer to the measured values, but still lower up to 37%. The scattering coefficients increased by a factor of 1.54 after including liquid water content in the aerosol mass, the absorption coefficients increased only 10%, and the single scattering albedo increased 0.04.

Key word: Absorption coefficient, aerosol liquid water content, scattering coefficient, volume average method

纳米流体注入过程中咸水层二氧化碳迁移数值分析

(杨多兴^{1,2}, 张毅²)

1 中国科学院工程地质力学重点实验室, 北京, 100029

2 日本地球环境产业技术研究机构, 京都, 6190292

摘 要: 二氧化碳地质封存是一个新型的地质工程热点问题, 仍然面临诸多挑战, 其中之一是如何利用纳米材料与技术提高储层的可注入性和有效储量。本文将纳米流体的对流-扩散方程与三维多孔介质多相流动模式相结合, 初步建立多孔介质中超临界 CO₂ 纳米流体多相流动理论模型, 采用高精度时空守恒元/解元 (CE/SE) 算法, 模拟非均质储层中 CO₂ 的前缘迁移和分布特征。计算结果显示, 疏水纳米粒子减弱流体边界层内流动的剪切力, 增强 CO₂ 在边界层内的移动性能, 即纳米粒子在流体边界层减阻机理; 同时, 纳米粒子增强流体内部的剪切作用, 促进 CO₂ 前缘迁移均匀化。上述结果初步揭示疏水纳米粒子降低了地层非均质性对 CO₂ 前缘迁移的影响, 可提高 CO₂ 有效地质储量。本文提出的纳米流体地质封存概念, 对商业化大规模 CO₂ 地质封存、深层干热岩地热资源的开发、致密油气藏的高效开发以及提高采收率 (EOR) 具有意义, 同时对纳米材料与技术的环境资源利用及资源高效再生中的应用研究领域具有一定的推动作用。

关键词: 纳米流体, 地质封存, 超临界 CO₂, 致密油气藏, 纳米技术

黏粉原料配比及粒徑對於拜香燃煙特徵之影響

(楊奇儒^{1*}, 林建佑¹, 葉秀緯², 李孫榮¹, 張翊峰³)

1 嘉南藥理科技大學 環境工程與科學系, 台南, 71710;

2 嘉南藥理科技大學 環境資源管理系, 台南, 71710;

3 嘉南藥理科技大學 觀光事業管理系, 台南, 71710;

*通訊作者, Tel: 06-2664911 轉6337, E-mail: chiru.yang@gmail.com

摘要：在市面上拜香種類多且原料配比不同，燃燒後所產生之空氣污染物特徵亦有相當差異。拜香之組成及作用有竹支(支撐)、木粉(香味)及黏粉(黏著)。本研究針對使用最廣泛使用之木粉（新山香）及黏粉（楠樹皮），先將各材料粉碎後進行熱分析，分別解析各項拜香原料之燃燒特徵；再以固相採樣模組全量收集並分析拜香燃煙之物理、化學特性，探討燃煙對人體傷害較低之黏粉配比及粒徑。研究結果顯示，在配比方面，黏粉比例增加（不超過50%）將可延長燃燒時間並減少懸浮微粒及固相多環芳香烴化合物及總毒性當量排放係數。在粒徑方面，細粒徑黏粉（粒徑<0.074 mm）之拜香燃燒時間較短，但黏粉粒徑與懸浮微粒及固相多環芳香烴化合物排放量及並無顯著之相關。此外，在拜香製造方面，黏粉比例達60%時，無法以半手動方式製香並持續燃燒。本研究成果將可作為研發製造低汙染拜香之重要參考依據。

關鍵字：拜香、黏粉、拜香燃煙、懸浮微粒、固相多環芳香烴化合物

Preparation of Titania-Silica Aerogels and Their Application to VOC Degradation

(Sun-Wen Yao¹ (姚尚汶), Hsiu-Po Kuo¹ (郭修伯))

1 Department of Chemical and Materials Engineering, Chang Gung University, Tao-Yuan, 333

Abstract: Titania-silica aerogels are prepared by sol-gel and carbon dioxide supercritical drying. The morphologies and microstructures of aerogels are characterized by FE-SEM, BET and BJH adsorptions. The crystalline and the mechanical structures of aerogels are also studied. Since titania-silica aerogels with very large specific surface area are effective for VOC adsorption and anatase titania reveals good photocatalytic activities under UV light exposure, the as-prepared aerogels are used for toluene degradation in a photocatalytic fluidized bed reactor. With the inlet toluene concentration of 600 ppm - 1000 ppm and gas flow rate of 5 L/min - 15 L/min, the toluene vapor is continuously degraded with the removal efficiency greater than about 40%. The toluene removal efficiency decreases with the increases of the inlet toluene concentration and the gas flow rate.

Key words: aerogel, photocatalytic, VOC degradation

不同尺度非控制型重油燃燒對多環芳香烴污染物排放的影響

(葉旗福^{1,*}, 賴進興², 林清和², 鄭立新³, 陳明仁³, 蔡匡忠⁴, 陳宣匡⁴)

1 國立中山大學海洋環境及工程學系, 高雄

2 輔英科技大學環境工程與科學系, 高雄;

3 輔英科技大學職業安全衛生系, 高雄;

4 國立第一科技大學環境與安全衛生工程系, 高雄

摘要: 本研究主要探討在 20、40 及 60 公三種不同尺度非控制型圓形油盤重油燃燒過程中, 對氣固相多環芳香烴污染物 (19 種) 排放的物理化學特徵的影響, 並計算重油燃燒所排放出多環芳香烴的排放係數。本研究的燃燒實驗室, 係參考 ISO 9705 標準方法建置。研究結果顯示總多環芳香烴排放濃度, 隨油盤尺度增加而增加, 濃度由 20 公分油盤的 $537\mu\text{g}/\text{Nm}^3$ 提高到 60 公分油盤的 $3075\mu\text{g}/\text{Nm}^3$, 顯示多環芳香烴的排放與燃燒尺度有關。多環芳香烴在三種燃燒尺度, 其濃度分布主要均以氣相為主。在三種不同尺度油盤燃燒, 多環芳香烴濃度在環數 (2 到 6 環) 的分布, 主要以 2 及 3 環為主, 占總量的 73.1 到 84.6 %; 但其百分比隨油盤燃燒尺度增加而下降。當油盤燃燒尺度增加時, 除 2 環含量百分比與尺度成反比, 其餘 3 到 6 環則均隨尺度增加而增加。此外, 多環芳香烴的同族物比例診斷結果, 在固、氣相及總量上, 顯示良好的一致性, 可用於未來重油燃燒, 來源指紋的診斷參考。多環芳香烴在三種不同尺度的排放係數, 分別為 $3752\mu\text{g}/\text{g-oil}$ (20 公分)、 $3416\mu\text{g}/\text{g-oil}$ (40 公分) 及 $1321\mu\text{g}/\text{g-oil}$ (60 公分), 此結果, 則顯示排放係數隨油盤尺度增加而下降。三種尺度油盤煙氣的多環芳香烴毒性當量, 隨尺度增加而增加。因此, 大尺度重油燃燒對人體健康的影響及環境的衝擊要特別注意。

關鍵字: 重油, 燃燒, 多環芳香烴, 排放係數, 毒性當量

工业纳米颗粒气溶胶测量及数值模型构建

(于明州¹, Martin Seinenbusch², Gerhard Kasper²)

1 中国计量学院, 杭州, 310018;

2 Karlsruhe Institute of Technology, Karlsruhe, Germany, 76131

摘 要: 纳米颗粒多相流实验测量及相关模型构建已成为多相流研究领域重要研究内容。本文基于欧盟 NANOPARTICLE PROJECT 实验平台, 对由不同尺度谱颗粒系统组成的分散体系进行实验测量, 并针对双峰系统颗粒动力学演变过程、颗粒壁面湍动以及热扩散沉积、复杂系统发生源信息获取等方面进行了模型构建。

关键字: 工业纳米颗粒; 气溶胶; 测量; 数值模拟

分光光度法测定大气气溶胶细粒子中的阴离子表面活性物质[#]

(于彦婷^{1,2}, 李红^{2*}, 张庆竹¹, 段鹏丽^{2,3}, 曹冠², 李雷^{2,4})

1 山东大学环境研究院, 山东济南 250100;

2 中国环境科学研究院 环境基准与风险评估国家重点实验室, 北京 100012;

3 山西大学环境与资源学院, 山西太原 030006;

4 山东科技大学化学与环境工程学院, 山东青岛 266510

摘 要: 借鉴分光光度法测定水样中阴离子表面活性物质的研究, 结合国内外大气气溶胶阴离子表面活性物质的研究结果, 开展了气溶胶中阴离子表面活性物质分光光度分析法的条件实验, 分别优化了亚甲蓝分光光度分析法和乙基紫分光光度分析法。结果表明, 两种分析方法的样品超声提取条件基本相同, 超声频率选择超声清洗器的最高频率 40 Hz, 起始水浴温度设定为 30 ℃, 以 30 min 为最佳超声提取时间。亚甲蓝显色剂的最佳使用量为 1 mL 中性亚甲蓝溶液 (0.35 g/L) 和 1 mL 酸性亚甲蓝溶液 (0.35 g/L), 乙基紫显色剂的最佳加入量为 0.2 mL 乙基紫溶液 (0.49 g/L)。亚甲蓝法萃取完成后应放置 30~45 min 再测定氯仿相的吸光度, 而乙基紫法样品的放置时间不宜过长, 在 30 min 时测定最好。乙基紫分光光度法中应依次加入 pH=5 的醋酸盐缓冲液 0.4 mL、EDTA 溶液 (0.1 mol/L) 0.1 mL 和硫酸钠溶液 (1 mol/L) 0.25 mL, 以此达到提高测定灵敏度和降低实验误差的目的。

关键字: 细粒子, 阴离子表面活性物质, 分光光度法, 亚甲蓝, 乙基紫

在线单颗粒气溶胶质谱仪在香烟口感及烟气气溶胶老化过程检测中的应用

(粘慧青¹, 庄雯¹, 李梅^{2,*}, 周振)

¹ 广州禾信分析仪器有限公司, 广州, 510530

² 暨南大学, 广州, 510632

摘要: 利用在线单颗粒气溶胶质谱仪 (single particle aerosol mass spectrometer, 简称 SPAMS) 对七种品牌香烟烟气气溶胶颗粒粒径及化学成分进行检测, 研究七种不同口味的香烟烟气气溶胶化学成分与粒径的差异及老化过程中硫酸盐、硝酸盐、氯离子、苯系物的变化情况。结果表明, 香烟烟气气溶胶化学成分与不同粒径段上颗粒数比例的差异可能是导致不同种香烟口感差异的原因之一; 烟气气溶胶老化硫酸盐和硝酸盐的数浓度百分含量增加, 这是因为硫氧化物和氮氧化物转化成硫酸盐和硝酸盐, 而氯离子含量的减少则可能是发生了非均相取代反应; 新鲜烟气中苯系物数浓度百分含量最低, 随着老化时间的增加, 苯系物的数浓度百分含量逐渐上升, 这可能是由于在老化过程中, 烟气中的苯系物由气相到粒相之间的转化。

关键字: 单颗粒气溶胶飞行时间质谱仪, 香烟烟气气溶胶, 老化烟气

The application of single particle aerosol mass spectrometer on study of taste and aged cigarette smoke aerosol

Huiqing Nian, Wen Zhuang, Mei Li*, Zhen Zhou

Guangzhou Hexin Analytical Instrument Company Limited, Guangzhou 510530

JiNan University, Guangzhou, 510632

Abstract: Particle size and chemical composition of seven kinds of cigarette smoke were detected by single particle aerosol mass spectrometer (SPAMS). The difference of particle size and chemical composition in seven kinds of cigarette smoke were studied. The change of number fraction for sulfate, nitrate, chloride and BTEX in ageing process were also studied. The results indicate that the differences of chemical composition and particle size distribution in cigarette smoke aerosol were the reasons that lead to difference taste of different kinds of cigarettes. The number fraction of sulfate and nitrate increased because of the translation of SOX and NOX. The reason for the reduction of chloride may be due to the heterogeneous reactions. The number fraction for BTEX in fresh cigarette smoke was lower than the aged cigarette smoke. As the aging time increases, the number fraction for BTEX gradually increased, which can be explained by the translation of gas phase to particle phase in the aging process.

Key words: SPAMS, cigarette smoke aerosol, aged cigarette smoke

Email: limei2007@163.com

VOCs 廢氣治理與溶劑回收之最佳可行技術與案例探討

(粘愷峻^{*}、簡弘民^{1**}、張豐堂^{***})

摘 要：在臺灣 VOCs 已進行空汙費之徵收及相關管制法令之推行，而大陸於十二五規劃關於大氣污染防治，就 VOCs 之管制，將會走向法令規範日趨嚴格的趨勢，工業界于制程中使用有機溶劑之機會相當大，因此製造過程造成 VOCs 污染機會也相對提高，進行 VOCs 污染減量也勢必成為產業界必須重視的課題。

製造過程會產生 VOCs 排放的產業相當多，就不同產業所進行的統計就有 15 大項以上的產業之相關制程會產生 VOCs，環保主管機關也持續將尚未納入規範之產業進行法規研訂及逐年納管，以及適用一般性之 VOCs 排放標準，以期將所有污染源進行全面管制。

VOCs 之減量技術隨著產業需求日益增加，處理技術主要是以減量效率為主要考慮因素，以符合相關法令為其主要訴求；回收技術則是將廢氣中 VOCs 進行回收，將有機溶劑原物料回收再利用為主要訴求，因此在選用技術上需重點考慮其投資及經濟效益，較能符合產業之需求。

VOCs 應用處理技術中，焚化法破壞效率較高(>95%)，亦可回收 VOCs 燃燒所產生之熱能(可搭配熱媒油鍋爐、蒸汽鍋爐、吸收式冰水主機...等系統)，可以兼具環保及節能需求，應用產業也越來越多；VOCs 回收技術可視產業之需求選擇適當之技術，應用之產業從高科技業到傳統產業都有相關需求。

關鍵字：VOCs，流體化浮動床，沸石，焚化爐，RTO，PU 合成皮，凹版印刷

铅锌冶炼区大气颗粒物中典型重金属及来源分析

(张 凯^{1*}, 柴发合¹, 李倦生³, 郑子龙^{1,2}, 王静¹, 杨 晴^{1,2})

1. 中国环境科学研究院环境基准与风险评估国家重点实验室, 北京 100012

2. 山东科技大学化学与环境工程学院, 山东 青岛 266510

3. 长沙环境保护职业技术学院, 湖南长沙 410004

摘 要: 湖南是我国有名的“有色冶炼之乡”, 有色冶炼排放的废气成为我国大气重金属的主要来源之一。为了了解铅锌冶炼所排放的废气中典型重金属元素组分, 在湖南省中部某铅锌冶炼工业区周边及铅锌冶炼企业进行了大气颗粒物样品采集及分析。研究表明, 位于铅锌冶炼工业区下风向的采样点大气颗粒物中镉(Cd)、铅(Pb)和砷(As)的浓度明显高于其它站点, 而铬(Cr)浓度与其它站点相差不大; 粒径分布也表明, 颗粒物、Cd、Pb和As的最大浓度位于1.1~2.1 μm 之间, 具有非常相似的变化趋势, 而Cr无明显的粒径分布特征; 对铅、锌冶炼企业废气、底渣的样品采集分析表明, Cd、Pb和As会以废气的形式排到大气中, Cr通常会进入废渣。

关键字: 铅锌冶炼, 大气颗粒物, 典型重金属

砒矶岛国家大气背景站 PM_{2.5} 化学组成及来源分析

(张帆¹, 王晓平², 陈颖军^{1*}, 田崇国¹, 王艳¹)

1 中国科学院烟台海岸带研究所, 烟台, 264003;

2 中国科学院广州地球化学研究所, 广州, 510640

摘 要: 为了更加准确地反映我国区域大尺度的环境空气质量状况, 掌握我国环境空气污染物的区域输送情况, 国家环境监测总站在山东省长岛县砒矶岛设立国家大气背景监测站山东长岛站, 此站点是全国建设的 14 个背景站中唯一的示范站。砒矶岛站位于胶东、辽东半岛之间, 黄、渤海交界处, 东与韩国、日本隔海相望, 且受长距离传输影响显著, PM_{2.5} 来源及组分复杂, 对研究东南亚地区污染物迁徙规律具有重要作用。从 2011 年 11 月份开始砒矶岛站点进行 PM_{2.5} 大流量滤膜连续采样工作, 本研究选取了 2011 年 12 月至 2012 年 12 月期间共 72 个样品进行质量浓度及 OC、EC、无机元素、水溶性离子等化学成分分析, 以期获得砒矶岛背景点 PM_{2.5} 的化学组成特点, 并进一步探究该站点 PM_{2.5} 的来源。研究结果显示: (1) 砒矶岛 PM_{2.5} 年均质量浓度为 54.6 $\mu\text{g}\cdot\text{m}^{-3}$, 相较于北部沿海地区质量浓度偏低, 但远高于福建地区背景点浓度, 表明砒矶岛 PM_{2.5} 受周边地区大气传输影响显著; 季节浓度变化表现为春季浓度最高 (73.6 $\mu\text{g}\cdot\text{m}^{-3}$), 秋季浓度最低 (38.9 $\mu\text{g}\cdot\text{m}^{-3}$), 夏季与冬季浓度水平相近, 不同于北方其他地区冬季 PM_{2.5} 浓度最高的特点, 且月均最高浓度出现在 3 月份, 主要原因是砒矶岛春季受风沙影响较大, 而冬季湿沉降作用明显。(2) 砒矶岛 PM_{2.5} 组分主要为有机质、SO₄²⁻、NO₃⁻、NH₄⁺以及金属氧化物等, 其所占比例随季节不同变化显著, 其中, 夏季 SO₄²⁻所占比例最大, 冬季有机质所占比例最高, 与夏季二次气溶胶的生成和冬季燃煤比重较大相符合; 砒矶岛地区 PM_{2.5} 中 NH₄⁺与 SO₄²⁻的结合形式主要为 NH₄HSO₄; 砒矶岛 PM_{2.5} 中较高的 V/Ni 比值 (1.5) 证实了砒矶岛地区受周围船舶排放影响较大。(3) 使用 PCA/APCS 法对砒矶岛 PM_{2.5} 及 20 种化学组分质量浓度进行 PM_{2.5} 源解析, 结果表明, 对砒矶岛 PM_{2.5} 来源贡献率最大的为二次气溶胶、煤炭及生物质的燃料燃烧以及包括汽车与船舶等燃油尾气排放等, 全年中贡献率之和均在 80%左右, 海盐也占了较大的比重。(4) 总之, 受长距离传输的影响, 砒矶岛 PM_{2.5} 及其绝大多数化学组分浓度低于环渤海城市, 且传输过程中不同的沉降速率导致了如 SO₄²⁻与 NO₃⁻等较差的相关性; 气团反演轨迹亦证明了不同主导风向条件下砒矶岛 PM_{2.5} 及其化学组分存在差异。即砒矶岛大气背景点的建立为环渤海地区城市污染状况提供了有效的对照, 并验证了 PM_{2.5} 受长距离传输作用影响的显著性。

关键字: 砒矶岛, PM_{2.5}, 水溶性离子, 金属元素, 源解析

武汉秋季灰霾和非灰霾天气 PM_{2.5} 中水溶性离子的特征研究

(张帆, 成海容, 王祖武*, 吕效谱)
(武汉大学资源与环境科学学院, 武汉 430072)

摘要: 分析了武汉地区武大和东新两个采样点秋季灰霾和非灰霾天气 PM_{2.5} 中的九种水溶性离子(F、Cl⁻、NO₃⁻、SO₄²⁻、Na⁺、NH₄⁺、K⁺、Mg²⁺、Ca²⁺)浓度。结果表明, NO₃⁻、SO₄²⁻和 NH₄⁺是武汉秋季 PM_{2.5} 中最重要三种水溶性离子, 且 PM_{2.5} 中各水溶性离子之间组成比例是相对稳定的。灰霾期 PM_{2.5} 中水溶性离子比重的增加是武汉秋季灰霾污染的重要特征, 它们可能来源于生物质燃烧、土壤扬尘、化石燃料燃烧、汽车尾气排放等过程, 其中东新站点的大气二次污染比武大站点严重。固定源对武汉两站点秋季灰霾期大气中 NO_x 与 SO₂ 相对贡献均比非灰霾期要大, 移动源对东新站点秋季大气中 NO_x 与 SO₂ 的相对贡献则比武大站点要大。

关键词: 武汉, 灰霾, 水溶性离子, PM_{2.5}

Characteristics of Water-soluble Ions in PM_{2.5} during Haze and Non-haze Period in Autumn in Wuhan

ZHANG Fan, CHENG Hai-rong, WANG Zu-wu*, LV Xiao-pu
(School of Resource and Environmental Science, Wuhan University, Wuhan 430072, China)

Abstract: Nine water-soluble ions of PM_{2.5} including F, Cl⁻, NO₃⁻, SO₄²⁻, Na⁺, NH₄⁺, K⁺, Mg²⁺ and Ca²⁺ were analyzed during haze and non-haze period in autumn in 2012 at Wuda and Dongxin in Wuhan. The results showed that NO₃⁻, SO₄²⁻ and NH₄⁺ were the most important ions in PM_{2.5} and the composition of the ions in PM_{2.5} was relatively stable. The increase of the proportion of water-soluble ions in PM_{2.5} during the haze period was an important feature of the air pollution in autumn in Wuhan. And they might be derived from the course of biomass burning, soil dust, combustion of fossil fuels, automobile exhaust emissions. The secondary air pollution in Dongxin was more serious than that in Wuda. The relative contribution of stationary sources to NO_x and SO₂ in Wuhan's atmosphere during the haze period was greater than that in the non-haze period. And the relative contribution of mobile sources to NO_x and SO₂ in Dongxin was greater than that in Wuda.

Key words: Wuhan; haze; PM_{2.5}; water-soluble ions.

基金项目: 国家 973 计划项目(2011CB707106), 湖北省重点实验室(武汉大学)开放基金项目, 中国科学院广州地球化学研究所有机地球化学国家重点实验室开放基金(OGL-201110)

***通讯作者:** 王祖武(1962-), 男, 教授, 博士生导师, 主要从事大气污染控制工程、大气环境化学的研究, (电子信箱)hjgc1891@163.com.

作者简介: 张帆(1983-), 男, 博士研究生, 主要从事大气环境化学、大气污染控制工程的研究, (电子信箱)whu_zf@163.com.

海峽兩岸大氣中懸浮微粒模擬結果之性能評估

(張良輝¹, 陳杜甫¹, 蔡長祐¹)

¹ 台灣雲林科技大學環境與安全衛生工程系, 雲林, 64002;

摘要: 由於空氣污染物受到大氣化學反應、沈降、傳輸等機制之影響, 空氣品質在時間與空間之變異性非常大, 為瞭解這些變異之特徵與原因, 以及進一步後續進行傳輸影響與管制策略評估探討, 需要一個能夠合理準確模擬時空變異之空氣品質模式, 而要瞭解模式模擬結果是否合理準確, 需要與觀測資料比較以進行性能評估。本研究以 MM5/CMAQ 模式為基礎進行 2007 一整年包括大氣中懸浮微粒(PM)及其前驅物與衍生物之模擬。模式模擬範圍將使用三層的巢狀網格套疊, 最大模擬範圍涵蓋東亞地區, 最小模擬範圍包含全台灣, 且網格解析度達 9 公里。在巢狀網格模擬架構下, 模擬系統還包括三大部分: 氣象前處理、排放資料前處理、初始與邊界條件。(1)氣象前處理: 使用 MM5 所模擬之四維氣象場, 經由氣象前處理程序輸出空品模式所需之氣象參數。(2)排放量前處理: 東亞其它地區人為源排放量主要使用 REAS (Ohara et al., 2007)推估資料(排放量資料解析度 $0.5^\circ \times 0.5^\circ$)並經適當處理而得, 而生物源排放量則是利用東亞生物源排放量推估模式配合氣象資料進行逐時排放推估(張等, 2005); 台灣排放的人為源排放量採用最新的 TEDS7.1 (排放量資料解析度 $1 \text{ km} \times 1 \text{ km}$), 並透過排放前處理程序配合氣象資料計算污染物之三維空間(煙流高度計算)及其隨時間之分布, 生物源排放量則是透過台灣生物源排放推估模式配合氣象資料進行逐時排放推估(Chang et al., 2009)。模擬結果經粒徑分佈處理成 PM₁₀ 與 PM_{2.5} 後, 再與各種空氣品質監測資料進行比較評估。研究結果顯示全台灣測站平均 PM₁₀ 低估約 11%, SO₂ 低估約 22%, NO₂ 低估 2%。PM₁₀ 模擬除在宜蘭與雲嘉南空品區明顯較差(低估 23-24%)外, 其餘空品區均低於 13%; SO₂ 與 NO₂ 模擬則是宜蘭與花東空品區明顯較差。而本研究針對大陸六大地區在模擬範圍內的 82 個重點城市所進行 2007 全年驗證統計顯示, 華東與華南地區模擬值均屬於高估(各約 33%、52%)且大部份城市均為高估; 東北與西北地區模擬值均屬低估(各約-32%、-55%)且幾乎所有城市均為低估; 華北與西南地區均有部份城市呈現低估、部份呈現高估, 使得兩地區整體平均值各別呈現略為低估(-10%)與略為高估(11%)。相對於大陸重點城市, 本研究對於台灣測站可以獲得較佳的模擬結果。造成此差異的主要原因應有二: (1)兩者模擬網格解析度不同(由於排放資料空間解析度的限制, 大陸使用粗網格、台灣使用細網格); (2)本研究目前可取得之台灣與大陸排放資料, 在空間及時間解析度、及完整性有明顯之差異。

关键字: 排放量, 空氣品質模式, 監測資料, 解析度

Chemical composition and source characterization of Fugitive Dust over Xi'an in the South Margin of the Loess Plateau, China

(Zhang Qian¹, Mu Jiao¹, Shen Zhenxing^{1,2})

¹ Department of Environmental Science and Engineering, Xi'an Jiaotong University, Xi'an 710049, China

² SKLLQG, Institute of Earth Environment, Chinese Academy of Sciences, Xi'an 710075, China

Abstract: A unique set of soil samples were collected to analyze the chemical composition and source characterization of Fugitive Dust over Xi'an city, namely, 2 soil dust samples, 19(4) paved road dust samples, 53(17) construction dust samples and 2 cement production samples. By the means of high-sensitivity X-ray fluorescence and ion chromatography, the samples were detected contained eighteen elements like Na, Mg, Al, Si, K, Ca, Ti, V, Cr, Mn, Fe, Co, Ni, Cu, Zn, As, Ba and Pb and eight ions like Na⁺, Mg²⁺, Ca²⁺, F⁻, Cl⁻, NO₃⁻ and SO₄²⁻, respectively. The most abundant elements in the samples were Al, Si, Ca and Fe. The elements of Ca, Zn, As and Pb had negative correlations to crustal elements (Si, Al, K and Ti) and were rich in Xi'an city, typically, which indicated that they were from non-crustal sources and can be used as the typical trace elements of construction dust emission. High correlations ($r > 0.84$; $**P < 0.01$) were observed among crustal elements except Fe in dust samples which indicated that the source of Fe is different from others as it may come from oil burning. The observed Si/Al, K/Al, Ti/Al and Mn/Al ratios were similar to the source of Composite loess in Chinese Loess Plateau (CLP) and Upper Continental Crust (UCC): Furthermore, Fe/Al and Mg/Al were consistent with the Dust storm over NW China, implying that the fugitive dust were mixedly influenced by them. In cement samples, the ratios of K/Ca, Si/Ca and Fe/Ca were higher than other dust samples in Asian dust but much lower than in other urban cities, indicating there were significantly differences in the contributions of the energy structure of K, Si and Fe in Xi'an. Most of the water-soluble calcium had high correlation with evaluated carbonate ($r=0.97$), implying that Ca²⁺ is in the form of CaCO₃ rather than other calcium minerals in Xi'an fugitive dust. The majority of K is insoluble ($K^+/K < 20\%$), showing that the fugitive dust can be separated from biomass burning contributions. A similarity of major elemental portions and variation tendency in accordance with the characteristics of construction dust were observed in four types of fugitive dust (soil dust, cement, construction, paved road dust) over Xi'an area which shows that construction sites have great influences on the composition of city fugitive dust in Xi'an.

Key words: Fugitive Dust, Xi'an city, Source apportionment, Construction dust

Spatial and Seasonal Variations of Mass and Chemical Composition for PM₁₀ in Xi'an, China

(T. Zhang¹, J.J. Cao^{1,2}, S.X. Liu¹, S.X. Yang¹)

¹ SKLLQG, Institute of Earth Environment, Chinese Academy of Sciences, Xi'an, 710075, China.

² Institute of Global Environmental Change, Xi'an Jiaotong University, Xi'an, 710049, China.

Abstract: PM₁₀ samples were simultaneously collected in six sampling sites during spring, summer, autumn and winter in 2010, and then their chemical composition, including elements of Ti, Mn, Fe, Zn, As and Pb, water-soluble inorganic ions of Na⁺, NH₄⁺, K⁺, Mg²⁺, Ca²⁺, Cl⁻, NO₃⁻, and SO₄²⁻, organic carbon (OC), and element carbon (EC), were determined to evaluate the PM₁₀ levels and their chemical characteristics in Xi'an. The annual mean value of PM₁₀ mass concentration was 302.6 µg m⁻³ at Shengzhengfu site (north), 293.1 µg m⁻³ at Weidianji site (western), 266.3 µg m⁻³ at Dihuansuo site (south), 223.7 µg m⁻³ at Chanba site (eastern) and 254.9 µg m⁻³ at Gaolin site (upwind zone), 211.1 µg m⁻³ at Heihe site (downwind zone). The CD values calculated for the urban and background stations were 0.25, 0.20, 0.17 and 0.22 during spring, summer, autumn, and winter, respectively. Low CD values reflect the similarities in the composition of the aerosol between sites. The PMF results revealed that construction dust (22.7%) contributed significantly to the detected PM₁₀ mass, followed by secondary aerosol (22.3%), motor vehicle (18.3%), coal combustion (17.8%), soil dust (13.1%) and biomass burning (5.8%) at the urban site.

Keywords: PM₁₀, chemical composition, mass balance.

1964—2010 年四川能见度及消光系数特征及变化趋势

(张小娟¹, 韩永翔¹, 陈娟², 郑小波²)

1. 南京信息工程大学大气物理学院, 南京, 210004

2. 贵州省气候中心, 贵阳, 550002

摘 要: 利用四川省 156 个气象观测站 1964—2010 年能见度、相对湿度、降水和天气现象等观测资料, 分析四川省 47 年来能见度的时空变化特征, 并采用线性倾向率法对能见度和大气消光系数的变化趋势进行了分析。结果表明, 有 57.7% 台站出现了能见度减少趋势。减少最多为 $-7.72 \text{ km}/10\text{a}$, 最少为 $-0.02 \text{ km}/10\text{a}$ 。减少的平均气候倾向率在 1964-2010 年为 $0.33 \text{ km}/10\text{a}$, 平均能见度从 60 年代的约 30 km 下降到目前的约 27km。另一方面, 有 42.3% 站能见度有增加趋势, 且多集中在人类活动较为稀少的高海拔山区。1964-1997 年, 四川平均消光系数迅速增大, 1997 年以来略有下降, 总体上说消光系数是增加的, 主要出现在四川盆地和四川南部人口和工业稠密区。认为能见度下降、消光系数增加的原因与人为排放污染物浓度增加有密切关系。

关键词: 能见度, 消光系数, 四川, 气溶胶, 大气污染

华北平原区域雾霾天气分析与数值试验

(张小玲¹ 唐宜西^{1,2} 赵秀娟¹ 熊亚军³)

1 中国气象局北京城市气象研究所, 北京, 100089

2 成都信息工程学院大气科学学院, 成都, 620225

3 北京市气象台, 北京, 100089

摘要: 2013年1月中国中东部地区发生了多次持续雾霾天气, 对人体健康、交通运输、日常生活以及生态环境造成了严重影响。本文选取1月27-31日华北平原地区持续5天的雾霾天气进行分析, 并利用气象化学在线耦合模式WRF-Chem对持续雾霾期间的PM_{2.5}浓度以及气象要素进行模拟研究。结果表明, 区域雾霾过程期间华北平原高空以平直纬向环流为主, 地面多为弱气压场, 低层空气湿度大, 并有强逆温存在且维持时间比较长, 造成大气层结稳定、低层风速小(多偏南风维持)、高湿的典型静稳天气, 北京及其以南地区几乎处于空气停滞区, 边界层内污染物的水平和垂直扩散能力差, 高湿条件更易导致PM_{2.5}浓度在短时间内迅速升高, 高湿及PM_{2.5}的高浓度共同导致雾霾天气维持。实时运行的9km分辨率的华北区域WRF-Chem模式对此次雾霾过程期间PM_{2.5}浓度的形成和高浓度持续时间、消散减弱和结束的时间做出了较好的预报, PM_{2.5}浓度表现为“北低南高”的分布趋势。数值试验结果表明, 由于受地形和华北平原城市群高污染物排放的影响, 在弱气象场条件的影响下, 逐渐通过本地积累和城市间的输送造成区域性的重污染。特别是北京地处华北平原的西北边缘, 除京津有明显的高排放源外, 北京西南方向延伸至河南北段的诸多城镇形成大面积污染排放带, 在静稳天气条件下, 弱的偏南气流有利于把西南污染物和水汽输逐渐送到北京地区, 与本地累计的污染物叠加形成区域性重污染, 导致能见度下降, 造成严重的区域性雾霾天气。同时利用数值模式, 对本次雾霾过程中区域污染源排放强度消减试验表明, 对北京城区PM_{2.5}浓度贡献由大到小排列为: 冬季采暖季民用源>电厂排放>交通源排放>工业源排放; 扣除北京人为污染源排放后, 北京城区PM_{2.5}平均浓度可降低50%以上, 说明区域输送对北京城区的污染物浓度有明显影响。因此, 应对典型静稳天气条件下雾霾与重污染, 需加强静稳天气和重污染的预报预警, 加强区域联防联控, 加大多种污染源排放的综合治理和区域治理。

关键词: 区域雾霾, PM_{2.5}浓度, 气象条件, WRF-Chem数值试验, 区域输送

Observation of submicron aerosols at Mount Tai in east China from 2010 to 2012: Impact of different air masses on chemical components and size distribution

(Y.M. Zhang¹, X.Y. Zhang^{1,*}, J.Y. Sun¹, G.Y. Hu², X.J. Shen¹, T.T. Wang³, D.Z. Wang⁴, Y. Zhao⁴)

1. Key Laboratory for Atmospheric Chemistry, Chinese Academy of Meteorological Sciences, Beijing, China;

2. Wu Han University, Wu Han, China

3. Heilongjiang Province Meteorological Bureau, Harbin, China

4. Tai An meteorological bureau, Shan Dong province, Tai An, China

* Correspondence to X.Y. Zhang (xiaoye@cma.gov.cn)

Abstract. Real-time measurements of non-refractory submicron aerosols (NR-PM₁) were conducted using an aerodyne mass spectrometry (Q-AMS) at the summit of Mount Tai (1534m above sea level) in Shandong province, located in the center of the Central East China (CEC) region, from June 2010 to January 2012, as a part of National basic research project monitoring campaign. The mass concentrations and size distributions of non-refractory submicron particle (NR-PM₁) species (i.e., sulfate, nitrate, ammonium, chloride, and organics) were measured in situ at 5-min time resolution. Overall, 146 days valid data was obtained during the whole campaign, which covers four different seasons. The average total mass concentration of NR-PM₁ was 42.9 g m⁻³, with 31% sulfate, 32% organics, 19% nitrate and 18% ammonium. The average mass concentration of NR-PM₁ is highest (59.9 g m⁻³) in summer and lowest (31.9 g m⁻³) in spring. Species occupied different percentages in different seasons, sulfate in summer, Organics in fall and winter, while nitrate dominates the NR-PM₁ in spring respectively. To investigate the size-resolved mass concentrations of aerosol chemical components from different sources, seven air masses were clustered based on the 72 hours back trajectory with HYSPLIT model. Cluster I, IV and V with short pathway represent the local and regional sources, and the concentrations from these clusters were higher than that from cluster III and VI which originated from remote and clean North-West sources. According to the results of diurnal cycles for chemical species in NR-PM₁ higher at noon and lower at midnight from seven clusters, it was concluded that the site was controlled under the transitions between PBL and FT at daytime and nighttime. The size distributions of chemical species were different from different air masses, cluster I, II, IV, V and VII showed same shape with accumulation mode (500-600nm), the concentration at nighttime is lower than at daytime. For cluster VI and III, it demonstrated wider shape peaking at 300 nm, and there were no obvious decrease in concentration at nighttime.

Keywords: NR-PM₁, Chemical species, mass concentration, Size distribution, Mt. Tai

北京市大气中醛酮化合物和 BTEX 来源和浓度变化特征

摘 要：本研究于 2008 年 7 月-2010 年 8 月期间对北京市大气中的醛酮化合物和 BTEX 进行了同步观测研究，对大气中的醛酮化合物主要采用了 2,4-二硝基苯肼(DNPH) 涂敷的硅胶柱吸附和高效液相色谱分析的方法，对大气中的 BTEX 主要采用了 Tenax-TA 吸附/二次热解析/毛细管气相色谱法(GC-PID4400)分析的方法。大气中主要醛酮类化合物(甲醛、乙醛和丙酮)存在明显的年际变化特征，甲醛和乙醛的浓度之和的年增长率为 10%左右，而不规则的丙酮浓度以及甲醛/丙酮和乙醛/丙酮比值的季节变化表明其可能受当地不规律排放源的影响。三种醛酮化合物的季节平均浓度分别为：夏季($50.5 \mu\text{g m}^{-3}$)>春季($39.7 \mu\text{g m}^{-3}$)>秋季($37.7 \mu\text{g m}^{-3}$)>冬季($31.3 \mu\text{g m}^{-3}$)，除冬季以外，浓度日变化最大值出现在 14:00 左右，表明光化学二次形成是大气醛酮类化合物的一种重要来源。利用特征比值法估算了夏季光化学二次形成对大气中甲醛和乙醛的最大贡献率为 47.6-60.3%。北京市大气中 BTEX 的浓度年增长率为 15%，并且存在显著日变化和季节变化特征：冬季($31.9 \mu\text{g m}^{-3}$)>秋季($27.2 \mu\text{g m}^{-3}$)>春季($23.2 \mu\text{g m}^{-3}$)>夏季($19.1 \mu\text{g m}^{-3}$)，浓度日变化呈现早晚峰值，中午低谷值，表明汽车尾气是北京市大气中 BTEX 的重要来源。采用苯与甲苯特征比值分析表明，北京市冬季民用煤炉取暖以及夏季高温加剧的溶剂剂和涂料的挥发对北京市大气中 BTEX 也具有重要贡献。

行驶车辆对城市街谷内空气流动与污染物扩散的影响-基于拉格朗日模型的数值模拟

(张云伟, 顾兆林*, 段翠娥, 苏磊杰)

西安交通大学, 西安, 中国, 710049

通讯作者: 顾兆林教授, e_mail: guzhaolin@mail.xjtu.edu.cn

摘 要: 行驶车辆诱导空气流动及湍流也是影响街谷内空气流动与污染物扩散的重要因素, 尤其在街谷的底部。本文通过街谷内单个车辆在任意时刻对空气的曳力计算, 提出更具一般意义的欧拉-拉格朗日方法, 实现对行驶车辆引起空气流动及湍流的模拟。模拟结果显示, 在不同的背景来流风速下, 行驶车辆对街谷内湍流有显著影响, 而对平均流场的影响相对较弱。行驶车辆诱导的湍流主要分布的靠近路面的区域, 且在靠近背风面的地方湍流强度增加最为显著。街谷内行驶车流诱导湍流强度及分布受背景来流风速的影响显著, 而受车辆行驶速度的影响相对较弱。模拟结果显示, 街谷内行驶车流对风场的影响非常复杂, 以至于简单的以车辆行驶速度或背景来流风速进行参数化的模型很难模拟不同情形下的流场特征。而本文提出的拉格朗日模型在模拟街谷内行驶车辆对风场的影响时具有更高的精度和灵活性。

关键词: 车辆诱导湍流, 城市街谷, 数值模拟, 风场, 拉格朗日模型

以臺南市大氣粒狀物所含重金屬比例判斷重金屬污染源變異性

(張皇珍¹、邱瑞基²、林徽雅³、涂良君⁴)

1 臺南市政府環境保護局 局長 臺南市

2 臺南市政府環境保護局空氣及噪音管理科 科長 臺南市

3 富立業工程顧問股份有限公司 專案經理 臺南市

4 富立業工程顧問股份有限公司 協理 臺南市

摘 要：由於重金屬具有型態多變性、遷移轉化之廣泛性、生物體之累積性、毒害性及無法分解之特性，故較一般有害物質對人體及環境之危害性更為嚴重，故臺南市政府環境保護局於 100 年~101 年期間，對轄區內進行大氣粒狀物中重金屬檢測作業，而本研究利用歷次粒狀物所含重金屬比例分析評估污染源變異情形。由檢測結果進行分析顯示，重金屬鉛及鎘歷次鉛占粒狀物比例差異性不大；重金屬砷之歷次比例變化性較大，顯示污染來源變異性大，尤其為顯宮國小(安南區)及官田國中測站(官田區)，可能受到偶發事件的影響較大，由結果發現重金屬砷污染源較不易掌握。

关键字：重金屬，污染源

臺南市細懸浮微粒變化趨勢及區域污染特性分析

(張皇珍¹, 邱瑞基¹, 呂鴻毅², 蔡宜倫², 黃琬鈴²)

1 臺南市政府環境保護局, 台南市

2 立境環境科技股份有限公司, 高雄市

摘要：依據台灣環保署設置於臺南市空氣品質監測站(新營站、善化站、安南站、臺南站)長期監測資料顯示,臺南市細懸浮微粒($PM_{2.5}$)累積第 98%日平均值(第八大值)有明顯改善趨勢,2006 年為 $91.1 \mu g/m^3$,2012 年為 $65.0 \mu g/m^3$,改善率達 28.5%; $PM_{2.5}$ 年平均值整體亦呈現改善趨勢,2006 年為 $40.4 \mu g/m^3$,2012 年為 $33.0 \mu g/m^3$,改善率達 18.3%,顯示近年臺南市政府環境保護局管制策略之成效。另外,分析臺南市 $PM_{2.5}$ 之區域污染特性,統計 2006 至 2012 年各測站 $PM_{2.5}/PM_{10}$ 之比值,新營站介於 0.44~0.54(平均 0.49),善化站 0.49~0.53(平均 0.52),安南站 0.43~0.57(平均 0.52),臺南站 0.54~0.66(平均 0.58),顯示南部測站(如台南站)明顯高於北部測站(如新營站),且位於都會區之測站(如臺南站) $PM_{2.5}/PM_{10}$ 比值亦明顯高於郊區之測站(如安南站),與相關文獻之研究結果吻合,表示位於郊區之測站受原生性懸浮微粒影響較大,而都會區之測站因受交通污染源影響,易產生衍生性二次氣膠及細懸浮微粒。

关键字：細懸浮微粒, $PM_{2.5}$, 台南市

福州與馬祖地區酸雨化學成份及雨水酸化之探討

(張章堂¹，林凱隆¹，袁中新²，施志恆³，陳玉利⁴，江士豪⁵，陳光暉¹)

¹ 台灣宜蘭大學環境工程學系，宜蘭；

² 台灣中山大學環境工程研究所，高雄

³ 昱山環境技術服務顧問有限公司，台北，10029；

⁴ 連江縣環保局，連江縣，10029；

⁵ 連江縣東引鄉環保科，連江縣，21241；

摘要：於馬祖地區及鄰近福州馬尾地區設置六處酸雨採樣站，分別位於南竿鄉南竿氣象站、北竿鄉中山國中、東引鄉民代表會、黃岐鎮黃岐中學、連江縣百勝中學及梅花鎮梅花中學等六處地點，進行酸雨採樣，並分析雨水酸鹼值(pH)及化學成份，藉以瞭解馬祖地區酸雨化學成份及雨水酸化原因。馬祖地區之盛行風向為東北風，歷年冬季降雨量普遍僅有 50 mm~100 mm 間。本計畫採樣期間 7 月至 9 月 pH 值主要分布在 4.0 至 6.0，進入秋季過後雨水 pH 值下降到 4.0~5.0 之間，明顯有下降的趨勢。而本計畫採樣期間，7 至 12 月每月酸雨發生率分別為 6.7%、19.2%、47.4%、48.9%、83.3%。由採樣結果顯示，10 月過後酸雨發生率明顯上升，其中又以連江縣百勝中學採樣站發生率最大，酸雨平均發生率達 60%。由雨水化學成份分析結果顯示，馬祖地區雨水中 Na^+ 、 Cl^- 濃度普遍較高，顯示海島型的馬祖地區容易受到海鹽影響此外，馬祖地區主要致酸離子為 SO_4^{2-} ，而福州馬尾地區主要致酸離子除 SO_4^{2-} 外， NO_3^- 亦是重要致酸物種。

关键字：酸雨、化學成分、酸性沈降物

Analysis and characteristics of visibility in Shenyang from 2010—2012

(Hujia ZHAO^{a,b,c}, Huizheng CHE^a, Xiaoye Zhang^a, Yanjun Ma^c, Yangfeng Wang^c,)

^aKey Laboratory for Atmospheric Chemistry (LAC), Institute of Atmospheric Composition, Chinese Academy of Meteorological Sciences (CAMS), CMA, 46 Zhong-Guan-Cun S. Ave., Beijing 100081, China

^bUniversity of Chinese Academy of Science, Beijing 100049, China

^cInstitute of Atmospheric Environment, China Meteorological Administration, Shenyang 110016, China

ABSTRACT: Using the visibility data during 2010 to 2012 obtained at Shenyang Atmosphere Observation Center, the relationships between visibility, PM mass concentration and meteorological elements were statistically analyzed. The results show that: The monthly averaged visibility over Shenyang is higher in March and September with values about 19.0 ± 4.3 km and 17.1 ± 4.3 km, respectively. Low visibilities over Shenyang occur in January about 11.0 ± 4.7 km. Among the meteorological elements, wind speed was the main meteorological factor that influenced visibility and the PM mass concentrations. The number of days with visibility >19.0 km and visibility <10.0 km in Shenyang are 59, 123, 145 and 132, 119, 121 from 2010 to 2012. The relationship between visibility and PM indicated that human activities are already main sources of the pollutants, especially the fine particles which is the most important factor for the deterioration of visibility. The study shows an obvious diurnal variation and weekend effect of visibility and PM which are mainly due to human activities.

Keyword: Visibility; Particulate Matter; Shenyang; Northeast China

新国标下峡口地形城市冬季大气污染的时空分布变化规律研究

(赵克明¹, 李霞^{2,3*}, 卢新玉¹, 冯志敏⁴, 王磊⁵, 马超¹)

(1. 新疆气象台, 新疆 乌鲁木齐, 820002;

2. 中国气象局乌鲁木齐沙漠气象研究所, 新疆 乌鲁木齐, 820002;

3. 中国科学院大气物理研究所中层大气与全球环境探测实验室 北京 100029;

4. 新疆维吾尔自治区气候中心, 新疆 乌鲁木齐, 820002;

5. 乌鲁木齐市气象局, 新疆 乌鲁木齐, 820002)

摘 要: 峡口地形城市乌鲁木齐是全国乃至世界大气污染最为严重的城市之一。本文基于 2013 年 1~3 月每日发布的六类污染物 (PM_{10} 、 SO_2 、 NO_2 、 $\text{PM}_{2.5}$ 、 CO 和 O_3) 逐时数据和同期的气象数据, 对乌鲁木齐污染物的时空分布变化规律进行了分析。结果表明, 乌鲁木齐污染物浓度空间分布型可分为两种, 即城区中心~外围过渡型和南北过渡型。 PM_{10} 是城区中心~外围递增型, SO_2 和 CO 则是城区中心~外围递减型。南北递增型是 $\text{PM}_{2.5}$ 和 O_3 , 南北递减型为 NO_2 。乌鲁木齐冬季六类污染物污染指数级别由轻到重依次是: O_3 达到优水平, SO_2 为 II 级良, NO_2 属于 II、III 级良~轻度污染之间, CO 为 III 级轻微污染, PM_{10} 达到 IV 级中度污染水平, $\text{PM}_{2.5}$ 则为 V 级重度污染水平。污染物日变化曲线大致为双峰结构 (PM_{10} 、 $\text{PM}_{2.5}$ 和 NO_2) 单峰结构 (SO_2 、 CO 和 O_3), 中午 13~16 时、凌晨 7~8 时分别是乌鲁木齐全天污染最为严重和相对较轻的时段。煤改气采暖工程极大地改善了乌鲁木齐的空气质量, 但是由细颗粒物 $\text{PM}_{2.5}$ 造成的霾天频率依然很高 (42.9%~88.9%), 其与相对湿度、能见度、风速、降水呈反相关关系, 与逆温差呈显著的正相关。

关键字: 乌鲁木齐, 污染物, 时空变化规律, 煤改气采暖工程, 霾日

基金项目: 新疆自然科学基金 (2011211A102)、中央级公益性科研院所基本科研业务费专项资金项目 (IDM2008003)、中国沙漠气象科学基金 (Sqj20080014) 联合资助。

作者简介: 赵克明 (1983—), 男, 新疆乌鲁木齐人, 硕士研究生, 助理工程师, 主要从事短期天气预报和研究工作。Email: zhaokeming_1983@163.com。

***通讯简介:** 李霞 (1969—), 女, 新疆石河子人, 博士研究生, 副研究员, 主要从事大气环境和天气气候研究。Email: susannaryy@163.com。

Effects of meteorological conditions on high BC concentration at Xi'an from 2003 to 2007

(Zhao Shuyu¹)

1 Institute of Earth Environment, Chinese Academy of Sciences, Xi'an China, 710075

Abstract This study mainly investigated the causes of high black carbon (BC) episodes and effects of meteorological conditions on air quality in winter at Xi'an. Continuous BC mass concentration was measured from September 2003 to August 2007 at the site of Institute of Earth Environment, an urban site at Xi'an. Averaged BC concentrations were higher in winter and autumn than those in summer and spring. High BC concentration often appeared in winter and the magnitude was higher than those measured at other urban sites. Annual averaged BC concentration showed a linear decline that indicated the reduction of emissions and proportion of coal burning in the total energy consumption in winter. Relationships between BC concentration and meteorological conditions showed that an inversion layer, descending motion in the low troposphere and weak surface wind jointly contributed to high BC concentration in winter at Xi'an. Significant negative relationships between BC concentration and boundary layer height, wind speed implied that meteorological conditions directly affected seasonal variation of BC concentration. Additionally, less precipitation was also a key factor that led to high BC concentration in winter at Xi'an due to BC accumulation in the atmosphere.

Keywords: BC, Xi'an, boundary layer height, wind speed, precipitation

大气边界层中 VOCs 层化分布与逆温现象之相关性探讨

(郑佳俊¹ 林启灿² 袁中新³ 洪崇轩⁴ 廖思婷¹)

¹ 高雄海洋科技大学海洋环境工程系(所)硕士生

² 高雄海洋科技大学海洋环境工程系(所)教授

³ 中山大学环境工程研究所教授

⁴ 高雄第一科技大学环境与安全卫生工程系助理教授

摘 要：VOCs 是产生臭氧空气质量污染物之前驱物，大气中 VOCs 浓度可能会受到气象条件影响，而产生层化现象；过去也有许多文献提出，大气中有逆温层、混合层等情况出现时，会导致大气成份的层化分布。然而，臭氧空气质量模式推估，长期以来皆假设前驱污染物在垂直高度范围是均匀混合；为印证大气逆温层化现象是否会导致 VOCs 层化分布，本研究监测大气边界层中 VOCs 浓度之垂直分布，并与逆温现象之相关性进行探讨，以供空气质量模式研究人员评估其可能会导致的推估误差。研究选用探空气球采样法，进行从地面至垂直高空 800 公尺间，大气温度量测与气体采集，并以热脱附冷冻装置做为前处理再搭配 GC/MSD 进行 VOCs 之检验工作。

研究显示，冬季大气温度稳定度日夜变化结果，白天时段先由中性稳定转至极不稳定的状态，再逐渐回转至中性弱稳定；夜间时段，在 21:00-23:00 之间，大气稳定度为极稳定，此时亦是逆温层容易出现之时段；冬季逆温层是以辐射逆温为主，且高度范围较接近地面在 200-500 公尺之间。夏季大气稳定度趋势变化与冬季相反，逆温层则容易出现在白天 07:00-10:00 间，出现高度范围变化也较大。当逆温层出现时，有观察到污染物会蓄积在逆温层下方之现象，符合逆温现象不利污染物垂直扩散之预期；另外，也观察到逆温层上方有高浓度出现，此现象可能是远程传输之污染所导致。

关键字：挥发性有机化合物（VOCs），逆温层，层化现象，臭氧空气质量，探空气球

株洲市工业区大气颗粒物污染特征研究

(郑子龙^{1,2} 张凯^{2*} 柴发合² 杨晴^{1,2} 李倦生³ 刘运年⁴)

(1. 山东科技大学化学与环境工程学院, 山东青岛 266510;

2. 中国环境科学研究院环境基准与风险评估国家重点实验室, 北京 100012;

3. 长沙环境保护职业技术学院, 湖南长沙 410004

4. 株洲市环境监测中心站, 湖南株洲 412000)

摘要: 为了解株洲市大气颗粒物的浓度特征, 于 2011 年 11 月至 2012 年 11 月在株洲市采集了 4 个季节的 TSP、PM₁₀ 和 PM_{2.5} 样品, 分析表明株洲市大气 $\rho(\text{TSP})$ 为 $187.8\mu\text{g}/\text{m}^3$, $\rho(\text{PM}_{10})$ 为 $157.3\mu\text{g}/\text{m}^3$, $\rho(\text{PM}_{2.5})$ 为 $79.1\mu\text{g}/\text{m}^3$ 。秋冬季颗粒物浓度高于春夏季 50% 左右。 $\rho(\text{PM}_{2.5})/\rho(\text{PM}_{10})$ 比值为 0.5, 接近或低于其他工业城市。

关键词: 大气颗粒物, 株洲, 污染特征

Study on the pollution characteristic of atmosphere particles in Industrial Zone of Zhuzhou city

ZHENG Zi-long^{1,2}, ZHANG Kai¹, CHAI Fa-he¹, YANG Qing^{1,2}, LI Juan-sheng³, LIU Yun-nian⁴

1State Key Laboratory of Environmental Criteria and Risk Assessment, Chinese Research Academy of Environmental Sciences, Beijing 100012, China

2Shandong University of Science and Technology, Qingdao 266510, China

3Changsha Environmental Protection College, Changsha 410004, China

4Zhuzhou Environment Monitoring Station, Zhuzhou 412000, China

Abstract: To understand the pollution characteristics of atmospheric particles and typical elements in Zhuzhou City, TSP PM₁₀ and PM_{2.5} samples of 4 seasons were collected in Zhuzhou from November 2011 to November 2012. Results show that the average TSP, PM₁₀ and PM_{2.5} concentrations in Zhuzhou were respectively $187.8\mu\text{g}/\text{m}^3$, $157.3\mu\text{g}/\text{m}^3$ and $79.1\mu\text{g}/\text{m}^3$, which in autumn and winter were about 50% higher than that in spring and summer. The average ratio of $\rho(\text{PM}_{2.5})/\rho(\text{PM}_{10})$ was 0.5, which was close to or below the other industrial cities.

Key words: atmospheric particles, Zhuzhou City, pollution characteristic

基金项目: 国家环保公益性行业科研专项 (201109005); 国家自然科学基金 (41205093)

*通讯作者:

探寻 IMPROVE 和 NIOSH 法元素碳（EC）测定结果的数学联系

（支国瑞^{1*}，陈颖军²，李洋¹）

（¹ 中国环境科学研究院，² 中科院烟台海岸带研究所）

摘 要：元素碳（EC）指大气气溶胶中有一定耐热作用的吸光碳，源于含碳物质的不完全燃烧，既是一种空气污染物，又是一种重要的气候影响因子。30 多年来，实践中出现了多种测定方法，但由于不同方法着眼于 EC 的不同性质，造成测定结果的较大差异，为基于 EC 测定的排放清单制定、空气污染模拟及气候效应评估带来极大不便。即使是目前较为普遍使用的两种热光法测定协议，即 IMPROVE 和 NIOSH（表 1），其 EC 测定结果的差异也很明显。因此建立方法间的数学联系，对于不同方法的数据共享具有重要的理论和实践意义。

表 1. NIOSH 和 IMPROVE 分析程序

| 载气 | 碳化分 | NIOSH ^a | | IMPROVE ^b | |
|-------------------|------|--------------------|--------|----------------------|---------|
| | | 温度 (°C) | 时间 (s) | 温度 (°C) | 时间 (s) |
| He | OC1 | 250 | 60 | 140 | 160~580 |
| | OC2 | 450 | 60 | 280 | 160~580 |
| | OC3 | 650 | 60 | 480 | 160~580 |
| | OC4 | 850 | 90 | 580 | 160~580 |
| | 炭化校正 | 透射 | | 反射 | |
| He/O ₂ | EC1 | 550 | 45 | 580 | 160~580 |
| | EC2 | 650 | 60 | 740 | 160~580 |
| | EC3 | 750 | 60 | 840 | 160~580 |
| | EC4 | 850 | 40 | | |
| | EC5 | 870 | 40 | | |

^a类似于 Birch (1998); ^b2005 年以后的 DRI Model 2001 仪器所使用的温度，每步驻留时间并不固定，但介于 160-580s 之间，依每个 FID 碳峰接近基线为准。

实验基于九种不同成熟度的煤（烟煤、无烟煤），以不同型态（煤块、蜂窝煤）在不同炉型（改进、简易）中燃烧，使用自制的烟气稀释采样系统采集烟气的颗粒物于石英滤膜上，共得到 27 个滤膜样品，分别进行 NIOSH 法和 IMPROVE 法的 EC 测定。以测定结果建立如图 1 的坐标体系，X 轴为 IMPROVE 法测得的 EC 与总碳（TC）的比值（ $R_{EC/TC}$ ），y 轴为两种测定结果的相对差（ $(EC_{IMPROVE}-EC_{NIOSH})/EC_{IMPROVE}$ ）。通观察数据的特点，初步设计了 x、y 的关系构架为 $y=(1-x)/(1+mx^n)$ 。使用 SPSS 统计分析软件，拟合最佳的 m 值和 n 值，最终确定经验方程 $y=(1-x)/(1+4.86x^2)$ 。一些其它的实验数据支持该关系的合理性，但仍需在更多地区开展大气气溶胶 EC 的实际对比，以便对此关系进行验证和改进。通过该经验方程，把来自于 NIOSH 和 IMPROVE 的两种 EC 分析结果联系起来了。

* 联系人：支国瑞，zhigr@craes.org.cn
基金：中国自然科学基金（41173121）；国家环境保护公益性行业科研专项（201209007）

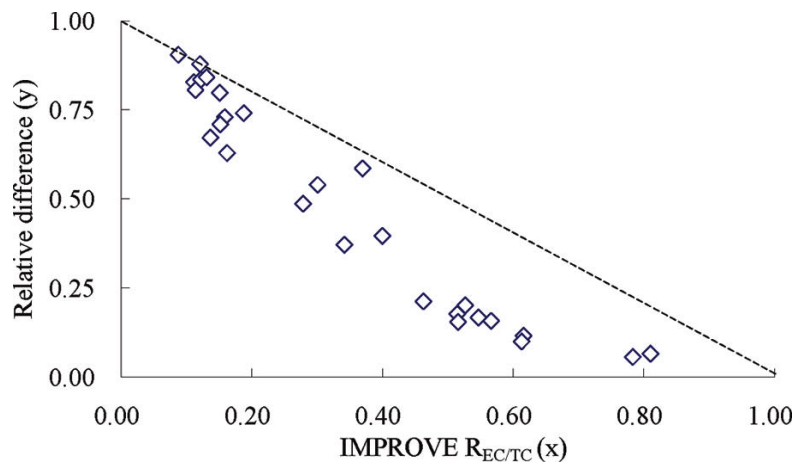


图 1 数据分布观察

参考文献

- (1) Birch, M. E. Analysis of carbonaceous aerosols: Interlaboratory comparison. *Analyst* **1998**, 123(5), 851-857.
- (2) Chow, J. C.; Watson, J. G.; Chen, L. W., et al. The IMPROVE_A temperature protocol for thermal/optical carbon analysis: maintaining consistency with a long-term database. *Journal of Air & Waste Management Association* **2007**, 57(9), 1014-1023.
- (3) Chow, J. C.; Watson, J. G.; Chen, L.-W. A., et al. Comparison of the DRI/OGC and Model 2001 Thermal/Optical carbon analyzers. Prepared for the IMPROVE Steering Committee, Fort Collins, CO, by Desert Research Institute, Reno, NV. **2005**,
- (4) Chow, J. C.; Watson, J. G.; Pritchett, L. C., et al. The DRI Thermal/Optical Reflectance carbon analysis system: Description, evaluation and applications in U.S. air quality studies. *Atmospheric Environment* **1993**, 27A(8), 1185-1201.
- (5) Zhi, G.; Chen, Y.; Sun, J., et al. Harmonizing aerosol carbon measurements between two conventional thermal/optical analysis methods. *Environmental Science & Technology* **2011**, 45(7), 2902-2908.

利用 CALIPSO 星载激光雷达资料研究我国 PM₁₀ 浓度分布特征

(周天, 黄忠伟)

兰州大学大气科学学院 半干旱气候变化教育部重点实验室, 甘肃, 兰州 730000

摘 要: 气溶胶显著的环境和气候效应使其成为影响环境和气候重要且不确定的因素之一。近年来, 可吸入颗粒物 PM₁₀ 对我国区域环境和气候的影响引起人们越来越多的关注。本文基于 CALIPSO 星载激光雷达可提供全球尺度气溶胶垂直结构和光学特性的优势, 综合分析了 2009 年 1 月至 2013 年 2 月期间的 CALIPSO 卫星资料与台湾中坜站 (24.95°N, 121.22°E, 135 米) PM₁₀ 观测资料的关系。首先, 利用统计学方法建立中坜站地区气溶胶层积分衰减后向散射系数、层积分退偏比和层积分色比与 PM₁₀ 浓度分布的关系, 初步结果显示该地区气溶胶光学特性与 PM₁₀ 浓度分布有很好的相关性; 其次, 将该关系推广至全国地区, 初步取得了我国 PM₁₀ 浓度的地域分布特点; 然后, 分析不同区域 PM₁₀ 浓度分布的月变化、季节变化和年际变化规律, 进一步深入了解我国不同地区 PM₁₀ 浓度的时空分布特征。本文研究结果不仅表明 CALIPSO 星载激光雷达在环境研究领域的独特优势, 而且获取我国 PM₁₀ 浓度的时空分布特征, 可为全球气候变化和环境科学等相关研究提供重要的观测资料。

关键词: CALIPSO, 星载激光雷达, PM₁₀

Investigations of the Chemical Characteristics from an Intensive Sainampling of Ambient Particles in Shanghai, China

(Chong-shu Zhu¹, Jun-ji Cao^{1,2})

¹ Key Laboratory of Aerosol, SKLLQG, Institute of Earth Environment, Chinese Academy of Sciences, Xi'an, China

² Institute of Global Environmental Change, Xi'an Jiaotong University, Xi'an, China

Abstract: Ambient daytime and nighttime PM_{2.5} and TSP samples were collected in parallel at two sites (named Pudong and Jinshan) in Shanghai, China. The samples were analyzed for carbon fractions, elements, water-soluble ions (WSIs) at both sites. The lower concentrations of particulates were found at Pudong, and higher level of PM_{2.5} and TSP concentrations were observed in daytime than nighttime for both sites. The variations of chemical components (OC, EC, ions and elements) as well as the species ratios were discussed in depth for daytime and nighttime. The results showed that organic aerosol and secondary sulfate are the most abundant components of the particle, and the contributions were variable during the different sampling periods due to the strength of local emission and the secondary production. The discussion indicated that the particulates were variable for different areas according to the local emissions and meteorology. The results can give some indications for the developing effective strategies for urban sub-zone pollution control.

Keywords: PM_{2.5}, TSP, carbonaceous fractions, ions, elements, Shanghai

大气细颗粒物对人体健康的影响

(朱彤)

北京大学环境科学与工程需要, 环境与健康研究中心

摘 要: 粒径小于 2.5 微米的大气细颗粒物(PM_{2.5})对人体健康有显著的危害。目前我国多个城市 PM_{2.5} 超标严重, 引起了社会和公众的广泛关注, 已成需要重点控制的大气污染物。尽管大量的流行病学和毒理学研究证实大气污染与心肺系统疾病发病率和死亡率增加显著相关, 但对于大气颗粒物的理化性质与健康效应之间的关系仍不清楚, 其危害机制亟待深入研究。为全面探索污染物对于心血管呼吸系统、机体代谢和免疫等功能的影响, 现代流行病学加速了与暴露组学、临床诊治、基因组学等学科的结合, 在人群调查中采用生物标志技术追踪污染物的暴露和代谢途径、分析污染物中的关键化学组分对于靶器官及组织的影响及交互作用机制。

流行病学研究显示空气污染是呼吸系统和心血管疾病的重要危险因素, 但人群研究的直接证据不足。目前主要的假设为空气污染首先诱发呼吸道局部氧化应激和炎症, 进而导致全身性炎症和氧化性损伤, 促进导致血栓形成、引发上皮细胞损伤、引发心脏自主神经功能和血管功能异常。2008 年北京奥运会和残奥会期间实施了大量的空气污染控制措施, 奥运会前后大气污染水平发生急剧变化, 为检验这些假设提供了难得的实验契机。北京大学和美国数所大学的研究人员在北京奥运前、中、后五个月密集追踪了 125 名健康年轻人的系统性炎症和血栓形成等生物性标记物水平的变化。检测的指标包括呼吸道炎症水平 (FeNO)、呼吸道氧化应激水平 (EBC Nitrite Nitrate)、DNA 损伤 (8-OHdG)、全身炎症 (纤维蛋白原、C-反应蛋白 CRP、白细胞 WBC 计数)、血栓形成或内皮功能障碍(可溶性血小板选择蛋白 sCD62P、可溶性 CD40 配基 sCD40L、血管假性血友病因子 vWF) 等有关的生物性标记物, 以及心率、血压等。结果显示北京奥运期间空气污染物水平与健康年轻人呼吸道炎症水平、呼吸道氧化应、DNA 损伤、血栓形成的生物标志物、心血管生理学指标的急性改变相关。

在奥运期间同期进行的患心血管疾病的老年人群追踪观测和小学儿童人群追踪观测。结果显示, 大气细颗粒物及气态污染物暴露后数小时内, 污染物浓度增加与呼吸系统炎症、交感/副交感神经功能的降低和血压的升高具有显著关联; 全身低炎症水平和肥胖可能进一步加剧污染物急性暴露的心血管功能损伤; 细颗粒物中的黑碳(Black Carbon)对于呼吸系统炎症和心血管健康的影响最为显著。

武汉市道路一侧 $\text{PM}_{2.5}$ 和 PM_{10} 浓度监测

(朱颖, 李可, 刘彬, 向荣彪)

华中农业大学资源与环境学院, 武汉, 430070

摘 要: 在2012年8月和10月采用重量法和PM质量分析仪对武汉市南湖大道一侧的 PM_{10} 和 $\text{PM}_{2.5}$ 进行了阶段性监测, 并与华中农业大学内 PM_{10} 和 $\text{PM}_{2.5}$ 浓度进行对比。结果表明, 南湖大道8月监测期间 PM_{10} 和 $\text{PM}_{2.5}$ 平均浓度分别达到 $137.2\mu\text{g}/\text{m}^3$, $61.4\mu\text{g}/\text{m}^3$; 超标率分别高达57%, 57%; 10月监测期间 PM_{10} 和 $\text{PM}_{2.5}$ 平均浓度分别达到 $187.4\mu\text{g}/\text{m}^3$, $100\mu\text{g}/\text{m}^3$; 超标率分别高达83%, 75%, 污染较为严重。通过 PM_{10} 和 $\text{PM}_{2.5}$ 小时平均浓度日变化趋势分析, 发现上午9时及晚上9时 PM_{10} 和 $\text{PM}_{2.5}$ 浓度出现峰值, 下午2时至3时空气质量相对较好。

关键字: PM_{10} , $\text{PM}_{2.5}$, 超标率

Comparing new particle formation events between in highly and less polluted atmosphere: Implication of a critical role of anthropogenic pollutants in growing new particles to CCN size

(Y.J. Zhu¹, H.W. Gao¹, Z.Q. Duan¹, G.J. Evans², X. H. Yao^{*12})

¹Key Lab of Marine Environmental Science and Ecology, Ministry of Education,
Ocean University of China, Qingdao 266100, China

²Southern Ontario Centre for Atmospheric Aerosol Research, University of Toronto, Canada

*Corresponding authors: Email: xhyao@ouc.edu.cn, Tel: 86-532-66782565, fax 1-831-618-6654

Abstract: When new particles formed in the atmosphere grow over 50-80 nm, they can be activated as cloud condensation nuclei (CCN) and lead to an increase of cloud albedo. Knowledge gaps still existed, e.g., 1) in what type of new particle formation (NPF) events new particles can grow over 50 nm? 2) which chemicals determine the growth of new particles to be over 50 nm? In this study, NPF events were investigated at two urban sites, in Qingdao and in Toronto, using two identical Fast Mobility Particle Sizer (FMPS) in spring. The satellite column density of pollution gases and the particular chemical concentration in PM_{2.5} both showed much higher concentrations of anthropogenic air pollutants in Qingdao than in Toronto. NPF events were observed in 16 days out of 39 sampling days in Qingdao and 13 days out of 31 sampling days in Toronto. The occurrence frequency of NPF events between Qingdao (41%) and Toronto (43%) was comparable to each other. In Qingdao, the geometric mean diameter of grown nucleated particles ($D_{pg,i}$) in 15 days grew to larger than 40 nm except in one day when the growth of new particles terminated at ~20 nm. In addition, new particles in 8 days out of the 15 days partly or entirely grew over 50 nm and they could even reached 100 nm in two days. Two-phase growth was generally observed in these NPF events of Qingdao. The first-phase growth occurred in daytime and the CMAQ modeling results suggested that formation of secondary organics was likely the major cause for the growth. The second-phase growth was observed at night and was associated with the increased concentrations of NH_4^+ and NO_3^- , implying that NH_4NO_3 condensation played an important role in the growth. In Toronto, NPF events in 4 days followed with the growth of new particles $< \sim 20$ nm while new particles grew up to ~ 40 nm in the remaining NPF events. A slight growth of new particles at night was observed only in 3-days NPF events when the increased concentrations of NH_4^+ , NO_3^- or the increased relative humidity were observed. However, the calculated $D_{pg,i}$ was less than 45 nm for all NPF events in Toronto, implying a negligible contribution of new particles to the population of CCN.

Key words: nucleation, particle growth, anthropogenic pollutants, NH_4NO_3 condensation

Characterization of Springtime Atmospheric Organic and Elemental Carbon of PM_{2.5} in a Typical Semi-Arid Area of Northeastern China

(Renjian Zhang^{1*}, Jun Tao², K.F. Ho^{3,4}, Zhenxing Shen⁵)

¹ RCE-TEA, Institute of Atmospheric Physics, Chinese Academy of Sciences, Beijing 100029, China

² South China Institute of Environmental Sciences, Guangzhou 510655, China

³ SKLLQG, Institute of Earth Environment, Chinese Academy of Sciences, Xi'an 710075, China

⁴ School of Public Health and Primary Care, The Chinese University of Hong Kong, Hongkong, China

⁵ Department of Environmental Science and Engineering, Xi'an Jiaotong University, Xi'an 710049, China

Abstract: Daily particulate matter (PM_{2.5}) aerosol samples were collected in Tongyu, a semi-arid area in northeastern China in spring. The concentrations of organic carbon (OC) and elemental carbon (EC) were determined with a thermal/optical carbon analyzer in the filter samples. The average concentrations of OC and EC in PM_{2.5} were 14.1 ± 8.7 and 2.0 ± 1.3 $\mu\text{g}/\text{m}^3$, respectively. A good correlation between OC and EC was observed during the spring season, suggesting that they might be derived from similar sources. The correlation between OC and K⁺ was high ($R = 0.74$) and the K⁺/OC ratio, as determined from their linear regression slope, reached 2.57. The good correlation and the high K⁺/OC ratio indicated that biomass-burning was probably one of the major sources of OC in this region. The concentrations of estimated secondary organic carbon (SOC) in PM_{2.5} in Tongyu ranged from below detection limit to 26.1 $\mu\text{g}/\text{m}^3$ (mean, 5.9 $\mu\text{g}/\text{m}^3$). The percentages of SOC in OC and in PM_{2.5} mass were 42.0% and 2.1%, respectively. The SOC concentrations during dust storms (DS) periods were higher than those during non-dust storm (NDS) periods, suggesting that chemical reaction processes involving gas-particle conversion should have occurred during the long-distance transport of aerosol particles.

Keywords: Semi-arid area; Organic carbon; Elemental carbon; Dust storm.

直接称量法环境空气颗粒物自动监测系统

摘 要：本文提出了一种新的环境空气颗粒物 $\text{PM}_{2.5}$ 自动监测方法——直接称量法。着重介绍了实现这种方法的仪器结构组成、工作原理、数据发布方式以及为提高称量精度而设立的标准化的称量环境。通过仪器的原理和工作过程描述论证了这种方法具有更高的准确性；通过初步监测数据证明这种系统具有良好的稳定性和一致性。作者认为这种监测 $\text{PM}_{2.5}$ 含量的直接称量法就是基础验证法的自动化和智能化，或者说是自动化和智能化的基础验证法。它消除了现行的间接监测方法的量值转换误差，是一种更科学、准确的环境空气颗粒物自动监测的方法，具有广阔应用和推广前景。

Real-time Measurements of Secondary Organic Aerosol from the Photooxidation of Naphthalene using Single Particle Mass Spectrometry

(ang Chen^{1,2}, Robert M. Healy², Shouming Zhou², and John C. Wenger²)

¹Institute of Earth Environment, Chinese Academy of Sciences, Xi'an China

²Department of Chemistry and Environmental Research Institute, University College Cork, Cork, Ireland

Abstract : Naphthalene is the most abundant polycyclic aromatic hydrocarbon detected in urban air and has recently been identified as an important precursor for the formation of secondary organic aerosol (SOA) in the atmosphere. In this work, a series of simulation chamber experiments has been performed on the photooxidation of naphthalene under a variety of reaction conditions. The decay of naphthalene was monitored using in situ FTIR spectroscopy and the formation and evolution of SOA was followed using a scanning mobility particle sizer. An Aerosol Time-of-Flight Mass Spectrometer (ATOFMS) was used to determine the chemical composition of the SOA in real-time. In experiments using NO_x as the hydroxyl radical precursor, the single particle mass spectra were found to change slowly over a period of hours. The positive ion mass spectra initially contained hydrocarbon fragments typical of aromatic species which are tentatively attributed to ring-retaining oxidation products such as naphthol and nitronaphthalene. After 3-4 hours the intensity of the hydrocarbon fragments was significantly reduced and the negative ion mass spectra displayed characteristic features of oxidized organic aerosol and nitrates. Interestingly, some of these peaks continued to increase after the lights were turned off, suggesting that particle phase processing was maintained, even under dark conditions. The results from these experiments indicate that ATOFMS can be used to monitor chemical changes in SOA in real-time and is a potentially useful tool for investigating aerosol formation and ageing.

Keyword: Secondary Organic Aerosol, Naphthalene, online single particle mass spectrometer.

半干旱区气溶胶物理特性的观测研究

(张武 冯岚 李娜 颜娇珑 王雅萍 柳丹 黄晨然)

半干旱气候变化教育部重点实验室 兰州大学大气科学学院, 兰州, 甘肃, 730000

摘 要:本文利用兰州大学半干旱气候与环境观测站(SACOL)在 2010 年 1 月-2011 年 2 月观测数据, 分析了气溶胶光学参数、不同粒径段气溶胶数浓度和数谱分布随时间变化的特点, 以及气象条件对这些参数的影响, 讨论了 AOD 与 PM_{10} 质量浓度的相关性。同时, 探讨了用 APS 资料拟合 PM_{10} 质量浓度的方法, 结果表明:

SACOL 站气溶胶光学厚度、浑浊度系数的年均值分别为 0.410 和 0.231, 季节平均值按春、冬、夏、秋顺序依次减少, 波长指数的年均值 0.840, 季节平均值则按春、冬、夏、秋依次增大。

SACOL 站大气中气溶胶总数浓度主要取决于 $PM_{2.5}$ 数浓度, 特别以粒径小于 $1.0\mu m$ 的积聚模态居多, 其中冬季粒径小于 $1\mu m$ 的气溶胶粒子数浓度又远远超出其它季节。

SACOL 站常年盛行东南和西北风, 这两个方向的上风向为兰州市和榆中县, 是人口聚集区, 人类活动产生的气溶胶被输送到下游, 气溶胶粒子数浓度出现高值的频次最多。

2010 年春季, SACOL 站所在区域沙尘天气频繁发生。沙尘天气中, AOD 增大, 浑浊度系数与 AOD 变化趋势保持一致, 呈正相关关系, 波长指数与它们呈较弱的负相关。沙尘暴发生前, $PM_{2.5}$ 数浓度急剧增大, 气溶胶总数浓度主要取决于粒径小于 $0.523\mu m$ 的颗粒物数浓度; 沙尘暴出现时, PM_{coarse} 数浓度急剧增加, PM_{total} 质量浓度主要取决于 PM_{coarse} 数浓度。

用 APS 数据拟合 PM_{10} 质量浓度的方法中, 多元线性回归在春季沙尘天气和冬季污染天气条件下的相关系数超过 0.950,

关键词: 气溶胶光学厚度, Angstrom 参数, 粒径分布, 半干旱区, SACOL

长三角臭氧和细颗粒污染及其对区域污染控制和污染-气候相互作用的启示：SORPES 观测站最新进展

(丁爱军¹, 符淙斌¹, 杨修群¹, 孙鉴淳¹, 聂玮¹, 谢郁宁¹, 齐西蒙¹, E. Herrmann^{1,2}, T. Petäjä², V.-M. Kerminen², M. Kulmala²)

¹ 南京大学气候与全球变化研究院/大气科学学院

² Dept. of Physics, University of Helsinki, Finland

摘要:南京大学气候与全球变化研究院与芬兰赫尔辛基大学合作于 2009 年起在南京大学仙林校区建立和发展了地球系统区域过程观测试验基地 (SORPES), 该基地致力于研究地表物理过程、大气化学-气候相互作用、生态系统-大气相互作用和水文过程及水循环。站点位于南京东郊、长三角西部的下风向区域背景地区, 具有很好的区域代表性。通过近 2 年的连续观测, 本研究获得了长三角西部地区臭氧和细颗粒物 $PM_{2.5}$ 及其相关前体物的季节变化特征, 发现了该地区臭氧、细颗粒污染的重要控制因子、天气过程及区域相互影响。本研究还发现在长三角地区高污染环境下也能出现频繁的新粒子生成事件, 并提出了区别于国外清洁环境的主要限制因子。研究同时发现该地区不同类型来源的高浓度颗粒物污染会实质性的改变天气乃至区域气候。2012 年 6.10 观测到的秸秆燃烧引起的高浓度气溶胶污染会导致天气预报对气温的严重高估和降水的“误报”, 多种计算机模型均不能重现该极端污染天气条件下的实际气温和降水分布。秸秆燃烧烟羽与城市及区域人为污染的混合, 进而通过复杂的大气边界层-污染-云和辐射的正反馈机制影响大气结构以及降水。基于此, 课题组将于 2013/14 两年在生物质燃烧的多发季节在 SOEPES 站点进行两期加强观测, 针对此问题进行进一步研究。

关键词: SORPES 观测基地, 区域代表性, 生物质燃烧, 反馈机制, 新粒子生成

亚洲沙尘的演化和非均相光化学过程研究

(聂玮¹, 王韬^{2,3}, 丁爱军¹, 薛丽坤³, 王文兴²)

¹ 南京大学气候与全球变化研究院/大气科学学院

² 山东大学环境研究院

³ 香港理工大学土木与环境工程系

摘 要: 沙尘表面的非均相化学对理解大气化学和辐射平衡至关重要。本研究于 2009 年春季在湖南衡山山顶（海拔 1269 米）进行了针对大气气体、气溶胶和气象参数的综合观测。研究目的主要关注于沙尘颗粒在传输过程中的化学演化和非均相光化学过程。观测期间捕获到两次沙尘暴个例，其中以 4 月 25-26 日发生的沙尘事件最为强烈。研究结果发现沙尘颗粒在传输过程中经历了显著的变化，二次成分（硫酸盐、硝酸盐和铵盐）在粗粒子模态有明显富集。用光化学年龄“时钟”法来量化了沙尘气团的大气反应时间，发现二次水溶性离子在沙尘颗粒上的富集随气团老化程度而显著增加。基于本次观测，我们提出了一个针对含碳酸钙沙尘颗粒的 4 步演化过程，包含了从初始排放沙尘颗粒到吸湿性物质（及酸性物质）覆盖的沙尘颗粒。此外，本研究还在沙尘暴过程的日间发现了高浓度的亚硝酸盐生成，实验室研究在近期验证的 NO_2 在 TiO_2 沙尘表面的光催化转化成 HONO 的过程是最可能的成因。本研究验证了非均相光化学反应在实际大气中的存在及其潜在的重要性。

关键词: 沙尘暴，衡山，化学演化，非均相光化学

西安 2008 年冬季地表臭氧变化模拟及其主要影响因素

摘 要:模拟了西安地区 2008 年 12 月份地表臭氧的分布及时间变化,并分析影响臭氧变化的主要因素。模拟发现,西安城区冬季 12 月份地表臭氧浓度普遍偏低,最低的时段接近于 0。地表臭氧浓度的日变化表现为在 15~16 时 (LT) 达到日最高 (~10ppb),在 7~8 时 (LT) 达到日最低 (< 1ppb),这与观测结果相吻合。西安地区风场状况较稳定,本地 NO_x 是地表大气臭氧浓度的主要决定因素,二者呈现出反相的变化规律,而冬季大气气溶胶和生物源排放对地表大气臭氧浓度的影响均很小。

Black carbon variation during a high pollution haze episode in Beijing, China

Qingyang Liu^{1,3}, Yanju Liu^{1,2*}, Yi Gao⁴, Meigen Zhang⁴, Renjian Zhang⁴, Hui Ding⁵, Xuekui Qi¹,

¹Beijing Center for Physical and Chemical Analysis, Beijing, 100089, China

²Beijing Milu Ecological Research Center, Beijing, 100076, China

³College of Resources and Environment, University of Chinese Academy of Sciences, Beijing, 100049, China

⁴State Key Laboratory of Atmospheric Boundary Layer Physics and Atmospheric Chemistry, Institute of Atmospheric Physics, Chinese Academy of Sciences, Beijing, 100029, China

⁵Beijing Academy of Sciences and Technology, Beijing, 100089, China

* Corresponding author

E-mail: liuyanju@hotmail.com

Tel/Fax: : +86-10-8817 6969

Abstract: Black carbon (BC) aerosol is esthetically displeasing as it is responsible for the brown appearance of urban hazes. In this study, atmospheric BC aerosol was measured using an aethalometer (AE-31) at an urban location of Haidian District, Beijing from May 2012 to March 2013. A logarithmic negative correlation ($R^2=0.5120$) between BC and visibility suggested that BC was an important air pollution factor to affect air quality in Beijing. BC concentration showed significant seasonal variation with mean concentration varying between $4.24 \mu\text{g m}^{-3}$ (summer) to $8.14 \mu\text{g m}^{-3}$ (winter). The highest daily mean concentration was recorded as high as $27.69 \mu\text{g m}^{-3}$. The highest concentration of BC occurred during a high pollution haze episode in winter. In a clear day, BC exhibited a distinct diurnal pattern, with three maximum peaks within a day. However, BC exhibited a multi-peak diurnal pattern during haze episodes from Dec 2012 to Jan 2013. Statistical factors analysis demonstrated that emission source factors were not increased, leading to multi-peak diurnal pattern in BC variation. Additionally, Weather Research and Forecasting Model showed that the boundary layer height during haze episodes hourly varied in a similar trend with normal days. All the evidence indicated that BC exhibited a rather higgledy-piggledy diurnal pattern during haze episodes, which played a key role in the stabilization of haze formation.

Keywords: Black carbon aerosol, Haze formation, Diurnal pattern, Seasonal trend.

大型环境舱协助改进外排式空气净化设备性能的评价测试

杨华, 王欣欣, 刘清珺, 刘艳菊, 邵薇
北京市理化分析测试中心, 北京, 100089

摘 要: 现行空气净化器评价标准不适于外排式净化设备的性能测试。本实验通过对外排式净化设备设计、添加采样装置, 在现行空气净化器评价标准基础上, 以大型环境舱为检测平台, 以香烟烟雾为颗粒物、甲醛、乙醛和巴豆醛等污染物的污染源, 实现了净化设备的性能改进, 污染物去除率从不足 5%最高升至 82.8%。

关键字: 外排式空气净化设备, 评价, 大型环境舱, 颗粒物, 气体污染物



AIR & WASTE MANAGEMENT
ASSOCIATION
SINCE 1907



禾信质谱
HEXIN MASS SPECTROMETRY



CAMBUSTION

BMET

EVERISE®

**TECHNO
SOLUTIONS**

